DEUTSCHES ELEKTRONEN-SYNCHROTRON DESY

DESY 77/79
December 1977

The Properties of Charmonium and Charm Particles

by

Herwig Schopper
Deutsches Elektronen-Synchrotron DESY, Hamburg
and
II. Institut für Experimentalphysik der Universität Hamburg

NOTKESTRASSE 85 · 2 HAMBURG 52

To be sure that your preprints are promptly included in the
HIGH ENERGY PHYSICS INDEX ,
send them to the following address (if possible by air mail) :

DESY
Bibliothek
Notkestrasse 85
2 Hamburg 52
Germany

THE PROPERTIES OF CHARMONIUM AND CHARM PARTICLES

by

Herwig Schopper
Deutsches Elektronen-Synchrotron DESY, Hamburg
and
II. Institut für Experimentalphysik der Universität Hamburg

Lecture given at Erice, Italy

(updated to January 1978)

Erice-School: The WHY's of Subnuclear Physics

Contents

1. INTRODUCTION

An impressive amount of data has been accumulated over the past three years which support strongly the idea that elementary particles are composed of four quarks instead of three. All the predictions based on the existence of the fourth, the charm quark, have in principal been born out by experiments and from detailed investigations very interesting results could be obtained for the strong and the weak interaction. Most of these results have been obtained with electron-positron storage rings, and only these will be discussed in this report. Additional data from hadronic or neutrino interactions are in general agreement with the e^+e^- data and will not be discussed here. This series of lectures will be entirely devoted to a discussion of mesons, i.e. quark - antiquark systems. Although some indications have been found for the existence of charmed baryons, these data are still rather scanty. In the last chapter we shall also discuss the upsilon particle.

1.1 Experimental techniques

1.11 Electron-positron storage rings

Most of the data have been obtained at SPEAR in Stanford, California, and DORIS at DESY, Hamburg. SPEAR is a single ring machine in which electrons and positrons circulate in the same vacuum chamber in opposite directions. The stored particles are concentrated in one bunch per beam thus colliding only at the two intersection regions. DORIS on the other hand, consists of two rings, one on top of each other. The beams are crossing at an angle of 24 mrad. As a consequence, each beam can contain up to 480 bunches, yielding higher luminosities at lower energies where the luminosity is limited by space charge effects. At higher energies where the rf power is the limitation, the single ring operation is more favourable.

The two rings of DORIS would make it possible also to study electron-electron and electron-proton collisions. These options have not been used so far, because of the strong interest in e^+e^- physics.

The lay-out of DORIS and injection scheme is shown in fig. 1.1. So far DORIS mostly has been operated at energies between 2×1.5 and 2×3 GeV. The electron and positron currents are usually about 200 mA and the beam lifetime is varying between 5 and 12 hours. Currents between 0.5 and 0.8 A have been achieved, but beam lifetime then became short and the momentum smearing in the beam gets bigger than 1 MeV. In October 1977 DORIS has been converted to single ring opera-

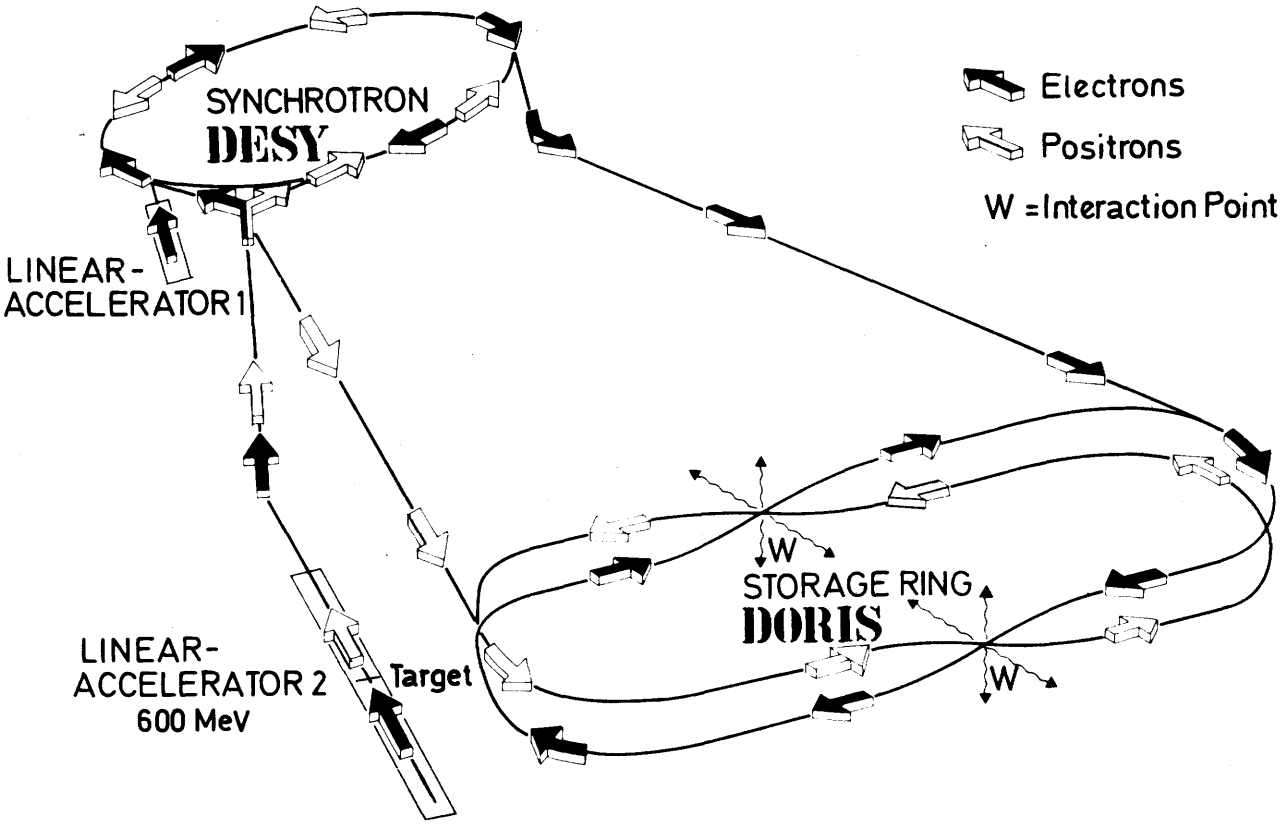

Fig. 1.1: layout of DORIS and injection scheme

tion and energies of 2 × 4 GeV have been achieved. The limitation is then given by the rf-power. It is planned to add two more PETRA cavities in DORIS which should make it possible to push the energy up to 2 × 5 GeV. This shall be tried during 1978.

In fig.1.2 luminosities as obtained with DORIS are shown. Going up in energy, the number of bunches is successively reduced, giving a tooth-structure. The dashed line indicates the luminosity expected for single ring operation. The cross over of the two curves is around 2.5 GeV per beam, indicating that at lower energies multi-bunch operation is more favourable than single ring operation.

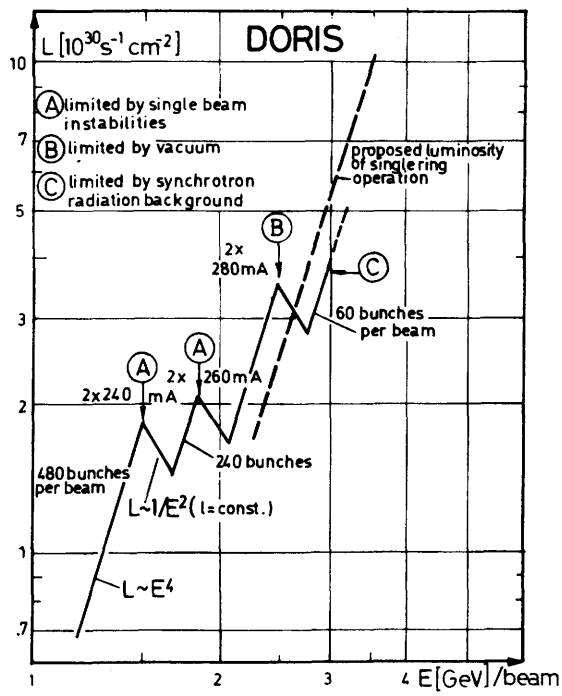

Fig. 1.2

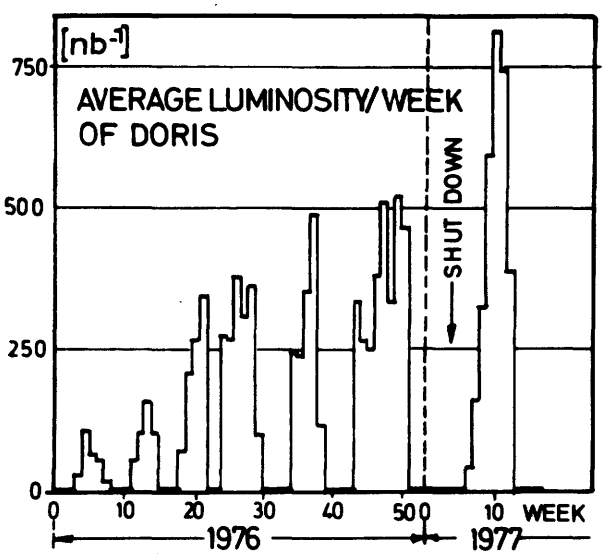

Fig. 1.3

Fig.1.3 shows the average luminosities per week obtained during '76 and beginning of '77. It is the average luminosity which is really important for the experiments. The continuous increase of the average luminosity is mainly due to improvements in the stability and reliability of the machine. With a total cross section of about 40 nb several hundred events can be observed per day.

1.12 Spectrometers

In order to observe and analyze the particles produced in e^+e^- annihilation magnetic spectrometers are used in most experiments.

Fig.1.4 shows a blow-up diagram of the magnetic detector at SPEAR. A coil with about 3 m diameter produces a longitudinal field parallel to the incident beams. Cylindrical chambers permit the detection of charged particles providing

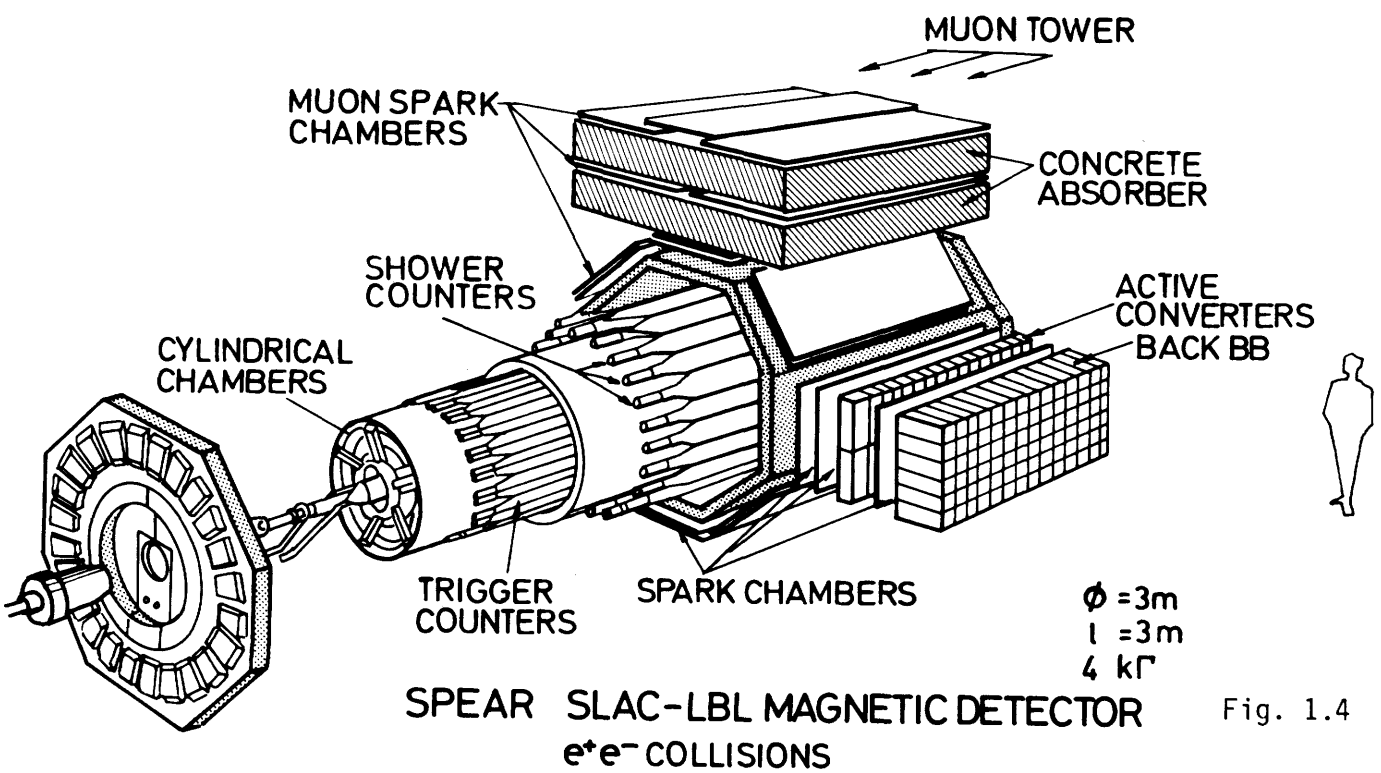

Fig. 1.4

very good momentum analysis which is one of the strengths of this spectrometer. A solid angle of about 65 % of 4π is covered. Electrons and γ-rays can be observed by shower counters, which are placed outside the coil. Time of flight measurements with scintillation counters make it possible to identify particles and in particular the separation of K and π's turned out to be very important for the discovery of charmed particles. Large spark chambers located outside the iron yoke allow the detection of muons. Since the iron yoke is not very thick, there is however some punch trough from hadrons. In order to provide a cleaner muon detection for at least a limited solid angle, additional concrete absorbers have been added later on top of the detector ("muon tower"). Very recently a lead glass wall with an active converter has been added which has proved to be very important for the clean detection of electrons.

Fig.1.5 shows the PLUTO spectrometer at DORIS. PLUTO also uses a longitudinal magnetic field which, however, is produced by a superconducting coil giving a field of about 2 Tesla. Since the diameter of the coil is only about 1 m, the

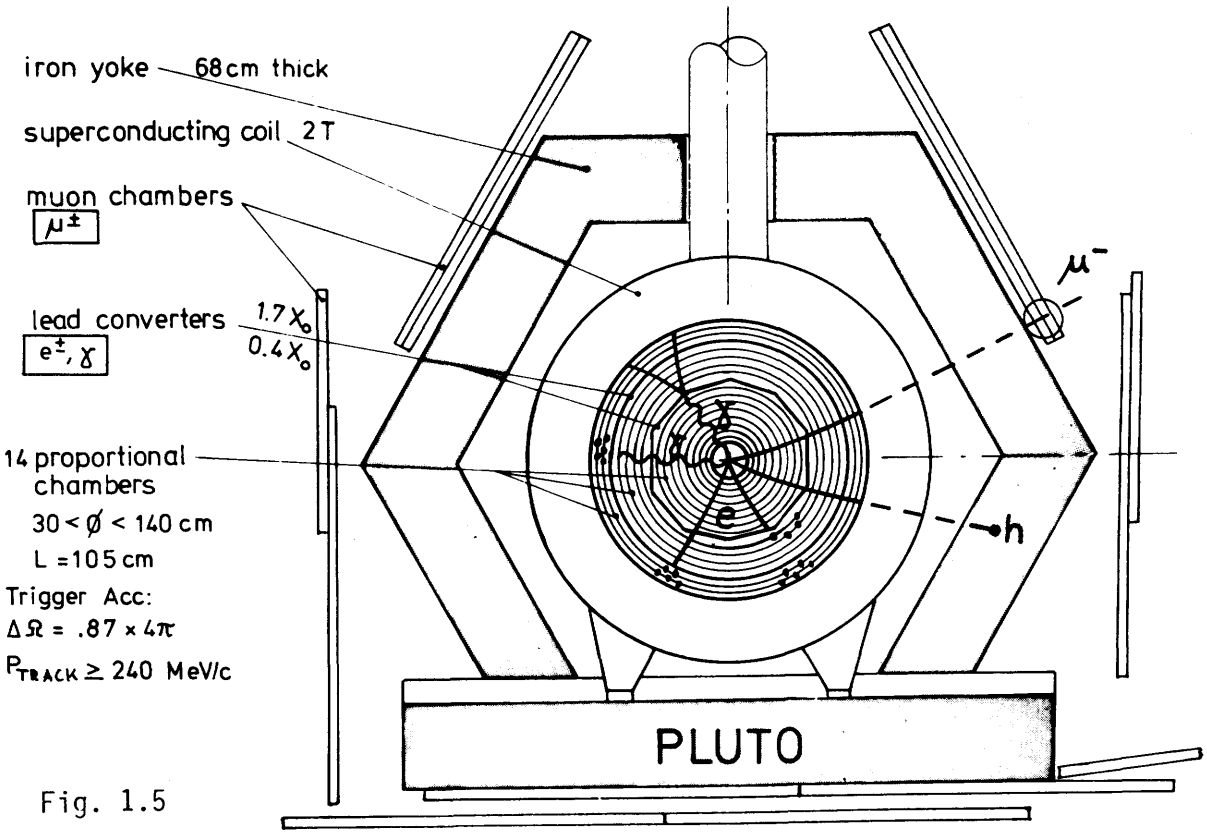

Fig. 1.5

momentum resolution is lower than that of SPEAR and time-of-flight measurements cannot be used to identify particles. On the other hand the cylindrical chambers inside the coil cover about 86 % of 4π. The cylindrical chambers are interspersed with two lead converters (0.4 and 1.7 radiation lengths thick, respectively)

which allow the detection of γ's and the identification of electrons. Large chambers outside the iron yoke are used to detect muons. Since the iron yoke provides a hadron absorber more than 60 cm thick in all directions, a very good muon identification can be obtained. Indeed, the mis-interpretation of a hadron for a muon is less than about 3 %. Also electrons can be identified quite reliably, again with a mis-identification probability of only a few percent. These properties have been very important in verifying the existence of a heavy lepton.

Fig.1.6 shows a schematical view of the double arm spectrometer DASP at DORIS. Here two big magnets provide a transverse field outside the interaction region. Particles entering the gap of the two magnets can be analyzed very precisely (momentum resolution better than 2 %). Since long distances are involved, particle identification by time-of-flight is possible. Electrons and γ are again identified with shower counters and μ are observed behind iron absorbers. Thus very good identification and momentum analysis of hadrons is achieved over a solid angle of 0.9 sr. Two cerenkov-counters have been installed covering the magnet gaps which allows a very clean electron identification. A central detector consisting of proportional tubes and shower counters but without magnetic

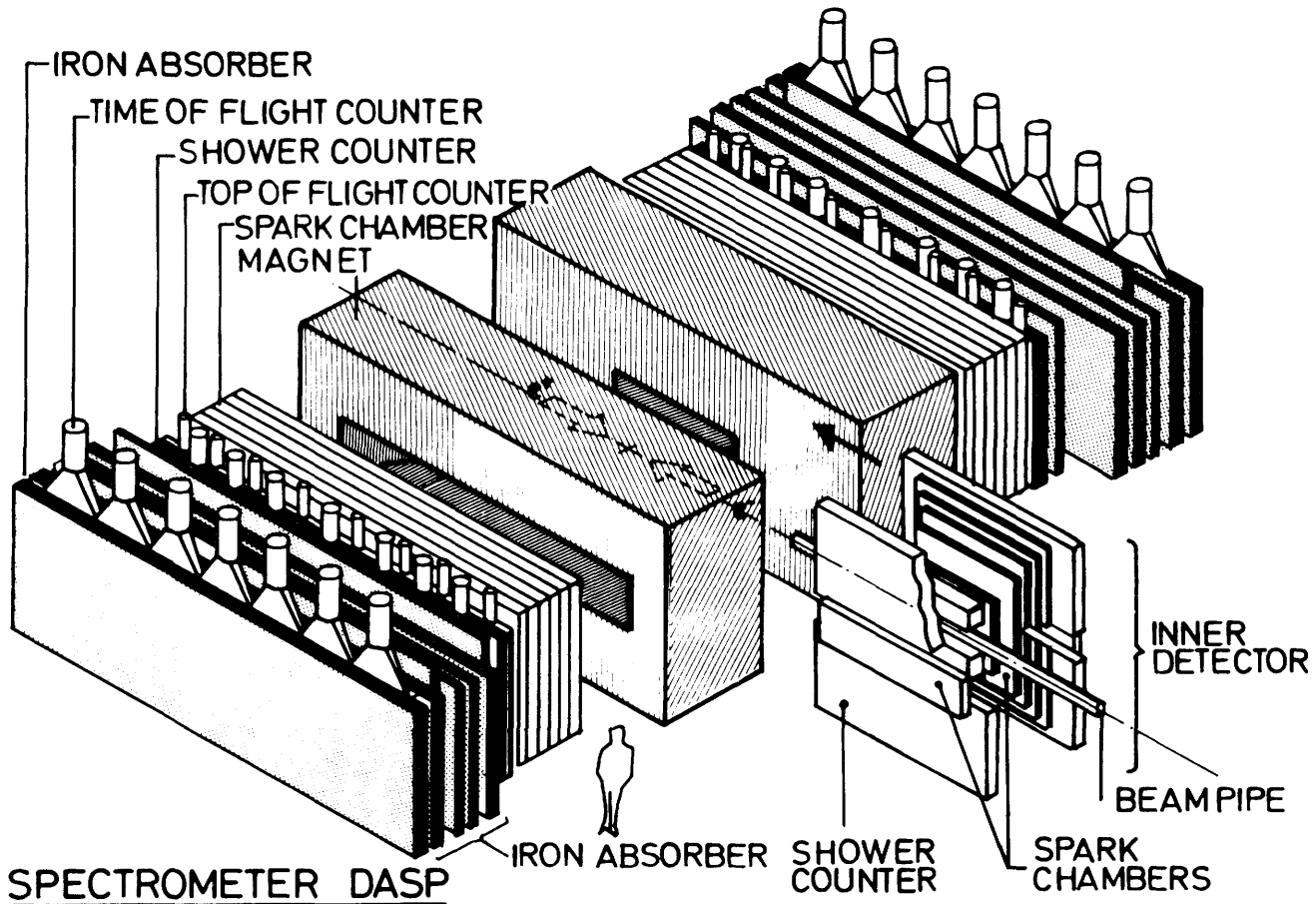

Fig. 1.6

analysis covers about 70 % of 4π. This central detector allows the determination of the direction of γ's and charged particles with an accuracy of about 2^{o}, which has been very essential in some of the experiments.

Several non-magnetic detectors using NaJ crystals, lead glass counters or large neutron counters, have been used at SPEAR as well as at DORIS. Unfortunately, there is not enough room here to describe all the experiments.

1.13 Types of experiments

If an electron and a positron annihilate, a virtual photon is produced which then decays either again into a lepton pair or into hadrons (fig. 1.7).

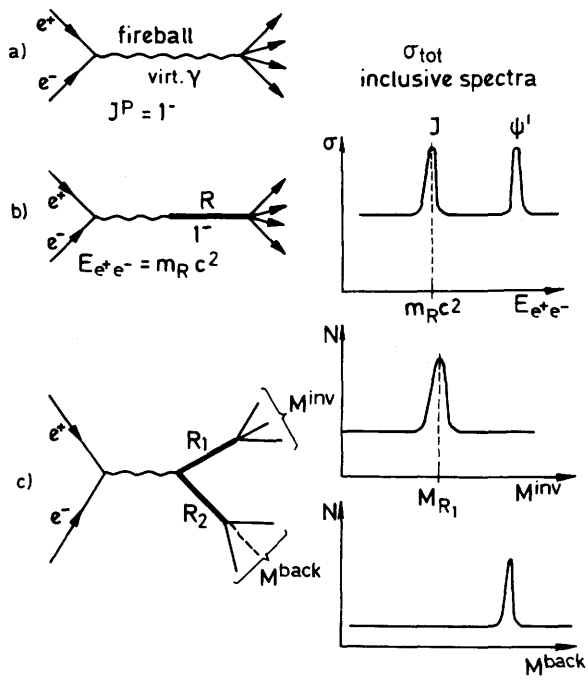

Fig. 1.7

The total final state must have the quantum numbers of the photon $J^P = 1^-$. Most of the experiments which have been performed and which will be described later fall into the following three classes:

1. Non-resonant hadron production (fig. 1.7a). Here one might ask questions like what is the multiplicity of produced hadrons, how varies the total cross section as a function of energy (excluding resonances), what are the inclusive spectra of different kinds of particles like, etc.
2. If the energy of the virtual photon coincides with the rest energy of a vector particle having the quantum numbers of the photon, the hadron production will be enhanced. Measuring the total cross section or special channels one will notice a resonance-like structure if plotting the data as function of the e^+e^- energy (fig. 1.7b). This is a very powerful method to detect new particles, however, only particles with the quantum numbers of the photon can be discovered in this way.
3. Other states can be found in the following way: assume that the virtual photon decays into two resonances (fig. 1.7c) which in turn decay into other hadrons. If the momenta of the final particles are measured, then one can combine two or more particles and calculate from the relativistic kinema-

tics the invariant mass of the object from whose decay they originate. Since one does not know a priori which particles come from the decay of the resonance, many wrong combinations of course are taken, which produce a smooth background. The right combinations of particles on the other hand, produce a sharp peak on top of this background. In this way states with other quantum numbers can be found; of course it is necessary to measure all decay particles in order to determine the invariant mass.

4. The kinematic allows to calculate also the mass of the system recoiling against the invariant mass determined as described. If the recoiling state also contains well defined resonances, peaks in the distribution of the recoil mass will be found. Since the recoil mass can be calculated from the momentum of the first resonance and the initial state, it is not necessary to observe the decay products of the recoiling resonance.

1.2 Phenomenological Models

The purpose of this review is to summarize the experimental facts and not to discuss various theories. To interprete the data phenomenological models will be used which have been developed over the past years and which are based on simple concepts. Most of these models are lacking a rigorous foundation and hence they are criticized by many theorists. On the other hand, these models have exhibited a surprising and extremely successful predictive power and therefore the usefulness of such models is beyond any doubt. Before discussing these models, it might be useful to recall some generally accepted ideas.

1.21 Quark model

The following discussions will be based on a $SU(4) \times SU(3)$ quark model implying that quarks have 4 flavours (u,d,s,c) and 3 colours (blue, red, yellow). One of the main questions will be to clarify if the experimental results are in agreement with the existence of a charm quark, which has been requested to restore quark-lepton symmetrie[106] and to explain the absence of neutral currents in K decay[107].

The colour SU(3) is supposed to be a perfect local symmetry implying that only colour neutral (white) particles can be observed. The following arguments support the existence of a colour-degree of freedom:

1) to explain the spin-statistics of baryons consisting of 3 quarks,
2) to obtain a non-Abelian group,
3) to explain some experimental results, e.g. decay probability of $\pi^0 \to \gamma\gamma$ (factor 3^2) and the ratio $R = (e^+e^- \to \text{hadrons}) / (e^+e^- \to \mu^+\mu^-)$ (factor 3),
4) to understand why particles consist only of $q_1\bar{q}_2$ (mesons) or $q_1q_2q_3$ (baryons).

The quantum numbers of the quarks are

flavour	Q	I_3	S	C	Y
u	2/3	1/2	0	0	1/3
d	- 1/3	- 1/2	0	0	1/3
s	- 1/3	0	- 1	0	- 2/3
c	2/3	0	0	1	- 2/3

and baryon number B = 1/3, spin = 1/2 for all quarks with $Q = I_3 + \frac{1}{2}(B+S+C)$. The SU(4) flavour symmetry is broken by the different quark masses.

Since experimental results on charmed baryons are still rather scarce, only mesons will be discussed. They consist of a quark and an antiquark. This leads to the group theoretical reduction

$$(4) \times (4) = 8 + 1 + 3 + \bar{3} + 1$$

with C = 0, 0, -1, +1, 0.

The octett and singlett with charm charge C = 0 correspond to the old SU(3) symmetry. The two tripletts require the existence of 3 particle states with charm C = +1 and -1, respectively. Finally the last singlett is associated with a state $c\bar{c}$, the two charm charges cancel and hence C = 0 ("hidden charm").

1.22 Chromodynamics QCD

QED can be generalized to a gauge field theory with local SU(3) colour symmetry[1]. The interaction between quarks is mediated by gluons in analogy to photons in the electromagnetic case.

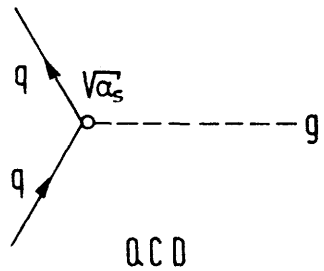

QCD

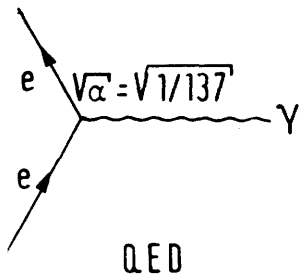

QED

The main differences are:

a) there are 8 massless neutral gluons with a quantum number colour (compared to only one neutral, colourless photon);
b) the coupling constant α_s is a function of the interaction energy E (instead of being a universal constant).

On the basis of very general assumptions one obtains[2)]

$$\alpha_s(E) = \frac{\alpha_s(E_0)}{1 + \frac{25}{12\pi}\,\alpha_s(E_0)\,\ln\,(E/E_0)^2} \qquad (1.1)$$

where E_0 is an arbitrarily chosen normalization energy. The factor $25/12\pi$ is derived from dimensional counting*) and this particular value is associated to 4 quarks. The ln-term corresponds to vacuum polarization in QED.

Equation (1.1) implies that α_s becomes small at high energies (corresponding to small distances) and gets big at low energies (large distances). This has important consequences:

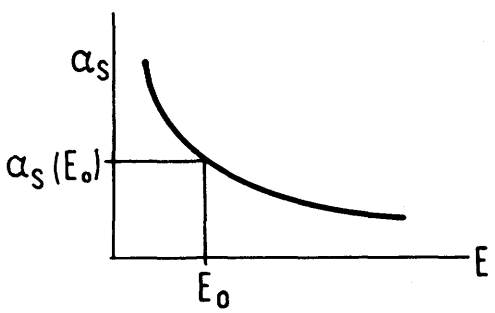

a) Asymptotic freedom: If the distance between two interacting quarks gets very small (the interaction energy is high) the coupling constant $\alpha_s < 1$ and one has a similar situation as in QED. One gluon exchange prevails and perturbation theory can be used. Many of the formulae developed for the hydrogen atom or positronium are applicable.

*) 33 - 2N where N is the number of flavours.

b) Quark confinement (infrared slavery):

At large distances the interaction energy is small and according to (1.1) α_s gets large. The strong coupling might prevent the liberation of quarks since the production of $q\bar{q}$ pairs is more likely. However, it is not yet well understood how this confinement mechanism works and in particular it is not clear whether it can be understood in terms of many gluon exchanges. In the frame work of a locally broken but globally conserved SU(3) colour symmetry free quarks and gluons might exist with quite strange properties[3a].

1.23 Potential models

For the interpretation of the experimental results various potential models have been developed. The choice of the q-q potential is based on the general arguments given above. In particular the Hamiltonian constists of 3 parts [4]

$$H = m_1 + m_2 + p_1^2/m_1 + p_2^2/m_2 + \\ + (\alpha\, Q_1Q_2 - k\,\alpha_s)\; S_{12} \quad + \\ + L(r) \qquad (1.2)$$

The first line is, of course, the free particle term where m_1 and p_1 stand for the masses and momenta of the 2 quarks. The second line is associated to the short range interaction whose radial and spin dependence expressed by S_{12} are assumed to be the same for the Coulomb force and the strong interaction. The only difference is the replacement of the fine structure constant α by α_s of (1.1) and of the electric charges Q_1Q_2 by a colour factor k which is $k = -4/3$ for a $q\bar{q}$ system and $k = -2/3$ for a three quark state.

The third line of (1.2) stands for the long range binding potential. A preferred guess for $L(r)$ is[5]

$$L(r) = a\, r \qquad (1.3)$$

i.e. a linear dependence on r and the constant a has to be determined from experiments. Sometimes[6] a harmonic osciallator potential $L(r) = a\, r^2$ is used instead of (1.3). Practically nothing is known from a theoretical point of view on the spin dependence of $L(r)$ and on the influence of the quark masses. Also

the properties under Lorentz transformations are under question. A first guess might be that L(r) transforms like a Lorentz vector but scalar contributions are possible. Various models differ by the assumptions made for L(r). Recently also logarithmic potentials have been considered[134)135)].

1.231 Standard model[3,5)]

The simplest model is based on the following assumptions:

a) non-relativistic potential (relativistic corrections up to $(v/c)^2$),

b) S_{12} is Coulomb-like, i.e. 1/r-behaviour, spin-spin, L·S and tensor couplings,

c) L(r) = ar, Lorentz vector.

The explicit form of S_{12} is[3,4)]

$$S_{12} = \frac{1}{r} - \frac{\pi}{2}\delta^3(\vec{r})\cdot\frac{4}{3}\frac{\vec{s}_1\cdot\vec{s}_2}{m_1\ m_2} - \frac{1}{m_1 m_2 r^3}\left\{\frac{3(\vec{s}_1\cdot r)\ (\vec{s}_2\cdot r)}{r^2} - s_1\cdot s_2 + \right.$$

$$\left. + (\vec{r}\times\vec{p}_1)\cdot\vec{s}_2 - (\vec{r}\times\vec{p}_2\cdot\vec{s}_1\right\} - \qquad (1.4)$$

$$- \frac{1}{2m_1\ m_2}\left(\frac{\vec{p}_1\cdot\vec{p}_2}{r} + \frac{(\vec{r}.\vec{p}_1)\ (\vec{r}\cdot\vec{p}_2)}{r^3}\right) -$$

$$- \frac{1}{2r^3}\left\{\frac{1}{m_1^2}(\vec{r}\times\vec{p}_1)\cdot\vec{s}_1 - \frac{1}{m_2^2}(\vec{r}\times\vec{p}_2)\cdot\vec{s}_2\right\} - \frac{\pi}{2}\delta^3(\vec{r})\left(\frac{1}{m_1^2} + \frac{1}{m_2^2}\right)$$

The second term in the first line describes the spin-spin interaction giving rise to the hyperfine splitting, the third term gives the tensor and the second line the L × S coupling. The third line originates from relativistic corrections of order $(v/c)^2$. The last line has no classical analog, its origin is the reduction of the relativistic α_i-matrices to the Pauli σ_i spinors.

1.232 More sophisticated models

a) General potential V(r)

Some authors[7,8)] consider a more general r-dependence of the potential V(r) than the Coulomb like 1/r. In this case the gluon propagator has to be modified

$$\gamma_{1\mu}\ \gamma_2^{\mu}\cdot\frac{1}{k^2} \rightarrow \gamma_{1\mu}\ \gamma_2^{\mu}\ v(k^2)$$

where $v(k^2)$ is the Fourier transform of V(r).

For simplicity S_{12} is given only for the case of equal masses of the two interacting quarks:

$$-\frac{4}{3}\,\alpha_s\,S_{12} = \frac{1}{3m^2}\left(\frac{d^2V}{dr} - \frac{1}{r}\frac{dV}{dr}\right)\left[\vec{s}_1\cdot\vec{s}_2 - 3\,(\vec{s}_1\cdot\hat{r})\,(\vec{s}_2\cdot\hat{r})\right]$$

$$+\frac{2}{3m^2}\,(\vec{s}_1\vec{s}_2)\,\nabla^2 V(r) \qquad (1.5)$$

$$+\frac{3}{2m^2}\left(\frac{1}{r}\frac{dV}{dr}\,(\vec{r}\times\vec{p})\,(\vec{s}_1+\vec{s}_2)\right.$$

$$+ \text{ spin independent terms}$$

The spin independent terms are the same as in (1.4), last two lines.

For $V(r) = -\alpha_s/r$ equ. (1.5) is transformed into (1.4). If the "naive" potential $V(r) = -\alpha_s'/r + ar$ is chosen then the confining potential contributes automatically to spin dependent effects.

The level ordering for quite general classes of potentials has been studied by Grosse and Martin[8b].

b) Lorentz properties of L(r)

Since very little is known about the long range potential L(r) it cannot be taken for granted that it behaves like a Lorentz vector. A more general ansatz is a mixture between vector and scalar [9,10]

$$L(r) = L_1(r)\,\gamma_{1\mu}\,\gamma_2^{\mu} + L_2(r)\,\mathbb{1}_1\cdot\mathbb{1}_2 \qquad (1.6)$$

where $\mathbb{1}_i$ are unit matrices.
For a linear potential

$$L(r) = (K_v\cdot\gamma_{1\mu}\,\gamma_2^{\mu} + K_s\cdot\mathbb{1}_1\,\mathbb{1}_2)\,r \qquad (1.7)$$

where the constants K_v and K_s determine the mixing ratio.

c) Anomalous Pauli coupling

In analogy to the anomalous magnetic moment it might be considered that quarks possess anomalous gluon couplings[11]. This implies that one makes the following substitution

$$\gamma_\mu \to \gamma_\mu + \frac{\varkappa}{2m}\,\sigma_{\mu\nu}\,k_\nu$$

where $\varkappa$ is the anomalous moment. As a result expression (1.5) has to be modified in the following way:

$$
\begin{aligned}
-\frac{4}{3}\,\alpha_s\,S_{12} = {} & \frac{(1+\varkappa)^2}{3m^2} + (\text{tensor term}) \\
& + \frac{2(1+\varkappa)^2}{3m} + (\text{spin-spin term}) \\
& + \frac{3}{2m^2}\left(1+\frac{2\varkappa}{3}\right) + (L\cdot S\text{-term}) \\
& + \text{unchanged term.}
\end{aligned}
\tag{1.8}
$$

From these coefficients it follows immediately that an anomalous coupling $\varkappa$ has a larger influence on the tensor and spin-spin terms than on the L·S-coupling.

Some people question why a fundamental structureless particle like a quark should have anomalous couplings. It does not seem clear if they could arise from higher order gluon terms[12]. However, some confinement mechanisms seem to require $\varkappa \neq 0$. For example the MIT bag[13] requires $(1+\varkappa) \to 0$ if the quark mass $m \to 0$.

d) Coupled decay channels

For a bound system like charmonium the decay channels above the binding energy (e.g. $c\bar{c} \to c\bar{u} + u\bar{c}$) are neglected in the first approximation. However, just below the dissociation threshold the virtual channels can modify the bound state. Such corrections have been calculated[5,14].

e) Annihilation graphs

In the charmonium system virtual transition $c\bar{c} \to \gamma \to q_i\,\overline{q_i}$ are possible, where q_i are other than c-quarks. These virtual transitions effect the bound $c\bar{c}$ state and lead to non-negligible corrections[14].

The influence of the improvements of the standard model will be discussed below for particular measurable quantities like level splittings, transition probabilities, etc.

1.24 Group theoretical models

Since the potential models are not relativistically invariant, even if relativistic corrections are included, some authors derive level schemes from group theoretical models. The group O(4) for example corresponds to the relativistic dynamics of charmonium[15]. Also broken SU(4) has been investigated[16].

These models yield level schemes with quantum numbers which differ from the standard model. However, it seems that they did not really help to solve some of the difficulties which will be discussed below and hence these models will not be discussed further.

2. MASS SPECTRA

Experimentally the masses of the new particles are determined by three classes of measurements (chap. 1.13):

1. Peaks in the cross section for $e^+e^- \to$ hadrons as function of the c.m. energy (fig. 8b). Since in this case the virtual photon is converted into the resonance, its quantum numbers must be the same, i.e. only $J^P = 1^-$-particles can be detected in this way. As is well known, the J/ψ, ψ' and the masses of higher excited states where determined in this way. For bound states the resonances are very narrow (narrower than the experimental resolution of a few MeV), whereas above the $D\bar{D}$ production threshold the resonances are several hundred MeV wide.
2. The masses of particles with other quantum numbers can be found as invariant masses calculated from the momenta of their (charged) decay products (fig. 1.7c).

   If the resonance decays into the particles 1 and 2 whose momenta enclose the angle Θ one finds the invariant mass of the resonance from

$$M^2_{inv} = m_1^2 + m_2^2 + 2\{E_1E_2 - |p_1|\,|p_2|\cos\Theta\} \qquad (2.1)$$

   Since a priori it is not known which particles in the final state originate from one resonance, one has to try all possible combinations. The wrong combinations and pure phase space decays produce a slowly varying background in the distribution of the invariant mass. Experimentally mass resolutions of the order of 20 MeV can be obtained. Sometimes the identification of the particles in the final state is not or only partially possible (e.g. π-K separation). In such a case the wrong assignment of a particle mass to a certain track leads to "kinematic reflections" in the distribution of invariant masses.

A few special cases are of particular interest. If the decaying system with mass M_o is at rest $\vec{p}_1 = -\vec{p}_2 = \vec{p}$ hence the Q-value of the decay is given by

$$Q = M_o - m_1 - m_2 = p^2 \{ \frac{1}{m_1 + \sqrt{p^2 + m_1^2}} + \frac{1}{m_2 + \sqrt{p^2 + m_2^2}} \}. \qquad (2.1a)$$

For $p << m_1, m_2$ the Q value is proportional to p^2 and hence a comparatively crude measurement of the momentum yields quite accurate values of M_o. This procedure is useful if particles are produced just above threshold, e.g. $e^+e^- \rightarrow \psi(3.77) \rightarrow D\bar{D}$.

If a particle moving with momentum $\vec{p}$ decays into 2 photons the most likely decay is the symmetrical one where the 2 photons have the same energy k and the angle between each photon and p is the same[17]. For this case one finds

$$\cos\Theta/2 = p/2k = (p/2) \cdot \sqrt{m^2 + p^2} \qquad (2.2)$$

where p and m are the momentum and mass of the decaying particle. The symmetrical decay angle Θ is also the minimum angle associated to a particular m and p. A cutt-off in the angle can therefore help to distinguish between different particles.

A special case are decays with 3 photons in the final state, e.g. $J/\psi \rightarrow \gamma X \rightarrow \gamma(X \rightarrow \gamma\gamma)$. Combining (2.1) and (2.2) one obtains for the invariant mass of the X-state

$$M_X = E_o \sin^2(\Theta/2) / (1 + \cos\Theta/2), \qquad (2.3)$$

where E_o is the total energy.
This implies that the mass can be determined from a measurement of the direction of the photons alone and this is still true in the general case of an asymmetric X-decay.

3. If not all of the decay products of a resonance can be detected (either because they are neutral or do not fall into the acceptance of the spectrometer), it is still possible to determine its mass if the resonance in question R_2 (fig.1.7c) is produced together with one other resonance R_1 or particle. From the masses m_i and momenta p_i of the decay products of R_1 the recoiling mass can be calculated.

$$M^2_{recoil} = (E_o - \Sigma \sqrt{p_i^2 + m_i^2})^2 - (\Sigma p_i)^2 \qquad (2.4)$$

If the recoiling mass is associated to a resonance, one finds a peak in the recoil mass distribution.

The results of such experiments are summarized in Table 1. The way how masses and the quantum numbers were determined, will be discussed below when the production and decay mechanisms of the new particles will be described.

Table 1a: Masses of charmonium states

Name	State	Mass (MeV)	Name	State	Mass (MeV)
J/ψ	$1\ ^3S_1$	3096 ± 2	$X \equiv \eta_c$?	$1\ ^1S_0$?	2830 ± 30
ψ'	$2\ ^3S_1$	3684 ± 5	η'_c ?	$2\ ^1S_0$?	3454 ± 7
			χ	$1\ ^3P_0$	3414 ± 4
			P_c	$1\ ^3P_1$	3508 ± 4
			χ	$1\ ^3P_2$	3552 ± 6
ψ''	$3\ ^3S_1$?	4028		$1\ ^3D_1$	3.772 ± 3
		~ 4150			
		4414 ± 5			

Table 1b: Masses of charmed particles

Name	State	Mass (MeV)	
D^o	^1S_o	1863.3 ± 0.9	MARK 1 [1o4]
D^+	^1S_o	1868.3 ± 0.9	
D^{o*}	$^3S_1$	2006 ± 1.5	
D^{+*}	$^3S_1$	2008.6 ± 1.0	
F^+	^1S_o	2030 ± 60	DASP [1o5]
F^{+*}	$^3S_1$	2140 ± 60	

2.1 Masses of $J^P = 1^-$ $c\bar{c}$ states

We now want to compare the experimental mass spectrum of the $c\bar{c}$ system with the theoretical expectations based on the simple models described in chapter 1.2. For the hamiltonian (1.2) one expects a hydrogen (or positronium) -like level scheme, as shown in fig. 2.1. One has different ladders for different angular momenta ℓ and the levels are split due to hyperfine splitting, spin orbit and tensor couplings. For a pure Coulomb potential the 2s and 1p states would be degenerate. Because of the confining term (1.3) in (1.2) the p and d-states are shifted to lower energies. Indeed for a r^2-potential (harmonic oscillator) the 1p-state would lie in the middle between the 1s and 2s-state. The lowest d-state has $J^P = 1^-$ and hence could interfere with the $2s_1$-state, if the shift is large enough.

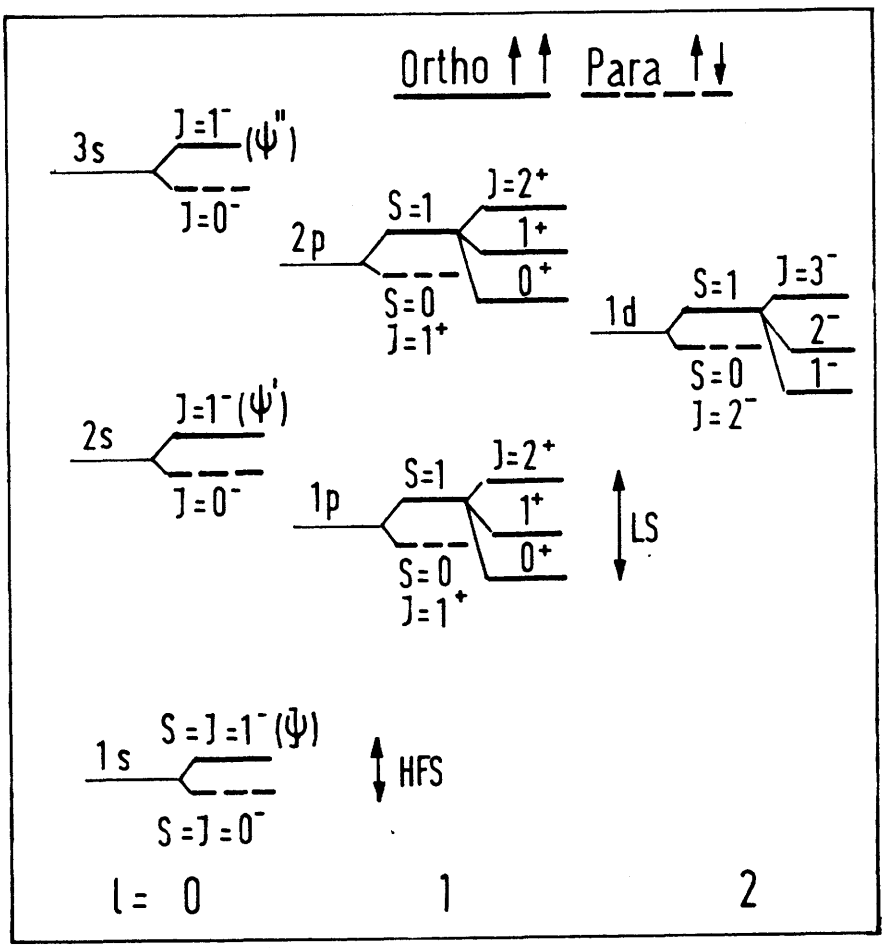

Fig. 2.1: Niveau scheme for charmonium

Soon after the discovery of the J/ψ and ψ' particles several authors solved the non-relativistic Schrödinger equation with the potential

$$V(r) = -\frac{\alpha_s}{r}\left\{1 - \left(\frac{r}{r_o}\right)^2\right\} \qquad (2.5)$$

Identifying J/ψ with the 1^3S_1 and ψ' with 2^3S_1 state the following parameters were found[5]):

$$\alpha_s(3.1\ \text{GeV}) = 0.2,\ r_o = 0.2\text{f},\ m_c = 1.6\ \text{GeV}/c^2$$

These values justify qualitatively the assumptions on which the naive model was based: the coulomb-like part is indeed short range, the coupling constant is smaller than 1 and the c-quark mass is large (non relativistic Schrödinger equation). On the basis of these parameters the masses of higher lying non-bound resonances were predicted[14]).

state	prediction	exp. (Table 1a)
1^2D_1	3.75	3.77
3^3S_1	4.2	4.15
3^3D_1	4.6	4.41

Keeping in mind the simplicity of the model, these predictions are extraordinary impressive. The difference between prediction and epxeriment for the two highest states can be attributed to neglecting coupled channels[14]) (see 1.232).

2.2 HFS-Splitting of S-levels

Because of the spin-spin coupling the states with opposite and parallel spins are split. If the X-particle found by DASP is identified with the 1^1S_o state (usually called η_c) and the resonance at 3.45 GeV with the 2^1S_o state (η_c') (table 1a) one finds the splittings

$$\Delta(\psi - \eta_c) = 266\ \text{MeV}, \qquad \Delta(\psi' - \eta'_c) = 230\ \text{MeV}.$$

These large splittings have been considered for quite some time as a major difficulty for the charm of model, since most calculations produced much smaller splittings.

If the spin-spin coupling is associated only to the short range part of the potential, one finds

a) for Coulomb-potential[7,8] $V(r) = -\frac{4}{3}\alpha_s/r$

$$\Delta M_{HFS}^{short} = \frac{32\pi\,\alpha_s}{m_1\,m_2}\,|\psi(0)|^2 \tag{2.6}$$

where m_1, m_2 are the masses of the bound quarks and $\psi(0)$ is the wave function at the origin.

b) for general short range potential $V(r)$[7,8]

$$\Delta M_{HFS}^{short} = \frac{2}{3\,m_1 m_2} < \nabla^2 V(r) > \tag{2.7}$$

c) If spin-spin coupling is assumed to exist also for the long range part of the potential, one obtains[18] for $V(r) = ar$

$$\Delta M_{HFS}^{long} = \frac{4}{3}\,\frac{(1+\varkappa_1)\,(1+\varkappa_2)}{m_1 m_2}\,a\,\left\langle\frac{1}{r}\right\rangle \tag{2.8}$$

Here anomalous couplings $\varkappa_1$, $\varkappa_2$ (see 1.232) for the long range force have been included. The total splitting is

$$\Delta M_{HFS} = \Delta M_{HFS}^{short} + \Delta M_{HFS}^{long} \tag{2.9}$$

2.21 Splitting of charmonium states

The experimental ratio $R_{HFS} = \Delta(\psi - \eta_c)\,/\Delta(\psi' - \eta_c') = 1.2$. According to (2.6) one has $R_{HFS} = |\psi(0)|^2_{\psi}/|\psi(0)|^2_{\psi'}$. The functions at the origin of the J/ψ and ψ' particles can be inferred from their leptonic decay widths and one finds $R_{HFS} = \Gamma_{\psi}(e^+e^-)/\Gamma_{\psi'})e^+e^- = 3.9/2.4 = 1.6$. The agreement is not so bad and supports the simple model.

For the absolute values of ΔM_{HFS} on the other hand one calculates much too small numbers on the basis of the standard model. Splittings of about 30 to 80 MeV were obtained[2,3,4,7] depending on various assumptions and on different values of $\psi(0)$. Using a more general potential $V(r)$ the splitting could be increased[8] to $\Delta(\psi - \eta_c) = 120$ MeV and $\Delta(\psi' - \eta_c') = 92$ MeV, still factors of 2 too small. With special potentials the right values could be derived but this leads to unnatural conditions for the leptonic decays[19].

The easiest way to explain the experimentally found HFS-splitting seems to be anomalous gluon couplings analogous to the anomalous magnetic moments.

Schnitzer[18] assumed that this coupling is small for the light quarks ($\varkappa_u$, $\varkappa_d \approx 0$) but appreciable for the charm quark ($\varkappa_c \approx 1$). With such a large $\varkappa_c$ the HFS-splittings and also the LS-splitting of the P-levels come out somewhat too big[11] *). A value $\varkappa_c \approx 0.4$ i.e. $(1 + \varkappa_c)^2 \approx 2$ in equ. (2.8) reproduces the experimental results better.

Recently it has been shown[62] that instantons may generate a spin-spin interaction between quarks. Here small quantum fluctuations about the perturbation-theoretic vacuum are replaced by a coherent superposition of vacua with different topological character. A quantitative estimate of these effects shows that the splitting between J/ψ and η_c may be dominated by them and this splitting might be a direct evidence for the existence of instantons.

2.22 Splitting of D and F mesons

It is very interesting to apply the idea of anomalous moments to the D and F mesons. From (2.5), (2.7) and (2.8) one derives

$$\Delta(D^*\text{-}D) = (100\pm30)\ \text{MeV} + (1+\varkappa_u)\,(1+\varkappa_c)\ 114\ \text{MeV}$$
$$\Delta(F^*\text{-}F) = (65\pm20)\ \text{MeV} + (1+\varkappa_s)\,(1+\varkappa_c)\ 144\ \text{MeV}. \qquad (2.1o)$$

Since in the meantime the experimental HFS-splittings of the charm mesons became known (table 1b) one can derive information on the $\varkappa_i$ from (2.1o). With $\Delta(D^*\text{-}D) = 145.3$ MeV and $\Delta(F^*\text{-}F) = (120\pm40)$ MeV one finds $(1+\varkappa_u)/(1+\varkappa_s) \approx 1$ and $1+\varkappa_c \approx 1.4$ as needed to explain the charmonium splittings (2.1o) yields $(1+\varkappa_u) \approx (1+\varkappa_s) \lesssim 0.25$. As a consequence the anomalous coupling is small for particles consisting of light quarks since $(1+\varkappa_u)^2 \approx (1+\varkappa_s)^2 \lesssim 0.06$; it contributes somewhat for the charmed mesons D and F since the mixed terms are of order $(1+\varkappa_u)\,(1+\varkappa_c) \approx (1+\varkappa_s)\,(1+\varkappa_c) \approx 0.3$ and it is most important for charmonium because $(1+\varkappa_c)^2 \approx 2$. It seems surprising that $1+\varkappa_u$ and $1+\varkappa_s$ should be so small. However, this fits very nicely with some ideas about quark confinement. For the MIT bag it has been shown[13] that $(1+\varkappa) \to 0$ if $m \to 0$ and hence it seems plausible that $1+\varkappa$ is small for the light quarks. Of course it would be nice if the anomalous gluon coupling could be derived from higher oder terms in analogy to g-2 of the electron. The lowest

*) $\Delta(\psi\text{-}\eta_c) = 300$ MeV, $\Delta(\psi'\text{-}\eta_c) = 250$ MeV,
$\Delta(^3P_2\text{-}^3P_1) = 125$ MeV, $\Delta(^3P_1\text{-}^3P_0) = 141$ MeV.

terms give[12] $1+\varkappa \approx 1 + (4/3)(\alpha_s/2\pi) = 1.04$ which is much too low. The matter gets quite complicated if the long range behaviour is included. In that case divergencies appear and arbitrary cut-offs have to be made.

Fritzsch[20] also considered the possible existence of anomalous gluon coupling and taking the analogy serious between colour and electromagnetic moments he derived:

$$\frac{\Delta(F^* - F)}{\Delta(D^* - D)} = \frac{\mu_s}{\mu_u} = \frac{-3\mu(\Lambda)}{\mu(p)} \qquad (2.11)$$

where the μ are the total magnetic moments. With $\mu(p) = 2.79$ and $\mu(\Lambda) = -0.67 \pm 0.06$ one expects for the ratio (2.1o) the value 0.72 ± 0.06 which is in excellent agreement with the experimental ratio $120/145 = 0.82 \pm 0.3$.

Finally it should be remarked that the introduction of an anomalous gluon coupling does not change the electromagnetic transition rates since the gluons carry no electric charge.

The splitting between the charged D^+ and the neutral D^o meson has been estimated by various authors. If the isospin breaking is calculated with a non-relativistic model[23] one finds $D^+ - D^o \approx 15$ MeV, whereas a more refined model[24] yields a value of 6.5 MeV in excellent agreement with the experimental value 5.1 ± 2.8 (see table 1b).

2.3 Splitting of P-states

Let us now turn to the splitting of the triplett P states which is associated to L·S and tensor couplings (see 1.23). For these states the quark spins are parallel and therefore the total spin $S = 1$ couples with the orbital angular momentum $\ell = 1$ to total spins $J = 0, 1, 2$. From equation (1.5) one can derive the following expressions for the masses of the triplett P-states:

$$
\begin{aligned}
{}^3P_2 &= A + B - \tfrac{2}{5} C \\
{}^3P_1 &= A - B + 2\,C \\
{}^3P_0 &= A - 2B - 4\,C
\end{aligned}
\qquad (2.12)
$$

with $B = \frac{3}{2m^2} \left\langle \frac{1}{r} \frac{dV}{dr} \right\rangle$ LS-term

$C = \frac{1}{12m^2} \left\langle \frac{1}{r} \frac{dV}{dr} - \frac{d^2V}{dr^2} \right\rangle$ Tensor-term

A arises from the S·S-term and the spin independent terms. It is useful to define the ratio

$$R_P = \frac{{}^3P_2 - {}^3P_1}{{}^3P_1 - {}^3P_0}$$

which assumes the following values:

	R_p
short range Coulomb potential (like positronium)	4/5
standard potential (2.4)	1.2
linear potential	1.4
harmonic oscillator potential (C = 0)	2

For the potential (1.5) the possible range is $0.8 \leq R_p \leq 1.4$.

From table 1a one deduces from the experimental masses

$$\left.\begin{aligned} {}^3P_2 - {}^3P_1 &= 44 \text{ MeV} \\ {}^3P_1 - {}^3P_0 &= 94 \text{ MeV} \end{aligned}\right| \quad R_p = 0.47.$$

This presents a serious difficulty since this value is outside the theoretically acceptable range. From the experimental splittings and (2.12) one finds $C/B \approx 0.3$ implying that Tensor forces have to be taken into account.

Difficulties arise not only for the ratio R_p but also for the absolute values of the splittings. Associating the spin effects only to the short range Coulomb potential gives splittings which are more than factors 5 too small[3]. Including the long range potential one obtains[3,5,14] about the right value for the ${}^3P_2$-${}^3P_1$

difference but the ratio R_p comes out wrong. The coupling to decay channels[14] and anomalous moments have little effect (see 1.232) and cannot explain the big discrepancy in R_p.

The only way proposed so far to remedy this difficulty is the assumption that the long range potential L(r) is not a Lorentz-vector but contains scalar contributions[21] (see 1.232 equ. 1.7). In this case the ratio R_p can have any value. Indeed for a pure scalar L(r), i.e. $K_v = 0$ in equ. (1.7) the ordering of the ^3P states is reversed, with the $^3P_0$ being the highest state, unless unreasonable values of α_s are permitted[22]. The experimental ratio $R_p \approx 0.5$ is reproduced[21] with $K_s/(K_s + K_v) \approx 0.8$ implying that the long range potential is mainly scalar. It should be noted, however, that $K_s \neq 0$ reduces the HFS splittings.

A few additional remarks will close the subject of mass splittings. The singlett P-state $^1P_1$ is expected to coincide with the center of gravity of the ^3P states. The $^1P_1$ state has not been seen yet; since being a 1^+ state it cannot be produced directly in the e^+e^- annihilation and is also hardly accessible by decays from higher states.

The 1^3D_1-state is expected to be suppressed by spin effects and coming close to the 2^3S_1 these two states are likely to interfere. This will be discussed further in chapter 4.1.

2.4 Summary of mass spectra

a) Experimentally almost all of the levels predicted by the charm model have been seen. The $^1P_1$ state is still missing but this fact is easily to be explained.
The existence of the X particle at 2.83 GeV is now well established and its mass value poses no serious problem. Its identification with the 1^1S_0 state, however, creates some troubles as far as decay rates are concerned (see 3.1).
The nature and existence of the state at 3.45 GeV has to be verified and its interpretation as 2^1S_0 is in question.

b) The potential $V(r) = \alpha_s/r + ar$ describes quite well the position of the bound charmonium states as well as the charmed particles. Indeed, some spectacular predictions could be made. Corrections due to coupled decay channels and virtual transitions are not negligible.

c) The HFS-splitting for the charmonium states and the D and F mesons can be understood in a common way if anomalous gluon ("magnetic") moments are introduced for the long range force. Alternatively this splitting might be explained in terms of instantons.

d) The experimental splitting of the triplett P-states can be reproduced by L.S and tensor couplings, however, the long range potential has to be a mixture between Lorentz vector and scalar, the latter being predominant.

In conclusion it might be said that it is quite astonishing how well the simple potential models are able to explain or at least correlate the experimental data. The predictions made and verified by experiments are particularly impressive.

Of course, many detailed questions are still to be answered. It can be hoped that more experimental and theoretical work will provide us with very interesting information on the forces between two quarks. In particular more knowledge on the long range binding potential will be valuable.

3. Hadronic and Radiative Decays of Charmonium

3.1 Possible decay modes of charmonium

The charm charge is expected to be conserved by the strong interaction like isospin and strangeness. Consequently there are only 3 possibilities for the charmonium system $c\bar{c}$ to decay.

a) The c and $\bar{c}$ quark separate and pick up another light quark pair to form a pair of charm particles, e.g. $c\bar{c} \to (c\bar{u}) + (\bar{c}u)$. The charm particle with the lowest mass is the D_0 with $m(D^0) = 1864$ MeV. The threshold for this decay is therefore E = 3728 MeV and the decays $J/\psi \to D\bar{D}$ and $\psi' \to D\bar{D}$ are forbidden by energy conservation. The disintegration of higher states into charm particles will be discussed in chap. 5.

b) Another possibility is that $c\bar{c}$ annihilates with the emission of gluons or photons depending whether we are dealing with a strong or electromagnetic decay. As in the case of positronium, a system with J = 0 can decay into 2 photons or gluons. The 2 photons can be real and such decays have been observed e.g. $X(2.83\ \text{GeV}) \to \gamma\gamma$. The 2 gluons will be transformed into hadrons and cannot be observed directly. However, for high mass states the 2 gluons are expected to appear as 2 hadron jets.
A system with J = 1 couples to 1 virtual photon or 3 gluons (compare the decay of ortho positronium into 3 real photons).

c) If the $c\bar{c}$-system is not in its ground state it can cascade down by emitting a photon or gluons with the $c\bar{c}$-system staying together.

Diagrams for the various possibilities are shown in fig. 3.1a and b. The $c\bar{c}$ states are bound by the exchange of many "soft" gluons. Since the energy of the gluons is low their coupling to the quarks given by $\alpha_s(E)$ is large (see 1.22).

If a virtual photon is emitted it can couple either to a lepton pair or a quark pair. These processes are proportional to $\frac{2}{3} e^2 \sim \frac{2}{3}\alpha$ since the coupling of the photon is proportional to the charges of the particles attached to the photon.

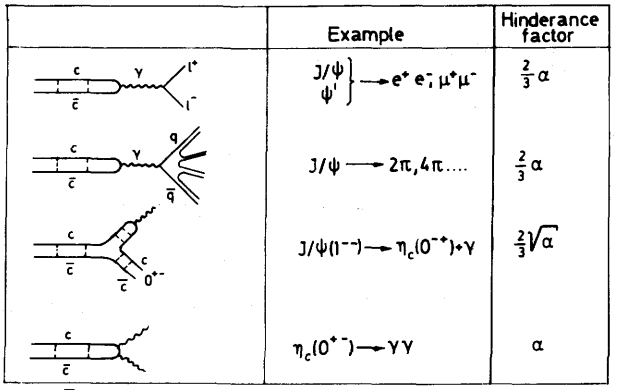

a) Electromagnetic decays of bound charmonium states

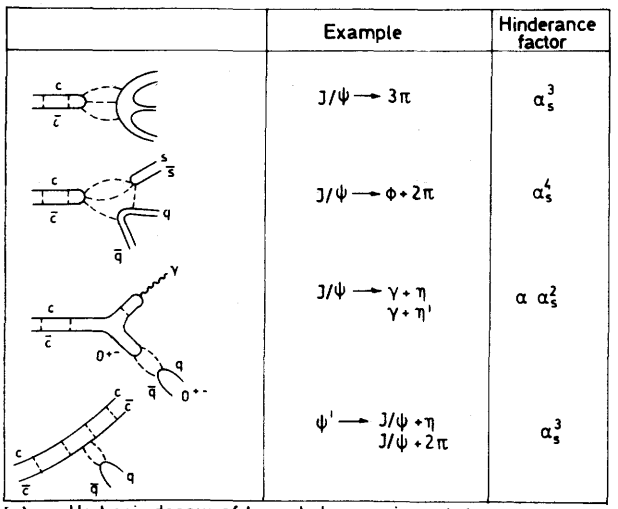

b) Hadronic decays of bound charmonium states

Fig. 3.1 a and b

If gluons emerge from the $c\bar{c}$ annihilation they couple to light quarks. Each of these gluons carries an appreciable fraction of the total energy ("hard gluons") and hence the coupling $\alpha_s(E)$ is small. As a consequence these processes are suppressed and the hinderance factor is determined by the number of exchanged gluons (again in complete analogy to QED).

3.2 Decays of J/ψ and ψ' (vector particles)

Vector particles with $J^{PC} = 1^{--}$ couple to the photon and hence can be produced directly in e^+e^- annihilation (see Fig. 1.7b). As is well known the J/ψ besides having been detected in p + Be → e^+e^- + anything at BNL[25], has been found at SPEAR[26] and soon later the ψ'[27]. The decay of these particles was investigated extensively at SPEAR[28] and at DORIS[29]. Since detailed summaries[28,29] have been published only the main points will be considered here.

3.21 Determination of total and leptonic decay widths

The width of the resonances turns out to be much narrower than the experimental resolution determined by the momentum smearing of the colliding e^+e^- beams which is about 1 to 2 MeV. But the true widths can be determined by a "trick". Assuming that the production cross section can be described by a Breit-Wigner formula we have for the process $e^+e^- \to J/\psi \to$ final state

$$\sigma_f = \frac{\pi(2J+1)}{m^2} \cdot \frac{\Gamma_{ee}\,\Gamma_f}{(E-m)^2 + \Gamma^2/4} \tag{3.1}$$

where m is the J/ψ mass, J its spin, Γ_{ee}, Γ_f are partial and Γ the total decay widths.
Integrating (3.1) over the energy E one obtains (with J = 1)

$$\Sigma_f = \int \sigma_f \, dE = \frac{6\pi^2}{m^2} \frac{\Gamma_{ee} \cdot \Gamma_f}{\Gamma} \tag{3.2}$$

If the three final states e^+e^-, $\mu^+\mu^-$ and hadrons are measured independently, one can solve for the widths Γ_{ee}, $\Gamma_{\mu\mu}$ and $\Gamma = \Gamma_h + \Gamma_{ee} + \Gamma_{\mu\mu}$. Since Γ_{ee} and $\Gamma_{\mu\mu}$ are found to be small compared to Γ_h one has $\Gamma_h \approx \Gamma$ and from (3.2)

$$\Gamma_{ee} = \frac{m^2}{6\pi^2} \Sigma_h$$
$$\Gamma \approx \Gamma_h = \frac{\Sigma_h}{\Sigma_{ee}} \cdot \Gamma_{ee} \quad . \tag{3.3}$$

The integrals Σ_h and Σ_{ee} (and $\Sigma_{\mu\mu}$) are found by integrating the experimental cross section for the proper channel over the energy E. It is assumed that because of the limited experimental resolution the resonance curve is widened but the area is not changed.However, the integrated cross section has to be corrected for

radiative effects[29] which amounted to about 40 %. The results are shown in table 3.1. Particularly striking are the narrow total widths which indicate the effectiveness of a new selection rule, i.e. charm charge conservation. As explained above, the $c\bar{c}$-system can only decay by higher order processes involving hard gluons or photons and which therefore are hindered (see fig. 3.1).

Table 3.1 Resonance parameters of J/ψ and ψ'

		ψ/J			ψ'	
		SPEAR[30]	DORIS[31,32]	ADONE	SPEAR[27]	DORIS[31,32]
m	(MeV)	3095 ± 4 *)	3096 ± 2	3103 ± 6	3684 ± 5	3687 ± 2
Σ_h	(μb MeV)	10.4 ± 1.5	9.7 ± 1.2	9.6 ± 1.7	3.7 ± 0.6	3.06 ± 0.34
Σ_{ee}	(nb MeV)	790	965 ± 141	790 ± 200		
$\Sigma_{\mu\mu}$	(nb MeV)		870 ± 100			
Γ_{tot}	(keV)	69 ± 15	87 ± 20	67 ± 25	228 ± 56	
Γ_{ee}	(keV)	4.8 ± 0.6		4.6 ± 0.8	2.1 ± 0.3 **)	
$\Gamma_{\mu\mu}$	(keV)	4.8 ± 0.6	6.0 ± 0.7	4.6 ± 1.0		

*) corrected value

**) assuming $\Gamma_{ee} = \Gamma_{\mu\mu}$

3.22 Determination of quantum numbers and discussion of hadronic decays

The most direct evidence for the photon-like quantum numbers of J/ψ and ψ' is an observation of the interference between $e^+e^- \to \gamma \to \mu^+\mu^-$ and $e^+e^- \to \psi \to \mu^+\mu^-$. The cross section is given by

$$\frac{d\sigma}{d\Theta} = \frac{9\pi}{8E^2}(1 + \cos^2\Theta)\left|-\frac{2\alpha}{3} + \frac{\Gamma_{ee}}{m - E - i\Gamma/2}\right|^2 \qquad (3.4)$$

implying destructive interference below and constructive interference above the resonance at m. The data are presented in fig. 3.2 and clearly indicate the pre-

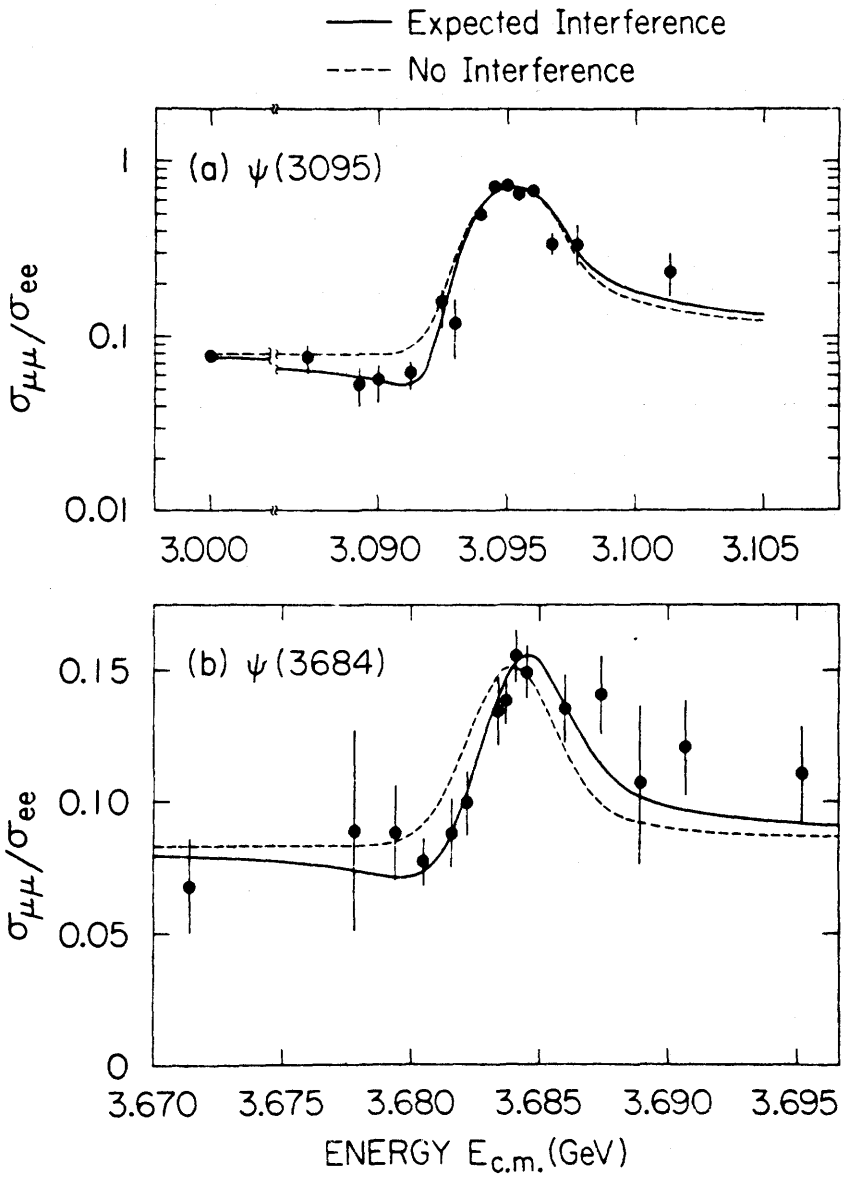

Fig. 3.2

sence of the interference[28]. Thus the assignment $J^{PC} = 1^{--}$ for J/ψ as well as ψ' is proven. It is corroborated by measurements of the angular dependence of e and μ emission.

More than 30 decay channels J/ψ → hadrons have been observed. They will not be discussed here since an extensive review has been published previously[28] (Appendix 1).

The main conclusions drawn from the hadronic decays of the J/ψ are the following. The J/ψ decays preferentially into final states with an odd number of π. The relation $C = (-1)^I \cdot G$ together with G = C = -1 implies[28,29] isospin $I^G = 0^-$, excluding I = 2 by the observed decay J/ψ → pp̄. The fact that J/ψ also decays into an even number of pions violating isospin can be understood quantitatively on the basis that the J/ψ couples to the photon.

The isospin and G-parity of ψ' can be inferred from the cascade decays ψ' → J/ψ + ππ and ψ' → J/ψ + η which account for 57 ± 8 % of the ψ' decays. For example the experimental ratio $(J/\psi \to \pi^0\pi^0) / (J/\psi \to \pi^+\pi^-) = 0.49 \pm 0.09$ has to be compared with the theoretical predictions 0.5, 0 and 2 for the isospin of the ππ system I = 0,1 and 2, respectively. So clearly the pions have I = 0 and consequently ψ' and J/ψ have the same isospin. The close similarity of the J/ψ and ψ' particles is obviously demonstrated by the fact that ψ' → J/ψ + ππ make up about half of all the decays, whereas ψ' → ωππ which has much more phase space is about two orders of magnitude rarer. Also ψ' → J/ψ + π^0 being I-forbidden is not seen whereas ψ' → J/ψ + η is allowed and was observed.

Finally it can be shown that J/ψ and ψ' behave as singletts with respect to the approximate SU(3) symmetry of the 3 light quarks which is expected for a charmonium state. The decays J/ψ → K^+K^- or $K^0\bar{K}^0$ are forbidden for a SU(3) singlett but allowed for an octett state. Indeed the experimentally observed branching ratios for both the J/ψ and ψ' are very small ($\lesssim 10^{-4}$ to 10^{-3}). The SU(3) singlett nature can also be inferred from a comparison of J/ψ → πρ and $K K^*(892)$. In particular DASP results[34,29] indicate that the octett admixture is very small.

Finally one might ask if we understand globally the decays of J/ψ and ψ' or if major decay components are still unknown. By summing up all known decays of J/ψ and adding those channels which can be estimated by I-conservation one arrives at about 70 % of the total decay width. It does not appear unreasonable that the major part of the missing 30 % is due to decays involving η's i.e. $J/\psi \to \eta$ + anything about which very little experimental information is available. Nevertheless a clarification of the situation would be welcome and in particular some channels on the percent level can provide very interesting information (see 3.24).

With respect to the ψ' decays a little more than 50 % are associated to cascade decays $\psi' \to \psi$ + hadrons. The decays to intermediate P-states (see 3.3) sum up to about 30 %. Adding the figure for electromagnetic decays ($\sim$ 5 %) and direct decays into hadrons ($\sim$ 10 %) one arrives[28] at a total of about 95 ± 12 %. Not much room is left here for unknown channels, but again some rare undetected decays might be of interest.

3.23 Discussion of leptonic decays

A 1^{--}-particle can convert to one virtual or 3 real photons. One real photon is forbidden by momentum conservation and 2 photons by charge conjugation. Since the transition via a virtual photon is of lower order it dominates.

The transition probability for $(1^{--}) \to \gamma \to e^+e^-$ is for an s-state and a Coulomb-like potential given by[2,4]

$$\Gamma(1^{--} \to e^+e^-) = 16\pi \frac{\alpha^2 Q^2}{m^2} |\psi(0)|^2 \cdot \qquad (3.5)$$

where Q and m are the charge and mass of the involved quark and $\psi(0)$ is the wave function at the origin (neglecting corrections as from annihilation channels). Taking into account[35] "gluonic radiative corrections" equ. (3.5) has to be multiplied by $\{1 - 16\,\alpha_s / 3\pi\}$. For a general potential (see 1.23) $|\psi(0)|^2$ has to be replaced by $m < dV/dr >$.

In table 3.2 the experimental results of Γ_{ee} are shown together with $|\psi(0)|^2$

as derived[4] according to equ. (3.5). For a "Coulomb" potential $|\psi(0)|^2$ is expected to rise ~ m^3, whereas for a linear potential ~ m. For the ground states the rise is approximately ~ m^2, indicating that the effective potential is somewhere in between "Coulomb" and linear, in full agreement with the standard potential (see 1.23). For a linear potential one expects that m <dV/dr> is the same for the ground and the excited states. This is not true as a comparison for

Table 3.2: Vector meson decays into e^+e^-

Meson	M (GeV)	Q^2	Γ(keV)	$\lvert\psi(0)\rvert^2$ $(GeV)^3\times10^2$
ρ	0.77	1/2	6.5 ± 0.8	0.29
ω	0.78	1/18	0.76 ± 0.17	0.31
ϕ	1.02	1/9	1.34 ± 0.08	0.47
J/ψ	3.95	4/9	4.8 ± 0.6	3.9
ψ'	3.68	4/9	2.1 ± 0.3	2.4
$^3D_1$	3.77	4/9	0.37 ± 0.09	0.44
ψ''	4.15	4/9	1.8 to 3.3	
ψ'''	4.41	4/9	0.44 ± 0.14	0.72

ground states above the line

ψ, ψ' and ψ''' shows. A more detailed analysis for the excited states has been carried out[6] for a harmonic potential and including S and D-wave mixing.

The regularities found for the leptonic widths of the vector meson ground states are useful in identifying new vector particles as the Υ (see chap. 6).

3.24 OZI-forbidden hadronic decays

The Okubo-Zweig-Iizuba[36] rule claims that decays described by connected quark lines are allowed whereas disconnected diagrams are suppressed.

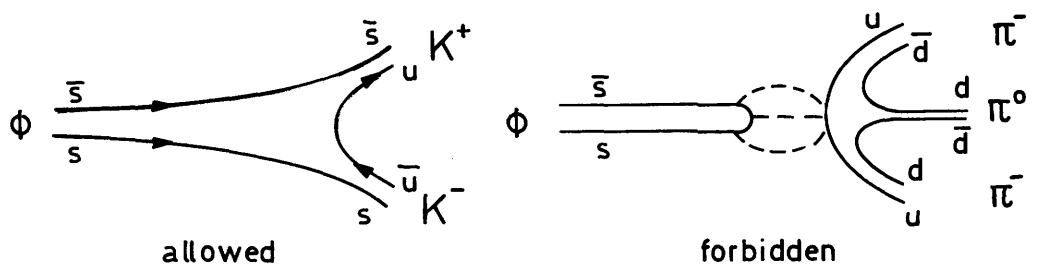

Here the ϕ decay is shown as an example. The decay $\phi \to K^+K^-$ is allowed but $\phi \to \pi^+\pi^0\pi^-$ is associated to a disconnected diagram and hence suppressed. This explains why the K^+K^- decay dominates inspite of its smaller phase space.

The functioning of the OZI-rule can be understood in terms of QCD. In connected diagrams the interaction between quarks is provided by "soft" gluons and hence is strong. In disconnected diagrams "hard" gluons have to be exchanged with $\alpha_s(E)$ being small. If QCD perturbation theory is applicable, the rate of a process involving n "hard" gluons, each carrying an energy E, should be proportional to $\left[\alpha_s(E)\right]^n$. We shall now see if this idea is compatible with experiments.

3.241 Singly disconnected diagrams

A $J = 1^-$ state can decay to 3 real photons as in the case of ortho positronium. In analogy we expect that it can also decay into 3 gluons. (In the electromagnetic case a transition to one virtual photon is also possible. One virtual gluon is excluded, however, because of conservation of colour charge.) Using the well-known expressions for positronium

$$\text{electromagn.} \quad \Gamma(1^- \to 3\gamma) = \frac{64}{9}(\pi^2-9)\frac{1}{m^2}\,|\psi(0)|^2\,\alpha^3 \tag{3.6}$$

and substituting α by α_s applying also a colour factor $\frac{5}{18}$ (see chapt. 1.22) one obtains[2)]

$$\text{strong} \quad \Gamma(1^- \to 3g) = \frac{64}{9}(\pi^2-9)\frac{1}{m^2}\,|\psi(0)|^2 \cdot \frac{5}{18}\,\alpha_s^3\,. \tag{3.7}$$

This offers a possibility to determine α_s. Assuming that the conversion of the 3 gluons to ordinary hadrons goes practically with 100 % probability $\Gamma(1^- \to 3g \to \text{hadrons})$ can be identified with the full hadronic width if connected diagrams are forbidden by energy conservation. This is the case for J/ψ. In the case of the ϕ only the decays into non-strange hadrons must be taken into account and for the ψ' the cascade and the radiative transitions have to be discarded since they do not proceed via a 3 gluon intermediate state.

Instead of using the absolute values of $\Gamma(1^{--} \to 3g \to \text{hadron})$ it is expedient to normalize them to the leptonic decay widths since then the unknown wave function cancels. From (3.5) and (3.7) one obtains

$$\frac{\Gamma\,(1^{--} \to 3g \to \text{hadrons})}{\Gamma\,(1^{--} \to e^+e^-)} = 1410\,\frac{(2/3)^2}{Q^2}\,\alpha_s^{\,3} \qquad (3.8)$$

where Q is the quark charge.
If we now take the experimental data for ϕ, J/ψ and ψ', particles which are almost pure $c\bar{c}$ states, one finds [4]

Table 3.3:

	M (GeV)	Γ_h/Γ_{ee}	α_s	Remark
ϕ	1.1	588	0.47	$\phi \to$ non-strange hadrons *)
J/ψ	3.1	14.4	0.22	
ψ'	3.7	8	0.2	without $\psi' \to J/\psi + \ldots$ $\psi' \to \gamma + \ldots$

The coupling constant α_s indeed decreases with increasing energy as expected in QCD (see 1.22) and is smaller than 1. Hence the application of first order perturbation theory is justified at least qualitatively. Inserting α_s from table 3.3 in (3.7) one derives $\Gamma(J/\psi \to \text{hadrons}) = 72$ KeV which agrees quite well with experiment.

In conclusion it can be stated that we understand in principle the narrow widths of the bound charmonium states on the basis of charm charge conservation and first order QCD perturbation theory. However, other models explaining the OZI-rule could be as satisfactory. In the following and in particular in chapt. 3.3 we shall see that on the basis of QCD one can understand many more experimental results than just the widths of J/ψ and ψ'.

Information on the inhibition by the exchange of hard gluons can also be obtained by comparing inhibited processes to allowed ones, i.e. to decays above threshold not forbidden by charm or strangeness conservation. Such a comparison will be of particular interest for diagrams involving 2 and

*) The reason for the small total width of ϕ is that the OZI-allowed decay $\phi \to KK$ is suppressed by the small available phase space.

3 gluons as for example*)

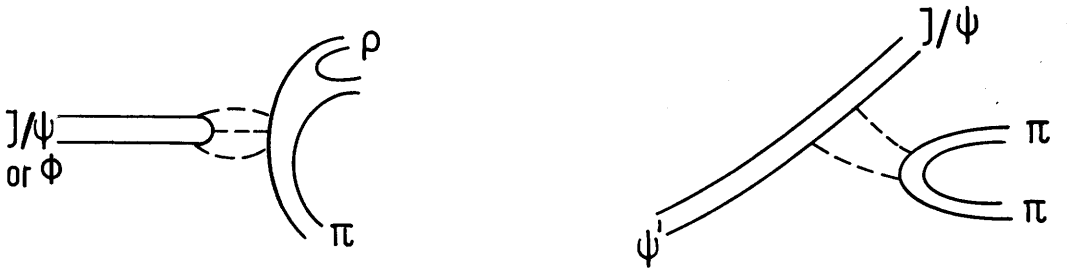

Table 3.4:

Forbidden decay / Allowed decay	Ratio[4] after phase space corr.	number of exchanged gluons	epexted inhibition factor
$J/\psi \to$ hadrons / $\psi(4.4) \to$ hadrons	~ 0.002	3	$\alpha_s^3 = 0.2^3 = 0.008$
$\psi' \to J/\psi\,\pi\pi$ / $\rho' \to \rho\,\pi\pi$	~ 0.013	2	$\alpha_s^2 = 0.2^2 = 0.04$
$\phi \to \rho\,\pi$ / $\phi \to KK$	~ 0.02	3	$\alpha_s^3 = 0.47^3 \approx 0.1$

From this table one infers that indeed $\psi' \to J/\psi\pi\pi$ involving only 2 gluons is less suppresssed than $J/\psi \to$ hadrons**). One cannot expect more than a very qualitative agreement since the gluons in the two cases carry different energies and hence α_s may differ. One further sees that $\phi \to \rho\pi$ is less suppressed than $J/\psi \to$ hadrons but the reason is quite different. Here it is the lower energy resulting in a larger α_s that causes less inhibition.

*) It might be mentioned that $\psi' \to J/\psi + \pi^0$ is forbidden by I-conservation and has not been observed

**) The decay $\psi' \to J/\psi + \eta$ has a large branching ratio[27] $(4.3\pm0.8)\times10^{-2}$ in view of the fact that it is p-wave and SU(3) forbidden, has very little phase space (Q = 40 MeV) and is OZI suppressed. The large decay rate can only be explained by an $c\bar{c}$ admixture to the η (see chap. 3.252) and hence no information on OZI can be obtained.

3.242 Doubly disconnected diagrams

The decay of J/ψ permits even more detailed studies of the mechanism of the OZI rule. Besides the singly disconnected diagrams discussed in the preceding section there exist also doubly disconnected ones. In fig. 3.3 different diagrams are shown which give rise to the decays $J/\psi \to \omega\pi\pi$, $\omega K\bar{K}$ and $J/\psi \to \phi\pi\pi$, $\phi K\bar{K}$. The left and right columns contain the singly and doubly connected diagrams, respectively. The two diagrams in the first line show the $\omega\pi\pi$ and $\phi\pi\pi$ decay without intermediate resonances, whereas the diagrams of the other two lines involve the tensor (2^{++}) particles f and f'. The f contains predominantly u and d quarks and can therefore be connected to the ω whereas the f' is made up essentially of $s\bar{s}$ and hence prefers to decay to $K\bar{K}$.

An interesting question is now whether the fourth gluon in the doubly connected diagrams (not attached to J/ψ) is also a "hard" one implying a suppression α_s^4 or whether it is comparatively soft yielding a hinderance $\sim \alpha_s^3$. An analysis of the experimental data with this aim is complicated, however, since the influence of the intermediate resonances has to be determined. For this reason the overall ratio[28)]

$$\frac{J/\psi \to \phi\pi\pi}{J/\psi \to \omega\pi\pi} = \frac{0.21 \pm 0.09}{1.0 \pm 0.3} \approx \frac{1}{5} \qquad (3.9)$$

is not very conclusive. In order to reduce the influence of intermediate resonances, only events with $M(\pi\pi) > 1$ GeV were selected[38)] and it seems that the suppression of the doubly disconnected $\phi\pi\pi$ decay is then stronger. Some interesting new

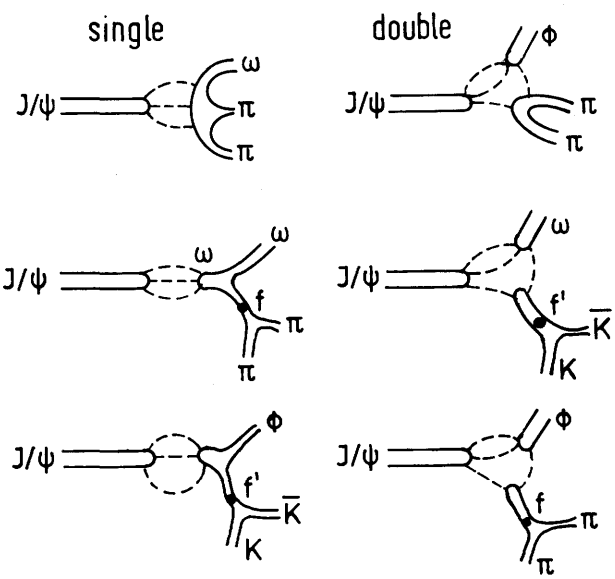

Fig. 3.3

Singly and doubly disconnected quark diagrams

information has recently become available from the PLUTO-collaboration[37]. They have studied the final state $J/\psi \to \pi^+\pi^+\pi^-\pi^-\pi^0$ and could observe the two decays $J/\psi \to B^+\pi^- \to (\omega\pi^+)\pi^- \to (\pi^+\pi^-\pi^0)\pi^+\pi^-$ and $J/\psi \to \omega f \to (\pi^+\pi^-\pi^0)\ (\pi^-\pi^+)$. The corresponding invariant or recoil mass peaks are shown in fig. 3.4. From these the following numbers were deduced.

Final state of J/ψ decay	Branching ratio %	Γ/eV
$\pi^+\pi^-\pi^+\pi^-\pi^0$	3.64 ± 0.52	2548 ± 360
$\omega\pi^+\pi^-$	0.78 ± 0.16	546 ± 110
ω f	0.40 ± 0.14	280 ± 100
$B\pi$	0.28 ± 0.07	196 ± 50

These results imply that most of the $\omega\pi^+\pi^-$ decay width is due to resonance decays. If these are subtracted the branching ratio for non-resonant $\omega\pi\pi$ is of the order of 0.1 % and hence comparable to $\phi\pi\pi$. This is confirmed by selecting only $\omega\pi\pi$ events with $M(\pi\pi) > 1.5$ GeV, thus reducing resonance contributions, and one finds $B\ R(J/\psi \to \omega\pi\pi) < 0.12$ %. These data seem to indicate that the doubly disconnected $\phi\pi\pi$ diagram is not much more suppressed than the simple disconnected $\omega\pi\pi$.

This result is, however, in contradcition to measurements involving the f and f' resonance. It was found[38] that the doubly disconnected decays $J/\psi \to \omega f'$ and ϕf are about a factor of 10 rarer than the singly disconnected decays $J/\psi \to \omega f$ and $\phi f'$.

More experimental work is needed to clarify the behaviour of doubly disconnected diagrams but certainly the decays of charmonium offer an excellent tool to this end.

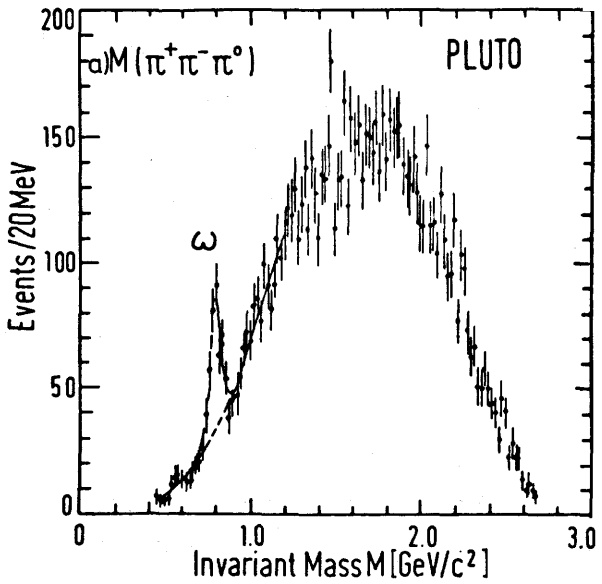

$e^+e^- \rightarrow J/\psi \rightarrow (\pi^+\pi^-\pi^0)\ \pi^-\pi^0$

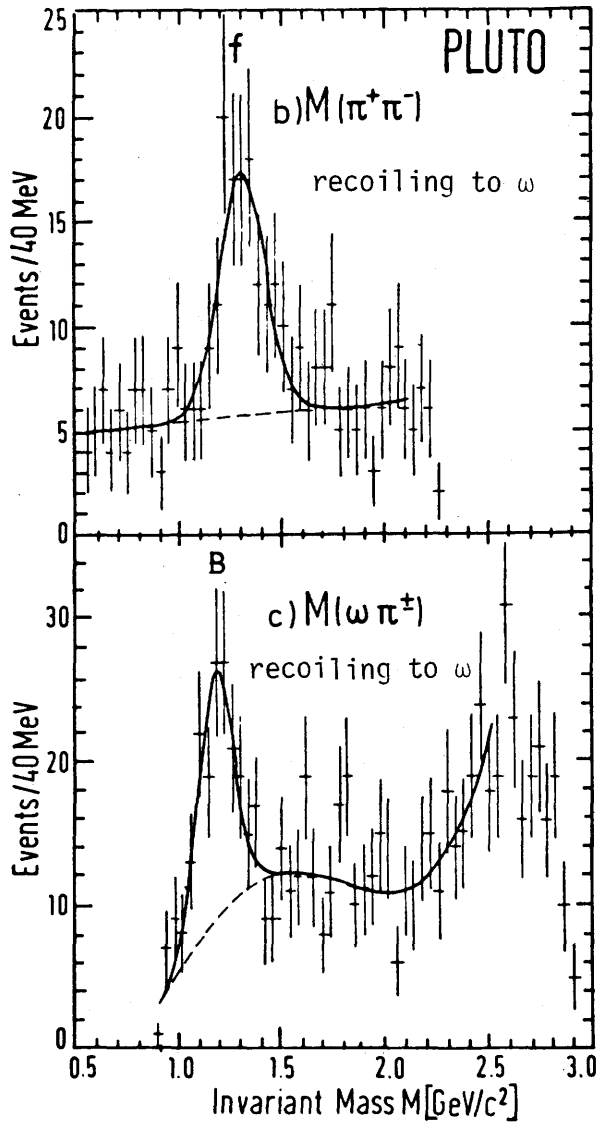

$e^+e^- \rightarrow J/\psi \rightarrow B^+\pi^- \rightarrow (\omega\pi^+)\pi^- \rightarrow (\pi^+\pi^-\pi^0)\ (\pi^+\pi^-)$

$\rightarrow \omega f \rightarrow (\pi^+\pi^-\pi^0)(\pi^+\pi^-)$

Fig. 3.4

3.25 Radiative decays of J/ψ and ψ' to ordinary hadrons

In this section we shall discuss the radiative decays $J/\psi \to \eta\gamma$, $\eta'\gamma$, $\pi^0\gamma$ and $f\gamma$. From these reactions interesting information on the admixture of $c\bar{c}$-states to the ordinary hadrons can be inferred. On the other hand radiative transitions from J/ψ and ψ' to other charmonium states (Pseudo-scalar and P-states) will be dealt with in chap. 3.3 and 3.4. Here the interpretation will be quite different since these transitions take place between practically pure $c\bar{c}$ states. In order to be able to discuss the decays like $\eta\gamma$, $\eta'\gamma$ a few ideas concerning the mixing of quark states have to be recalled (3.252). The puzzle to be explained is the experimental fact that the decays $\eta\gamma$ and $\eta'\gamma$ are more than an order of magnitude more probable than $J/\psi \to \pi^0\gamma$.

3.251 Experimental decay rates ($\eta\gamma$, $\eta'\gamma$ puzzle)

The decays $J/\psi \to \eta\gamma$, $\eta'\gamma$, $\pi^0\gamma$ and $f\gamma$ are two-body decays and hence photons should be monoenergetic. The search for narrow lines in the inclusive photon spectrum at SPEAR was negative[39], but the first 3 decays could be detected at DORIS by investigating the decays with 3 photons in the final state[40,41], e.g. $J/\psi \to \eta\gamma \to (\gamma\gamma)\gamma$ but also in the decay[42] $J/\psi \to \gamma\eta' \to \gamma\,(\gamma\rho^0) \to \gamma\gamma\pi^+\pi^-$. The corresponding invariant mass plots $M(\gamma\gamma)$ show the η and η' peaks (fig. 3.5). and $M(\pi^+\pi^-\gamma)$ show (fig. 3.6) a clear η' peak provided $M(\pi^+\pi^-)$ is restricted to the ρ region.

Very recently the decay $J/\psi \to f\gamma$ could be detected by PLUTO[43] by studying $\pi^+\pi^-\gamma$ final states, i.e. the decay $J/\psi \to f\gamma \to (\pi^+\pi^-)\gamma$. The invariant mass plot $M(\pi^+\pi^-)$ is shown in fig. 3.7. Besides the f peak also the ρ shows up. This peak is attributed to the channel $J/\psi \to \rho\pi^0 \to (\pi^+\pi^-)\ (\gamma\gamma)$ and a branching ratio of $(1.6\pm0.4)\times10^{-2}$ was inferred. Also DASP[50] has observed the $f\gamma \to \pi^+\pi^-\gamma$ final states.

The results are summarized in the following table:

Table 3.5: Radiative decays of J/ψ

Final state	Branching ratio ($\times 10^{-3}$)	Γ(eV)	Experiment
$\eta\gamma$	0.82 ± 0.10	55 ± 12	DASP[40,80]
	1.30 ± 0.4	87 ± 27	DESY-Heidelberg[41]
$\eta'\gamma$	2.9 ± 1.1	152 ±117	DASP[40]
	2.3 ± 0.7	160 ± 50	DESY-Heidelberg[41,42]
$\pi^0\gamma$	0.073 ± 0.047	5. ± 3.2	DASP[40]
$f^0\gamma$	2.0 ± 0.7	138 ± 48	PLUTO[43]

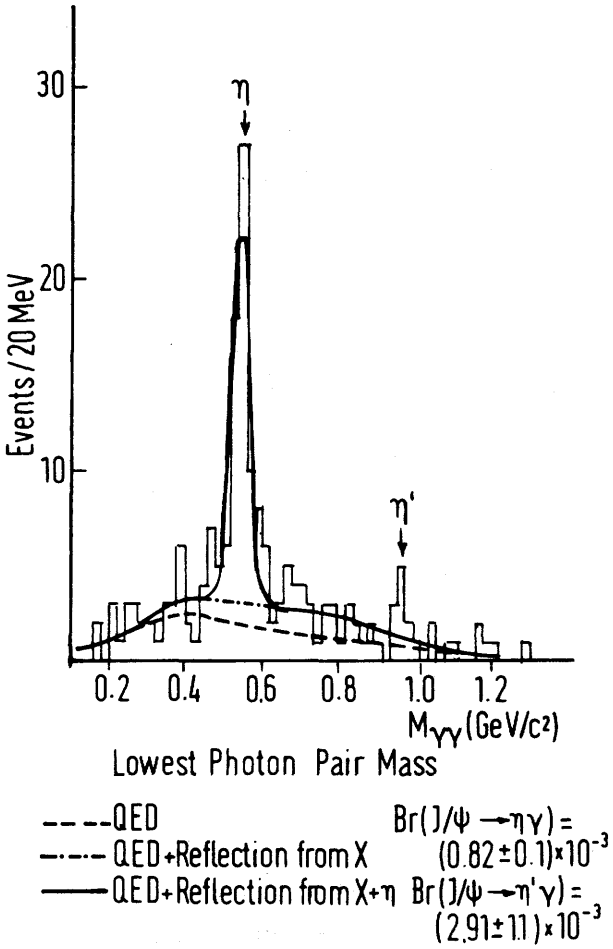

Fig. 3.5 DASP Preliminary
$e^+e^- \to \gamma\gamma\gamma$ at J/ψ
$\sphericalangle\,\gamma\gamma > 30^0$
$J/\psi \to \eta\gamma$
$\hookrightarrow \gamma\gamma$

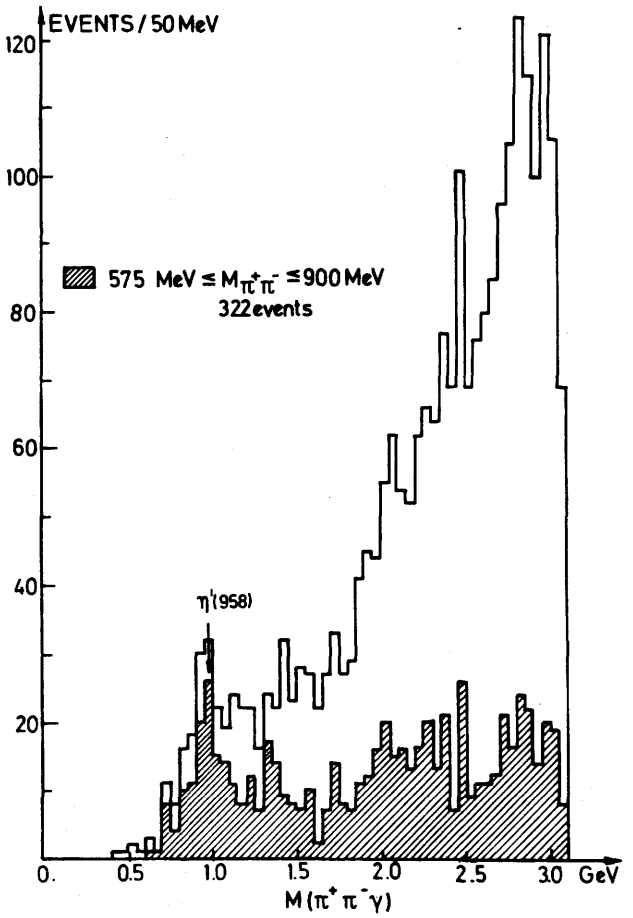

Fig. 3.6 DESY-Heidelberg Preliminary
$J/\psi\ (3.1) \to \pi^+\pi^-\gamma\gamma$
1241 events

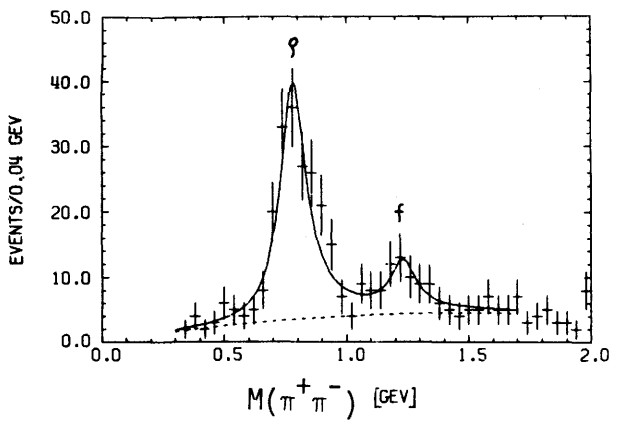

Fig. 3.7 PLUTO Preliminary
$J/\psi \to f\gamma \to \pi^+\pi^-\gamma$
$\to \rho\pi^0 \to \pi^+\pi^-\gamma\gamma$

These figures are quite surprising at first sight. In terms of vector dominance one would expect that $\Gamma(J/\psi \to \gamma\pi^0) \approx (\alpha/\gamma_\rho^2)\ \Gamma(J/\psi \to \rho^0\pi^0) \approx$ 1 eV with $\Gamma(J/\psi \to \rho^0\pi^0) \approx 260$ eV. This order of magnitude agrees with the experimental finding, but why are $\Gamma(J/\psi \to \eta\gamma)$ and $\Gamma(J/\psi \to \eta'\gamma)$ almost two orders of magnitude larger with $\Gamma(J/\psi \to \eta'\gamma) \approx \Gamma(J/\psi \to \rho^0\pi^0)$? And why is the ratio $\Gamma(\eta'\gamma) / \Gamma(\eta\gamma) = 3.5 \pm 1.0$ so large?

A similar argument applies to the $J/\psi \to f^0\gamma$ decay which by vector dominance is related to $J/\psi \to f^0\omega$ with a measured[37,38] branching ratio of $(0.40 \pm 0.14) \times 10^{-2}$. Hence the rate for the final state $f^0\gamma$ should be comparable to $\pi^0\gamma$ but experimentally it is much larger.
As will be discussed in the next section these anomalies can be understood in terms of $c\bar{c}$ admixture to ordinary $q\bar{q}$ states.

Finally it should be mentioned that the corresponding decays $\psi' \to \eta\gamma$, etc. have been looked for but not found[42,27].

3.252 The mixing of $q\bar{q}$ states

The $\eta\gamma$ and $\gamma'\eta$ puzzle and some other experimental results (see chap. 3.3) can only be explained in terms of mixing between $c\bar{c}$ states and $q\bar{q}$ states of ordinary quarks. This mixing can be understood by extending the description of the mixing of ordinary quarks.

It is well known that states of the ordinary vector and tensor mesons are well segregated according to quark flavour. The neutral mass eigenstates exhibiting "ideal mixing" with $(1/\sqrt{2})\ (\bar{u}u \pm \bar{d}d)$ and $\bar{s}s$. As a consequence one expects $M(\omega) = M(\rho)$ and $M(\phi) = 2M(K^*) - M(\rho)$. Both relations are fullfilled on the percent level.

The pseudo scalar mesons on the other hand show a strong mixing between non-strange and strange quarks inspite of their different masses. As a consequence the relations $M(\eta) = M(\pi)$ and $M(\eta') = 2M(K) - M(\pi)$ are strongly violated, 548 MeV against 138 MeV and 958 MeV against 854 MeV, respectively. The proper masses are obtained with wave functions[44]

$$\begin{Bmatrix} \eta \\ \eta' \end{Bmatrix} \approx \frac{1}{\sqrt{2}}(\bar{u}u + \bar{d}d)\begin{Bmatrix} \mp \end{Bmatrix}\sqrt{2}\,\bar{s}s \qquad (3.1o)$$

which amusingly implies that the probability to find a $\bar{s}s$ or a $\bar{u}u/\bar{d}d$ pair in the η or η' meson are approximately equal.

The different mixing for the vector and pseudo scalar particles can be understood[3,45,49] qualitatively in terms of gluon exchanges (see 1.22). To the mass matrix correction terms λ_{ij} have to be added which take into account annihilation terms $\bar{q}_i q_i \rightleftarrows \bar{q}_j q_j$. If the 2 quarks are in a $J^P = 1^-$ state (vector particle) the annihilation can only proceed via 3 gluons because of conservation laws. For a $J^P = 0^-$ state (pseudo scalar particle) annihilation via 2 gluons is possible. In terms of QCD perturbation theory the first process is proportional to α_s^3, the latter to α_s^2. For sufficiently large masses $\alpha_s < 1$ and as a consequence the annihilation corrections will be much more important for pseudo scalar particles than for vector states, for which the λ_{ij} are negligible. Thus the different mixing for the two kinds of particles can be explained in terms of QCD, but of course one should not expect too precise results at low masses where α_s is still big.

If the charm quarks are included in the discussion the mass matrix for pseudoscalar mesons can be written in lowest order perturbation theory:

$$M_{\bar{q}q}^2 = \begin{pmatrix} M_u^2 + \lambda_{uu} & \lambda_{ud} & \lambda_{us} & \lambda_{uc} \\ \lambda_{ud} & M_d^2+\lambda_{dd} & \lambda_{ds} & \lambda_{dc} \\ \lambda_{us} & \lambda_{ds} & M_s^2+\lambda_{ss} & \lambda_{sc} \\ \lambda_{uc} & \lambda_{dc} & \lambda_{sc} & M_c^2+\lambda_{cc} \end{pmatrix} \qquad (3.11)$$

with $M_u^2 = M_d^2 = m_\pi^2$, $M_s^2 = 2m_K^2 - m_\pi^2$, $M_c^2 = m_{\eta_c}^2$.

Isospin symmetry gives $\lambda_{uu} = \lambda_{dd} = \lambda_{ud}$. Since $M_c \approx 3$ GeV one may assume $\lambda / M_c^2 \ll 1$ and in a first step to determine the λ_{ij} the annihilation $\bar{q}_i q_i \rightleftarrows \bar{c}c$ may be neglected. With the experimental masses of π, K,η and η' as input one can solve equ. (3.11) and finds[46]

$$\lambda_{uu} = 0.30, \qquad \lambda_{us} = 0.21, \qquad \lambda_{ss} = 0.12. \qquad (3.12)$$

(all in GeV^2)

SU(3) symmetric annihilation would require $\lambda_{uu} = \lambda_{us} = \lambda_{ss}$ and therefore it is obvious that this symmetry is broken substantially. Also these findings can be interpreted in terms of QCD. In lowest order perturbation theory one expects

$$\lambda_{ij} \sim \alpha_s(m_{q_i}) \cdot \alpha_s(m_{q_j}). \tag{3.13}$$

The immediate consequence of equ. (1.1) should be $\lambda_{uu} > \lambda_{us} > \lambda_{ss}$, as indeed is found empirically. Furthermore, the elements λ_{ij} should satisfy the factorization relation $\lambda_{ii} \cdot \lambda_{jj} = \lambda_{ij}^2$. From (3.12) one finds $(\lambda_{uu}\ \lambda_{ss})^{1/2} = 0.19$ in good agreement with $\lambda_{us} = 0.21$.

As a next step one tries to predict the annihilation corrections for charm quarks[46]. From table 3.3 one takes $\alpha_s(M_s^2) / \alpha_s(M_c^2) \approx 2$ which is also in approximate agreement with equ. (1.1). Thus one obtains

$$\begin{aligned} \lambda_{sc} &= \lambda_{ss} \cdot \frac{\alpha_s(M_c^2)}{\alpha_s(M_s^2)} \simeq 0.06 \\ \lambda_{cc} &= \lambda_{ss} \cdot \left[\frac{\alpha_s(M_c^2)}{\alpha_s(M_s^2)}\right]^2 \approx 0.03. \end{aligned} \tag{3.14}$$

Hence as expected the annihilation corrections for the charm quark are smaller than for the ordinary ones and consequently $M(\eta_c) \approx M_c$ to a very good approximation.

The quark content of η_c is given in lowest order by

$$\eta_c = \bar{c}c + (\lambda_{uc}\ \bar{u}u + \lambda_{dc}\ \bar{d}d + \lambda_{sc}\ \bar{s}s) / M_c^2 \tag{3.15}$$

which can be written using $\lambda_{uc} = \lambda_{dc} = \lambda_{us} \cdot \lambda_{sc}/\lambda_{ss}$ as

$$\eta_c = \bar{c}c + \left[\lambda_{us}/\lambda_{ss}\ (\bar{u}u + \bar{d}d) + \bar{s}s\right] \lambda_{sc} / M^2 \tag{3.16}$$

and using (3.1o)

$$\eta_c = \bar{c}c + \varepsilon \cdot \eta + \varepsilon' \cdot \eta' \tag{3.17}$$

with $\varepsilon \approx 10^{-2}$ and $\varepsilon' \approx 2 \cdot 10^{-2}$.

We see that there is an admixture of ordinary quarks to the charm quark state and again we notice SU(3) breaking since the admixture of strange and non-strange quarks is different.

A similar approach for the vector mesons is possible in principle but difficult in practice, since the relevant mass difference $m_\omega - m_\rho$ is not known precisely enough. If an equation analogous to (3.17) is written for the J/ψ one has

$$J/\psi = \bar{c}c + \varepsilon_V \cdot \omega + \varepsilon_V' \phi \tag{3.18}$$

Estimating the coefficients ε_V and ε_V' from the decay of J/ψ into ordinary hadrons one finds ε_V, $\varepsilon_V' \lesssim 10^{-4}$. As mentioned above such a small admixture for the vector charmonium states is exactly what one expects since in this case the annihilation corrections are associated to 3 gluon exchange and hence

$$\lambda_{ij}^V \sim \left[\alpha_s (m_{qi}) \cdot \alpha_s (m_{qj})\right]^{3/2} \tag{3.19}$$

implying that the λ_{ij}^V are about one order of magnitude smaller than the λ_{ij} for the pseudoscalar states.

3.253 Discussion of radiative decays

The decay $(1^{--}) \to (0^{-+}) + \gamma$ is associated to an electromagnetic M1 transition. If the quark content of the initial and final state is the same the transition probability is given by (see also fig. 3.8a):

$$\Gamma(1^{--} \to 0^{-+}) = \frac{4}{3} \alpha \left(\frac{Q}{m_q}\right)^2 k^3 \cdot \Omega^2 \tag{3.2o}$$

where Q and m_q are the quark charge and mass and k is the photon energy. The overlap integral Ω is expected to be of order 1 if the transition takes place by a spin flip without changing the other quantum numbers. Indeed for transitions with ordinary quarks like $\omega \to \pi^0\gamma$, $\rho \to \pi\gamma$, $\phi \to \eta\gamma$, $K^{0*} \to K^0\gamma$ one finds values of Ω between 0.6 and 0.9. Transitions with charm quarks in the initial and final state like $J/\psi \to \eta_c + \gamma$ will be discussed in chapter 3.3.

Let us now discuss the case with charm quarks in the initial and ordinary quarks in the final states like $J/\psi \to \eta\gamma$, $\eta'\gamma$, $\pi^0\gamma$ and $f^0\gamma$. Since the emission of the photon changes only the spin of the system but not the quark content such transitions cannot go via diagram a) of fig.3.8. A mixing of states has to take place which can either happen after (Fig. 3.8b) or before (Fig. 3.8c)

photon emission. As a consequence the overlap integral Ω in (3.20) has to be replaced by $\varepsilon \ \Omega$ where ε is one of the mixing parameters of equ. (3.17) or (3.18).

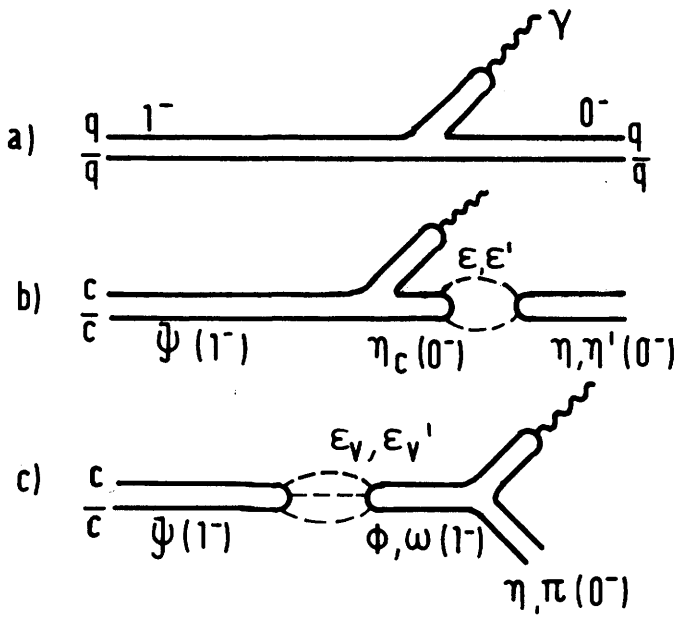

Fig. 3.8

3.2531 The $\eta\gamma$, $\eta'\gamma$ and $f\gamma$ final states

In the previous section arguments have been given that the admixture of ϕ and ω to J/ψ are very small (ε, $\varepsilon' \lesssim 10^{-4}$) whereas the admixture of η, η' to η_c is of the order of 10^{-2}. Hence diagram[46,49] c) in fig. 3.8 can be neglected and transitions like $J/\psi \to \eta\gamma$, $\eta'\gamma$ will go by diagram b). In this case one expects from equ. (3.2o):

$$\frac{\Gamma(J/\psi \to \eta'\gamma)}{\Gamma(J/\psi \to \eta\gamma)} = \left(\frac{k_\eta}{k_{\eta'}}\right)^3 \left(\frac{\varepsilon'}{\varepsilon}\right)^2 \simeq 3.9 \qquad (3.21)$$

with the ε, ε' values given after (3.17). The experimental ratio (see Table 3.5) is 2.9 ± 0.8 in good agreement with (3.21). Thus the unexpected ratio between these two decays becomes plausible.

With respect to the absolute rate equ. (3.2o) yields

$$\Gamma(J/\psi \to \eta\gamma) = 5400 \ \varepsilon^2 \ \Omega^2 \text{keV} \qquad (3.22)$$

Simple calculation[46] based on harmonic oscillator wave functions whose parameters are adjusted to give the $|\psi(0)|^2$ values as obtained from the leptonic widths (see chap. 3.23) suggest $\Omega^2 \simeq 0.1$. The overlap integral is relatively small because the transition energy is 1.5 GeV compared to decays of ordinary hadrons like $\omega \to \pi^0\gamma$, $\phi \to \eta\gamma$ where the transition energies are less than 400 MeV and consequently Ω close to 1. As a result one expects according to (3.22) with

$\varepsilon^2 \approx 0.01$ a width $\Gamma(J/\psi \to \eta\gamma) \approx 54$ eV which agrees very well with the measured width (see Table 3.5) of 55 ± 12 eV. For $J/\psi \to \eta'\gamma$ the corresponding values are 220 eV and 160 ± 50 eV. These excellent agreements might be fortuitous in view of the theoretical uncertainties but they indicate that lowest order QCD permits to understand qualitatively the experimental results.

The situation seems to be very similar for the $J/\psi \to f^0\gamma$ decay. Its branching ratio is of the same order as the $J/\psi \to f^0\omega$ and hence vector dominance with $\omega \to \gamma$ as the source of the photons must be discarded, since it predicts a $f\gamma/f\omega$ ratio of order $\pi\gamma/\gamma_\omega^2 \approx 10^{-3}$. Again a diagram of the type b) in fig. 3.8, where the photon is emitted by the $c\bar{c}$ must be dominant, this time leading to a $c\bar{c}$ state with $J^{PC} = 2^{++}$ which then mixes with the f. A quantitative analysis[51] has recently been carried out. There it is shown that the angular distribution of the photon contains interesting information.

3.2532 The decay $J/\psi \to \pi^0\gamma$

For this decay the situation is reversed. Since $\eta_c - \pi^0$ mixing is forbidden by isospin symmetry it is diagram c) of fig. 3.8 which is dominant and b) is neglegible. Since the J/ψ -ω mixing is quite small, as explained in 3.2552, it is plausible that the rate $J/\psi \to \pi^0\gamma$ is much smaller than $J/\psi \to \eta\gamma$, $\eta'\gamma$.

From eq. (3.2o) one derives

$$\varepsilon^2_{\psi\omega} = \frac{\Gamma(J/\psi \to \pi^0\,\gamma_1)}{\Gamma(\omega \to \pi^0\gamma_2)} \cdot \left(\frac{k_2}{k_1}\right)^2 \cdot \frac{\Omega_{\omega\pi}}{\Omega_{\psi\pi}} \tag{3.23}$$

with $\Omega_{\omega\pi} \simeq 1$ and assuming $\Omega_{\psi\pi} \simeq \Omega_{\psi\eta} \simeq 0.3$ (see 3.2531) one infers from the experimental values of the transition rates (Table 3.5) $|\varepsilon_{\psi\omega}| \simeq 9 \times 10^{-4}$. This is indeed the order of magnitude expected from 3 gluon exchange (see 3.252). More quantitatively one expects[46]

$$\frac{\varepsilon_{\phi\omega}}{\varepsilon_{\psi\omega}} = \left[\frac{\alpha_s(\phi)}{\alpha_s(J/\psi)}\right]^{3/2} \cdot \frac{m_\psi^2 - m_\omega^2}{m_\phi^2 - m_\omega^2} \simeq 41 \tag{3.24}$$

The parameter $\varepsilon_{\phi\omega}$ can be inferred from experiments in a similar way as $\varepsilon_{\psi\omega}$. Analogous to (3.23) one has $\varepsilon^2_{\phi\omega} = \Gamma(\phi \to \pi^0\gamma_1) \,/\, \Gamma(\omega \to \pi^0\gamma_2) \cdot (k_2/k_1)^3$ assuming equal Ω. Inserting the experimental widths one obtains $|\varepsilon_{\phi\omega}| = (5.4 \pm 0.9) \cdot 10^{-2}$. This combined with the "experimental" $|\varepsilon_{\psi\omega}| = 9 \times 10^{-4}$ yields a ratio $\varepsilon_{\phi\omega}/\varepsilon_{\psi\omega} \simeq 61$ which is again in reasonable agreement with the theoretical expectation 41 of equ. (3.24).

In conclusion one might say that first order QCD calculations provide a consistent picture for the radiative decays of charmonium into ordinary hadrons explaining in particular the drastic difference between $J/\psi \to \eta\gamma$, $\eta'\gamma$ and $\pi^0\gamma$. A study of these decays gives simultanously a deeper insight into the mixing of $q\bar{q}$ states.

Of course besides QCD there are other possibilities to understand the data. Schemes involving SU(4) breaking have for example been developed[16,48] which do not need an explicite potential. Many relations between various decay channels could be deduced.

3.2533 OZI transitions without $c\bar{c} \not\to g\bar{g}$ and $\psi' \to \psi + \eta$

If the transition rates are calculated[49] taking into account only SU(3) singlett and octett mixing for η and η' one obtains for OZI forbidden diagrams with 3 gluon exchange (fig. 3.8c) for the final states the ratios

$$\Gamma(\pi^0\gamma) : \Gamma(\eta\gamma) : \Gamma(\eta'\gamma) = 3 : \cos^2\Theta : \sin^2\Theta$$

with the mixing angle $\Theta \approx 11^0$. This is obviously in drastic disagreement with experiment.
The 2 gluon diagram (fig. 3.8b) yields

$$\Gamma(\pi^0\gamma) : \Gamma(\eta\gamma) : \Gamma(\eta'\gamma) = 0 : \sin^2\Theta : \cos^2\Theta$$

Here the enhancement of $\eta\gamma$ and $\eta'\gamma$ with respect to $\pi^0\gamma$ is properly reproduced but the ratio $\Gamma(\eta'\gamma) / \Gamma(\eta\gamma) = \cot an^2\Theta \simeq 30$ is much too large compared to the experimental value 3.1 ± 1.

In conclusion it should be stated that ordinary OZI diagrams successful in explaining the hadronic decays of J/ψ and ψ' (see 3.24) have to be modified by taking into account η_c - η mixing in order to understand the radiative decays.

It seems that the decay $\psi' \to J/\psi + \eta$ is more analogous to the radiative transitions than usual OZI forbidden decays. Its width[27] $\Gamma(\psi' \to \psi\eta) = 9.3 \pm 1.6$ keV is very large for its little phase space (Q = 40 MeV) and being p-wave, SU(3) and OZI suppressed. Hence this decay seems to confirm the $c\bar{c} \leftrightarrow q\bar{q}$ mixing as estabilished in the radiative decays.

3.3 The pseudoscalar states

In terms of the charmonium picture one expects that the vector particles J/ψ, ψ' etc. with parallel quark spins ($^3S_1$ states) are accompanied by pseudoscalar states with opposite quark spins ($^1S_0$ states) (see chap. 2.2). These states have the quantum numbers $J^{pc} = 0^{-+}$. Since they are analogous to the η particle of the light quarks these states are usually denoted by η_c ($\equiv 1^1S_0$) and η_c' ($\equiv 2^1S_0$). Because of the hyperfine splitting one expects these states to be somewhat below the J/ψ and ψ', respectively.

3.31 Experimental results for the X(2.83) and χ(3.45) states

Since the pseudoscalar states have even C they cannot be produced directly in e^+e^- annihilation but can only be reached by decays from J/ψ and ψ'. Since these decays are rather weak our experimental information on the η_c and η_c' states is very scanty compared to the rather complete knowledge of the vector states J/ψ and ψ'. Indeed the existence of the η_c and η_c' has been in doubt for quite some time. There is positive evidence now for η_c which is identified with the X(2.83) particle detected by DASP, whereas the existence of the χ(3.45) level still needs definite confirmation.

The possible transitions leading to η_c and η_c' are shown in fig. 3.9.

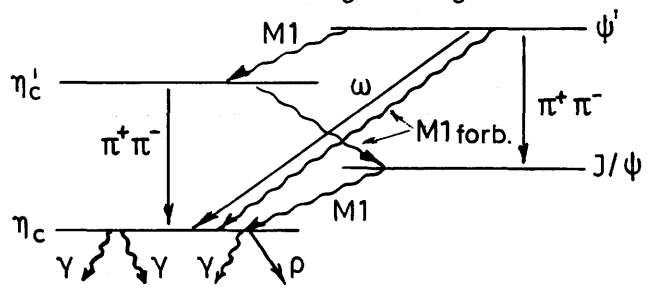

Fig. 3.9 Transitions involving η_c and η_c'

A particle called X with a mass below J/ψ has been detected by DASP[52] looking for 3γ final states from the decay chain $J/\psi \to \gamma X \to \gamma(\gamma\gamma)$. The invariant mass plot for $\gamma\gamma$ (high mass solution is shown in fig. 3.1o and exhibits a clear peak over the smoothly varying background[8o] at a mass of (2.83 ± 0.03) GeV/c^2 and a width of $\Gamma = (29 \pm 14)$ MeV which is consistent with the experimental mass resolution.

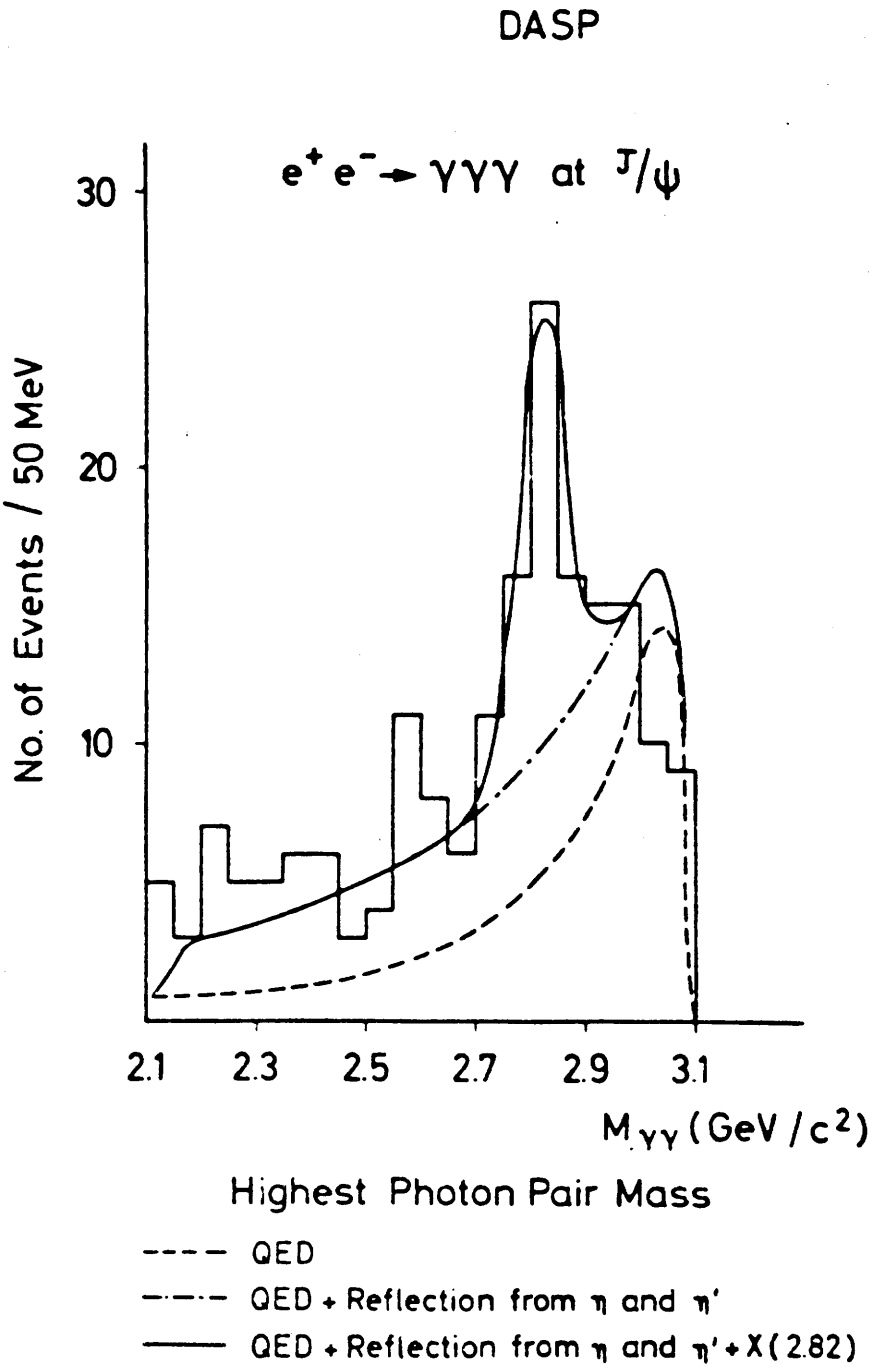
DASP
$e^+e^- \to \gamma\gamma\gamma$ at J/ψ
30
20
10
No. of Events / 50 MeV
2.1
2.3
2.5
2.7
2.9
3.1
$M_{\gamma\gamma}$ (GeV / c^2)
Highest Photon Pair Mass
---- QED
-·-·- QED + Reflection from η and η'
—— QED + Reflection from η and η' + X(2.82)

Fig. 3.10

The branching ratio of the decay chain is given in Table 3.6. The DESY-Heidelberg[53] experiment sees also an excess of events in this mass region but because of their worse mass resolution they cannot give but an upper limit of the branching ratio. The X particle has recently be seen in a pion-proton scattering experiment at Serpukhov[56] and hence its existence seems to be well established.

Table 3.6 Branching ratios of electromagnetic transitions involving pseudoscalar states η_c and η_c'

Transition	Product of Branching ratios in 10^{-3}	Experiment
$J/\psi \to \eta_c$		
$J/\psi \to \gamma\, \eta_c \to \gamma(\gamma\gamma)$	(0.14 ± 0.04)	DASP[52] 80)
	< 0.32	DESY-Heidelberg[53]
$J/\psi \to \gamma\eta_c$	< 17	MPPSSSD[54]
$\eta_c \to \gamma\gamma$	$> (8 \pm 3.5)$	calculated
$J/\psi \to \gamma\, \eta_c \to \gamma(\gamma\rho^0) \to \gamma(\gamma\pi\pi)$	< 0.26	DESY-Heidelberg[53]
$J/\psi \to \gamma\, \eta_c \to \gamma(p\bar{p})$	< 0.2	DASP[52]
	< 0.01	SLAC - LBL[55]
$\psi' \to \eta_c$		
$\psi' \to \gamma\, \eta_c \to \gamma(\gamma\gamma)$	< 0.14	DASP[57] 80)
	< 0.5	DESY-Heidelberg[53]
$\psi' \to \gamma\, \eta_c$	< 11	SLAC - LBL[55]
	< 10	DASP[57]
$\psi' \to \gamma\, \eta_c \to \gamma(\gamma\rho^0)$	< 0.18	DESY-Heidelberg[53]
$\psi' \to \omega\, \eta_c \to \omega(\gamma\gamma)$	< 0.23	- " -
$\psi' \to \eta_c'$		
$\psi' \to \gamma\, \eta_c' \to \gamma(\gamma J/\psi)$	6 ± 4	SLAC - LBL[55], PLUTO[55]
$\psi' \to \gamma\, \eta_c' \to \gamma(\gamma\gamma)$	< 0.07	DASP[57] 80)
$\psi' \to \gamma\, \eta_c'$	< 29	SLAC - LBL[55]
$\eta_c' \to \gamma\, J/\psi$	> 320	calculated
$\psi' \to \gamma\, \eta_c' \to \gamma\, (\eta_c\pi\pi) \to \gamma(\gamma\gamma\pi\pi)$	< 0.06	DESY-Heidelberg[53]

Because $X \to 2\gamma$ the particle has even C and spin 1 is excluded. This is in agreement with the expectation for η_c.

The monoenergetic γ-line associated to the allowed M1 transition $J/\psi \to \eta_c$ has not been seen[54]. Some indications were found[57] for $\psi' \to \eta_c \to (\gamma\gamma)\gamma$ but statistics is still too poor. The most puzzling fact is the negative search for hadronic decays of the η_c. In particular upper limits have been obtained for $\eta_c \to p\bar{p}$ and $\eta_c \to \gamma\rho^0$ which are summarized in Table 3.6. The transition probabilities will be discussed in chap. 3.33.

Evidence for a level at 3.45 GeV comes from an observation of the cascade $\psi' \to \gamma\chi(3.45)$ and $\chi(3.45) \to \gamma J/\psi$. This state has been observed with the intermediate P-states (see chap. 3.4) but does not fit such an interpretation. Hence the identification $\chi(3.45) \equiv \eta_c'$ may be reasonable, although the only information about its quantum numbers is even C, since it is reached by an electromagnetic transition from ψ'. Four cascade events have been found by SLAC-LBL, one by DASP and three by PLUTO (see fig. 3.11), some of which might originate from background. Hence more experimental data are urgently needed to establish this level.

The monoenergetic γ-line arising from $\psi' \to \eta_c'$ has not been seen (see Table 3.6) as well as hadronic decays. The situation is similar to that for the η_c.

3.32 Theoretical expectation of transition rates

3.321 M1 transitions

The decays $J/\psi \to \eta_c\gamma$ and $\psi' \to \eta_c'$ are allowed magnetic dipole transitions. The transition rate is given by

$$\Gamma(1^{--} \to 0^{-+}) = \frac{4}{3} \frac{Q^2\alpha}{M^2} k^3 \Omega^2 \qquad (3.27)$$

where Q and M are the c quark charge and mass, k is the photon energy and Ω is the overlap integral of the initial and final wave function. Allowed M1 transitions are those between states which have essentially the same spatial wave function and differ only in the spin state. Hence $\Omega \approx 1$ if spin-orbit coupling and other spin-dependent effects are neglected.

With these assumptions one calculates[4,59] from (3.27) a decay width of $\Gamma(J/\psi \to \gamma\eta_c) \simeq 29$ keV. From the branching ratio in table (3.6) the limit

$\Gamma(J/\psi \to \gamma\eta_c) \lesssim 1.2$ keV can be inferred, implying $\Omega^2 < 0.04$.

Similarly one calculates[59] the decay width $\Gamma(\psi' \to \gamma\, \eta_c') \simeq 17$ keV whereas the observed limit is $\Gamma < 6$ keV and hence $\Omega^2 < 0.3$.

These comparatively small values of Ω have caused some concern. M1 transitions between hyperfine partners should be rather insensitive to wave functions and indeed this kind of calculation works to within factors of 2 or so for the light mesons, where relativistic effects should make life much more difficult. On the other hand, the large J/ψ - η_c and ψ' - η_c' splittings might indicate that the Russel-Saunders approximation is poor. The discrepancy of a factor of 20 is certainly worrying.

The two "cross" transitions $\eta_c' \to \gamma\, J/\psi$ and $\psi' \to \gamma\, \eta_c$ are forbidden M1 since the main quantum number n changes from 2 to 1. Hence the wave functions are orthogonal if spin-dependent forces are neglected. The width corresponding to the second term in the power series of exp(ikr) is given by

$$\Gamma_{\text{forbidden}}\,(M1) \approx \frac{Q^2}{432}\,\frac{\alpha}{M^2}\;k^7\quad \Omega^2_{\text{forb.}} \tag{3.28}$$

where $\Omega_{\text{forb}} = \langle f \mid r^2 \mid i\rangle$ and the meaning of the other symbols is the same as in (3.27).

Using different wave functions $\Gamma(\psi' \to \gamma\, \eta_c)$ between 1 keV and 10 keV was found[4,5,14] which should be compared to the experimental partial width $\Gamma(\psi' \to \gamma\, \eta_c) \lesssim 2.5$ keV. This agreement, however, has not much relevance. It turns out that relativistic corrections to (3.28) are important[60] and factors of 10 are possible.

The situation for the decay $\eta_c' \to \gamma\, J/\psi$ is more complicated. From the data given in Table 3.6 one calculates a branching ratio $B(\eta_c' \to \gamma\, J/\psi) > (0.3 \pm 0.16)$ which is very large. Since the total width of η_c' is not known it is not possible to give an experimental partial width corresponding to this branching ratio. On the other hand the theoretical estimates deliver only $\Gamma(\eta_c' \to \gamma J/\psi)$ and not the branching ratio. Because of the unreliability of equ. (3.28) a better "theoretical" estimate can be obtained by assuming that the matrix elements of $\eta_c' \to \gamma\, J/\psi$ and $\psi' \to \gamma\, \eta_c$ are the same and correcting for phase space one obtains $\Gamma(\eta_c' \to \gamma\, J/\psi) \approx (1/4)\Gamma\,(\psi' \to \gamma\eta_c) < (1/4) \cdot 2{,}5$ keV $\simeq$ 0.6 keV.

In order to compare Γ and B it has been tried to estimate the hadronic width $\Gamma(\eta_c' \to \text{hadrons})$ which should be practically equal to the total width. As will be shown in 3.323 the hadronic width should be of the order of a few MeV. This yields a branching ratio $B < 10^{-3}$ in contrast to the experimental limit $B > 0.3$.

Another way to compare experiment and theory is to consider the cascade branching ratio $B(\psi' \to \eta_c' \gamma \to J/\psi\, \gamma\gamma)$ which experimentally is $(6 \pm 4) \times 10^{-3}$, whereas theoretically one expects $\simeq 3 \times 10^{-6}$. This again is a large discrepancy, however, the uncertainties for the calculated forbidden M1 transitions are very large.

3.322 $\eta_c \to \gamma\gamma$

Transcribing the QED results for the singlett state of positronium one finds for the decay rate[2,4]

$$\Gamma(0^- \to \gamma\gamma) = \frac{48\pi\, \alpha^2\, Q^4}{M^2} \, |\psi(0)|^2 \qquad (3.29)$$

Taking $\psi(0)$ as determined for the J/ψ (chap. 3.23) one obtains $\Gamma(\eta_c \to \gamma\gamma) \simeq 8$ keV.

The experimental branching ratio $B(\eta_c \to \gamma\gamma) > (8 \pm 3.5) \times 10^{-3}$ cannot be compared to this expectation since the experimental total width of η_c is not known. Theoretical estimates will be discussed in the next section.

3.323 Hadronic decays of η_c and η_c'

Following the analogy between QED and QCD the pseudoscalar η_c and η_c' can annihilate into 2 gluons besides into 2 photons. To derive the 2 gluon annihilation rate from (3.29) one has to make the replacement[35] $\alpha^2\, Q^4 \to 2\alpha_s^2\, /9$ and obtains

$$\Gamma(0^- \to \text{hadrons}) \simeq \Gamma(0^- \to g\, g) = \frac{32\pi}{3} \frac{\alpha_s^2}{M^2} |\psi(0)|^2 \qquad (3.30)$$

Inserting $\alpha_s = 0.2$ and using $\psi(0)$ as determined from the J/ψ one has $\Gamma(\eta_c \to \text{hadrons}) \simeq 6.4$ MeV. This can be checked by an estimate which is independent of the wave function and is obtained by taking the ratio of (3.30) and (3.7)

$$\frac{\Gamma(\eta_c \to g\, g)}{\Gamma(J/\psi \to ggg\,)} = \frac{27\, \pi}{5(\pi^2 - 9)\, \alpha_s} \approx 100 \qquad (3.31)$$

Taking the measured width $\Gamma(J/\psi \to \text{hadrons}) = 69$ keV one arrives at $\Gamma(\eta_c \to \text{hadrons}) \simeq 7$ MeV in good agreement with the previous estimate. This total width corresponds to a OZI hinderance factor of about $\gtrsim 50$.

The total width of η_c' can be estimated according to

$$\frac{\Gamma(\eta_c' \to \text{hadrons})}{\Gamma(\eta_c \to \text{hadrons})} \simeq \frac{\Gamma(\psi' \to \text{hadrons})}{\Gamma(\psi \to \text{hadrons})} \simeq \left| \frac{\psi(0)}{M} \right|^2_{\psi'} \times \left| \frac{M}{\psi(0)} \right|^2_{\psi} \simeq \tag{3.32}$$

$$\simeq \frac{2.4}{3.9} \times \left(\frac{3.1}{3.7}\right)^2 = 0.43$$

and hence $\Gamma(\eta_c' \to \text{hadrons}) \simeq 3$ MeV.

With this theoretical hadronic width one can now calculate the branching ratios $B(\eta_c \to \gamma\gamma) = \Gamma(\eta_c \to \gamma\gamma) \,/\, \Gamma(\eta_c' \to \text{hadrons}) \simeq 8$ keV/7 MeV $\simeq 1.2 \times 10^{-3}$. If this is compared to the experimental limit $B(\eta_c \to \gamma\gamma) > (8 \pm 3.5) \times 10^{-3}$ one obtains a factor $> (7 \pm 3)$ of discrepancy. In view of the uncertainties this does not seem too worrysome.

A more serious problem is the fact that so far no hadronic decays of either the η_c nor the η_c' have been observed. One way out could be that these particles decay to many different final states which are difficult to identify. With statistical model calculations some authors[61] have tried to estimate the probability of different final states. They find that indeed each channel contributes only a few percent, e.g. $\eta_c \to 2\,\pi^+\,2\,\pi^-\,2\pi^0$ 7 to 15 %, $\eta_c \to 2\,\pi^+\,2\,\pi^-$, $3\pi^+\pi^-$ 2 to 5 % each, $\eta_c \to p\bar{p}$ + anything a few percent. The first channel which is dominant is hard to find. The limits given in table 3.6 may still be compatible with these rates.

3.33 Discussion of pseudoscalar states

The comparison between experimental results and theoretical expectations concerning the $\eta_c \equiv X(2.83)$ and $\eta_c' \equiv \chi(3.45)$ particles can be summarized in the following way:

a) Whereas the existence of the X(2.83) is well established, the $\chi(3.45)$ needs confirmation.

b) The large splitting between the ^3S and ^1S states which originally has caused much concern does not seem too much of a problem. It can be understood quite coherently by attributing an anomalous gluon coupling

to the quarks (see chap. 2.2). Recently it has been shown[62] that the existence of instantons may be responsible for the large splitting and indeed it could be considered as direct evidence for the instantons.

c) Serious difficulties exist for the M1 transition rates. In particular it seems difficult to explain the large discrepancies for the allowed M1 transitions between HFS partners. The even larger discrepancies for the forbidden M1 "cross transitions" are perhaps less worrying because of the large theoretical uncertainties.

d) The real puzzle is the fact that no hadronic decays of η_c and η_c' have been seen, although partial width of several MeV are expected. The hadronic transitions seem to be suppressed and one puzzling consequence is the very large $B(\eta_c' \to \gamma J/\psi) > 32$ %.

Because of these difficulties some authors have questioned whether the X(2.83) and χ(3.45) are really the $^1S_0$ states[87]. Harari tried to identify the χ(3.45) with the $^1D_2$ ($J = 2^{-+}$) and Krasemann and Krammer[63] interpreted this state as a relativistic "time like" P-state. Both proposals are not very attractive since they do not solve the problems for the X particle and where is then the η_c' state?

Several authors[16,48,64] have shown that the transitions $J/\psi \to \eta_c \gamma$ and $\eta_c \to \gamma\gamma$ can be hindered by SU(4) symmetry breaking. Indeed by a proper choice of the parameters $\Gamma(\eta_c \to \gamma\gamma) < 3.7$ keV can be obtained. May be relativistic models are needed to interprete the decays involving η_c and η_c'.

As a possibility to verify the nature of the X(2.83) and χ(3.45) particles it has been suggested[65] to look for the decay $\psi' \to \gamma \chi \to \gamma(\pi^+\pi^-)X \to \gamma(\pi^+\pi^-)(\gamma\gamma)$ for which a branching ratio larger than 4×10^{-5} has been estimated. Unfortunately the upper limit given in table 3.6 has about this value and the hope that this decay chain is strong does not seem to be realized.

In conclusion one has to state that more experimental information is desperately required to solve the puzzle of the pseudoscalar charmonium states. With all the success of the charm model this seems to be the only major trouble that remains to be eliminated.

3.4 The intermediate P-states

According to the standard charmonium model one expects 3 triplett-P-states and one singlett P-state with masses between the J/ψ and the ψ'. As explained in chap. 2 these P-states fall inbetween the two lowest $^3S_1$ states because the potential deviates from a pure Coulomb shape and hence the P-states are lowered. Having C even the ^{3}P-states cannot be produced directly in e^+e^- annihilation but can be reached by an electromagnetic E1 transition from ψ'. They can decay eather by a E1 transition to J/ψ or into ordinary hadrons.

The $^1P_1$ state with $J^{PC} = 1^{+-}$ cannot be reached from ψ' by electromagnetic transitions because of its negative charge conjugation. The decay $^3P_2(2^{++}) \to \gamma\, ^1P_1(1^{+-})$ is possible but phase space is probably very small. Hence it is not surprising that the $^1P_1$ state has not been observed so far. The following discussion has to be restricted therefor to the ^{3}P states.

3.41 Experimental results for ^{3}P-states

The first evidence for an intermediate state called P_c was found by DASP[66] in the cascade $\psi' \to \gamma P_c \to \gamma\,(\gamma\, J/\psi)$. Later this and cascades to other intermediate states, which were given the generic name χ, were seen at SPEAR[54,55], by DESY-Heidelberg[68] and PLUTO[69]. The results are shown in fig. 3.11. Clustering in the $(J/\psi\,\gamma)$ invariant mass can be seen at 3.42,3.45,3.50 and 3.55 GeV. All these states have even C since they are reached by an electromagnetic transition from a 1^{--} state. The state at 3.45 GeV has a different character than the others since its decay into hadrons has not been observed. As discussed in chap. 3.3 it is tempting to identify this state with the 2^1S_0 level and since the relevant experimental data have been given in chap. 3.31 we shall not discuss it here.

The mass distribution of the γ J/ψ system in the decay $\psi' \to \gamma\gamma J/\psi$ as obtained in recent measurements[68)80)] is shown in fig. 3.12 a and b. The peaks at 3.51 and 3.55 GeV are clearly seen, there is a small indication at 3.41 GeV, whereas no significant structure is observed at 3.45 GeV.

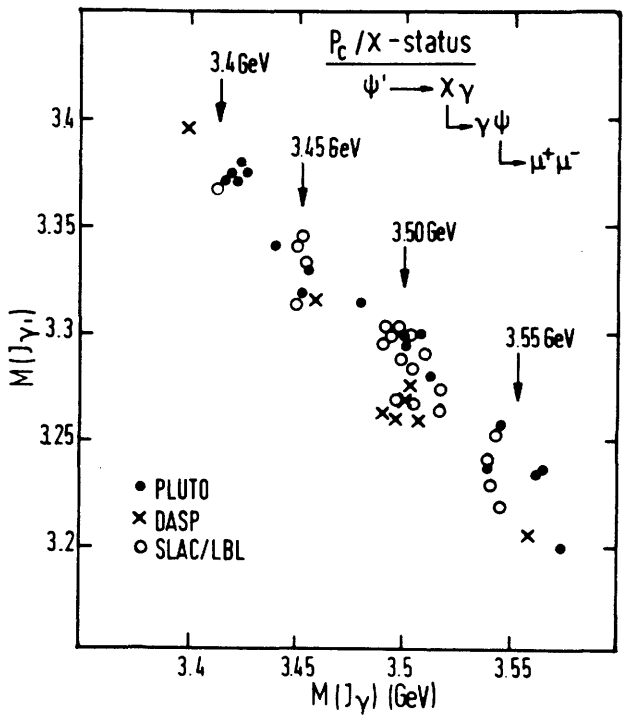

Fig. 3.11

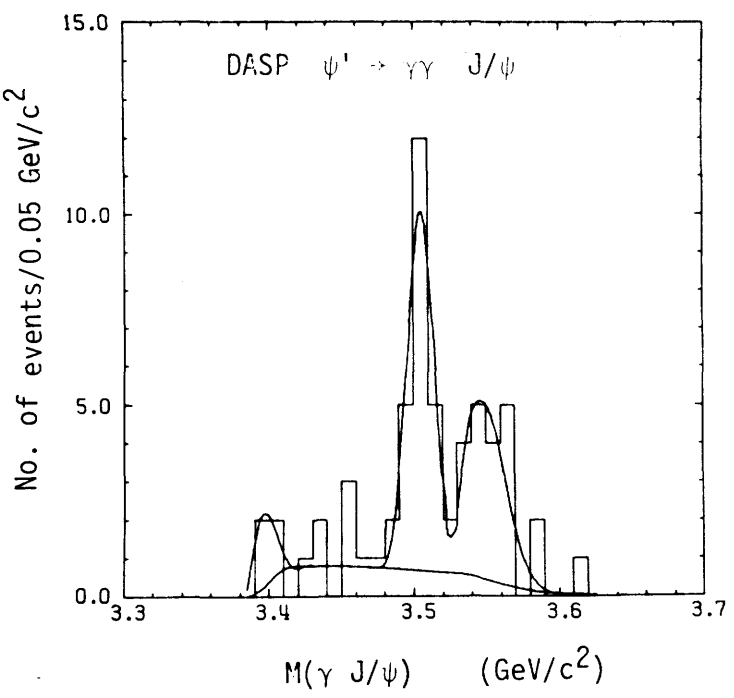

Fig. 3.12a

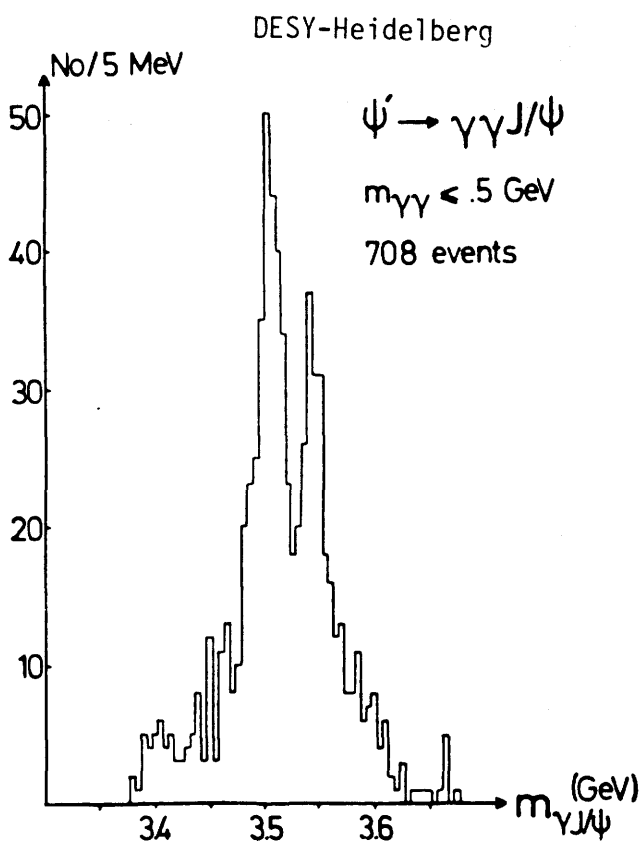

Fig. 3.12b

For the three P-states the monoenergetic lines corresponding to the transitions $\psi' \rightarrow \gamma\,^3P$ have been observed (fig. 3.13) and the branching ratios were determined. These branching ratios together with those for the $\gamma\gamma$ cascade are collected in table 3.7.

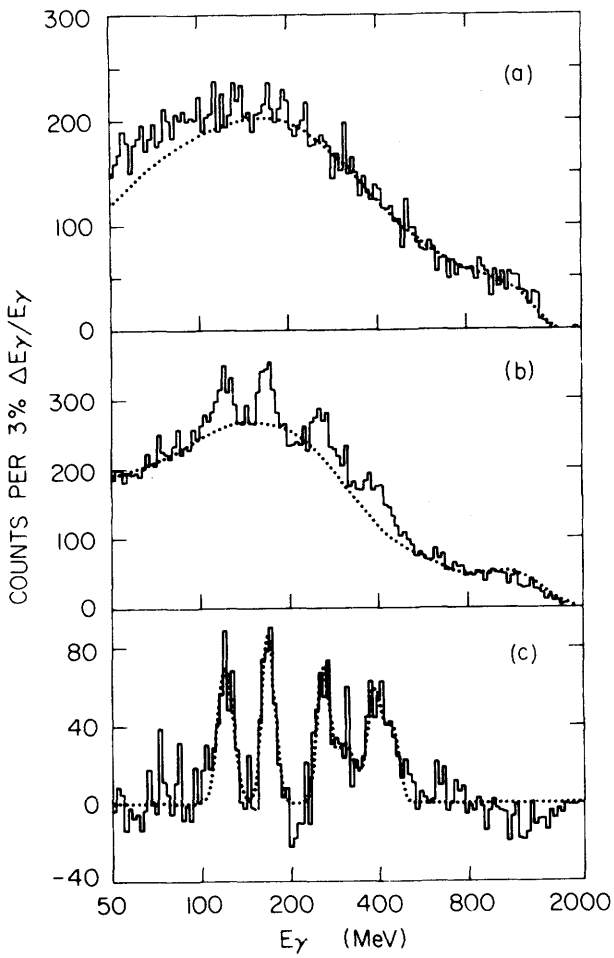

Fig. 3.13

MPPSSSD[54])

Table 3.7 $\psi' \to \gamma P \to \gamma\gamma\, J/\psi$ cascades

State MeV[+]	$B(\psi' \to \gamma\, ^3P)$ (%)	$B(\psi' \to \gamma\, ^3P \to \gamma(\gamma J/\psi))$ (%)	Parameter[++] a of $1 + a\cos^2\Theta$	Experiment
		1 ± 0.2		DASP[66)80)]
3543 ± 7		1.0 ± 0.6	a = 0.3 ± 0.4	SLAC-LBL[55)]
3561 ± 7	7.0 ± 2	2.2 ± 1.0		MPPSSSD[54)]
		2.3 ± 0.6		DESY-Heidel.[68)]
		1.1 ± 0.3		DASP[66)80)]
3504 ± 5		2.4 ± 0.8	a = 0.1 ± 0.4	SLAC-LBL
3511 ± 7	7.1 ± 1.9	5.0 ± 1.5		MPPSSSD
		3.3 ± 0.8	- 0.1 ± 0.3	DESY-Heidel.[68)]
	~ 1.4	0.34± 0.20		DASP[80)]
3413 ± 11	7.5 ± 2.6	0.2 ± 0.2	a = 1.4 ± 0.4	SLAC-LBL
3413 ± 9	7.2 ± 2.3	3.3 ± 1.7		MPPSSSD
		0.2 ± 0.1		DESY-Heidel.[68)]

+) Mass from hadronic decays

++) For J = 0, a = 1, for J = 1 and 2, a = - 1/3 and 0.08 for pure dipole transitions.

Information about the spin of a ^3P state can be obtained from the angular distribution of the first (low energy) γ in the cascade with respect to the beam axis. One expects a distribution proportional to $1 + a\cos^2\Theta$ where Θ is the angle between the first photon and the beam axis. With J = 0 for the intermediate state one has a = 1. For J = 1 or 2 the prediction for a is not unique since mixing of multipoles is possible. The experimental results for a are also shown in Table 3.7.
No $^3P \to \gamma\gamma$ were observed[69)].

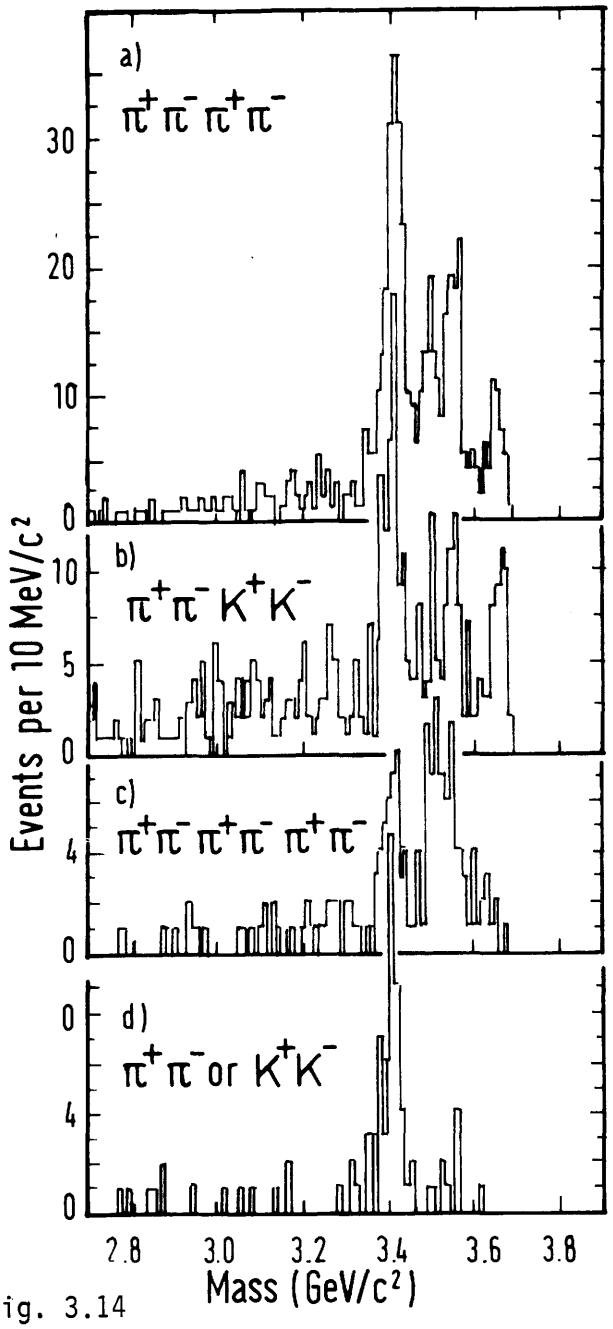

Fig. 3.14

The hadronic branching ratios of the P-states have been determined by the SLAC-LBL experiment. Invariant mass spectra for different final states are shown in fig. 3.14 and the branching ratios have been summarized by G. Goldhaber[70] (Table 3.8). The most striking fact is that the 3.41 and 3.55 GeV states decay into $\pi^+\pi^-$ and K^+K^- whereas the 3.50 GeV level does not.

3.42 Assignment of quantum numbers

On the basis of the experimental material presented in the previous section one can try to determine the quantum numbers of the 3 levels with even C and see if they are compatible with ^3P states.

3.41 GeV: The observed decay into $\pi^+\pi^-$ and K^+K^- implies natural spin-parity for this state, i.e. 0^{++}, 2^{++}... and it has to be an isoscalar. The angular distribution is in agreement with J = 0 and hence one can safely design this state to $J^{PC}=0^{++}$.

3.51 GeV: The absence of $\pi^+\pi^-$ and K^+K^- final states indicates unnatural spin-parity 0^-, 1^+, ... The two experiments which measured the angular distribution disagree but both require $J \neq 0$. Hence the assignment $J^{PC} = 1^{++}$ seems plausible but needs confirmation.

3.55 GeV: The presence of $\pi^+\pi^-$ or K^+K^- decays is again in favour of a 0^{++}, 2^{++}, ... state. The angular distribution indicates $J \neq 0$ and hence the assignment $J^{PC} = 2^{++}$ seems plausible.

These assignments[71] are in perfect agreement with the expectation for ^3P levels. This ordering of the spins is further corroborated by the discussion of the E1 transition probabilities (see next section).

The 3.45 GeV level which is the fourth intermediate state with even C does not fit into the ^3P level sequence and hence it is suggested to associate

Table 3.8 [70]

$\chi(3415)$ branching ratios

Decay Mode	Events	Efficiency	$B(\psi' \to \gamma\chi)\ B(\chi \to f)$	$B(\chi \to f)$ [a]
$\pi^+\pi^-$	32 ± 6	0.19	$(7.5\pm2.1)\times10^{-4}$	$(1.0\pm0.3)\times10^{-2}$
K^+K^-	27 ± 5.5	0.16	$(7.8\pm2.3)\times10^{-4}$	$(1.0\pm0.3)\times10^{-2}$
$\pi^+\pi^-\pi^+\pi^-$	181 ± 16	0.19	$(3.5\pm0.7)\times10^{-3}$	$(4.6\pm0.9)\times10^{-2}$
$\pi^+\pi^-K^+K^-$	83 ± 11	0.11	$(2.8\pm0.7\ \times10^{-3}$	$(3.7\pm0.9)\times10^{-2}$
$\pi^+\pi^-p\bar{p}$	23 ± 6	0.18	$(4.7\pm1.3)\times10^{-4}$	$(0.6\pm0.2)\times10^{-2}$
$\pi^+\pi^-\pi^+\pi^-\pi^+\pi^-$	37 ± 8	0.08	$(1.4\pm0.5)\times10^{-3}$	$(1.9\pm0.7)\times10^{-2}$
$\psi\gamma$	1 1	0.0011	$(2\ \pm2\ )\times10^{-3}$	$(3\ \pm3\ )\times10^{-2}$

a) We use $B(\psi' \to \gamma\chi) = 0.075$. The errors quoted for $B(\chi \to f)$ do not include the overall scale uncertainty of 35 % due to the error (± 0.0026) in $B(\psi' \to \gamma\chi)$.

$\chi(3505)$ branching ratios

Decay Mode	Events	Efficiency	$B(\psi' \to \gamma\chi)\ B(\chi \to f)$	$B(\chi \to f)$ [a]
$\pi^+\pi^-\pi^+\pi^-$	74 ± 12	0.20	$(1.4\pm0.4)\times10^{-3}$	$(2.0\pm0.6)\times10^{-2}$
$\pi^+\pi^-K^+K^-$	24 ± 7	0.11	$(0.8\pm0.3)\times10^{-3}$	$(1.1\pm0.4)\times10^{-2}$
$\pi^+\pi^-pp$	6 ± 4	0.19	$(1.2\pm0.8)\times10^{-4}$	$(1.7\pm1.1)\times10^{-3}$
$\pi^+\pi^-\pi^+\pi^-\pi^+\pi^-$	48 ± 15	0.08	$(1.9\pm0.7)\times10^{-3}$	$(2.7\pm1.1)\times10^{-2}$
$\psi\gamma$	12 ± 4	0.0011	$(2.4\pm0.8)\times10^{-2}$	$(34\ \pm11\ )\times10^{-2}$

a) We use $B(\psi' \to \gamma\chi) = 0.071$. The errors quoted for $B(\chi \to f)$ do not include the overall scale uncertainty of 27 % due to the error (± 0.019) in $B(\psi' \to \gamma\chi)$.

$\chi(3550)$ branching ratios

Decay Mode	Events	Efficiency	$B(\psi' \to \gamma\chi)\ B(\chi \to f)$	$B(\chi \to f)$ [a]
$\pi^+\pi^-$ or K^+K^-	9 ± 4	0.18	$(1.9\pm0.8)\times10^{-4}$	$(2.7\pm1.1)\times10^{-3}$
$\pi^+\pi^-\pi^+\pi^-$	89 ± 12	0.20	$(1.7\pm0.4)\times10^{-3}$	$(2.4\pm0.6)\times10^{-2}$
$\pi^+\pi^-K^+K^-$	47 ± 8	0.12	$(1.5\pm0.4)\times10^{-3}$	$(2.1\pm0.6)\times10^{-2}$
$\pi^+\pi^-p\bar{p}$	13 ± 5	0.19	$(2.6\pm1.0)\times10^{-4}$	$(3.7\pm1.4)\times10^{-3}$
$\pi^+\pi^-\pi^+\pi^-\pi^+\pi^-$	23 ± 15	0.08	$(0.9\pm0.6)\times10^{-3}$	$(1.3\pm0.8)\times10^{-2}$
$\psi\gamma$	4 ± 2	0.0009	$(1.0\pm0.6)\times10^{-2}$	$(14\ \pm8\ )\times10^{-2}$

a) We use $B(\psi' \to \gamma\chi) = 0.070$. The errors quoted for $B(\chi \to f)$ do not include the overall scale uncertainty of 29 % due to the error (± 0.020) in $B(\psi' \to \gamma\chi)$.

it to the 2^1S level as discussed in chap. 3.3. However, since neather hadronic decays nor angular distributions could be observed there is no direct experimental information on the quantum numbers of this state except its even charge conjugation.

3.43 Theoretical expectation for E1 transition rates

The transitions from ψ' to the ^3P levels and from these to J/ψ are electric dipole transitions.
For $\psi' \to \gamma\ ^3P_J$ one finds[4] for the partial width

$$\Gamma_J(E1) = \frac{4\alpha}{27} Q^2\ (2J + 1)\ k^3 [\ <2\ p|\ r|\ 2\ s>\ ]^2 \qquad (3.33)$$

where Q is the quark charge, k the photon energy and J the spin of the final state.

The experimental values for the branching ratio B (taken from Table 3.7) and the partial width Γ_J (calculated with $\Gamma_{tot}(\psi') = 228$ keV) are shown in table 3.9. The width Γ_J for the 3 transitions are remarkably constant. This is due to the circumstance that $(2J + 1)\ k^3$ which according to (3.33) determines Γ_J turns out to change only by a factor of 2 (see table 3.9) because of the balancing between $(2J + 1)$ and k^3. The factor k^3 alone changes by a factor of 50. As a consequence the experimental constancy of Γ_J supports very strongly the assumed spin ordering since for different spins Γ_J would change by large factors. This statement is independent of detailed calculations of the matrix element.

Original estimates[2,4] of the absolute decay rate were based on too crude approximations and lack of precise knowledge of the transition energies. The results of later calculations are given in table 3.9. They are in very good agreement with the experimental Γ_J. This confirms that the c-quark charge is $Q = 2/3$ since for $Q = -1/3$ a discrepancy by a factor of 4 would emerge.

The transition probabilities for the decays $^3P_J \to \gamma J/\psi$ are given by

$$\Gamma_J(E1) = \frac{12\alpha}{27}\ Q^2\ k^3 |<1s\ |r|\ 2p>|. \qquad (3.34)$$

Table 3.9

$\psi' \to \gamma\ ^3P_J$ transitions

J	k (MeV)	(2J+1) ($\times 10^7$)	k^3 $B(\psi' \to \gamma\ ^3P_J)$ %	exp. Γ_J (keV)	theoretical Γ_J (keV) Jackson[4]	Henriques[72]
2	123	0.93	7 ±2	16 ± 5	19	14
1	173	1.55	7.1±1.9	16 ± 4	27	21
0	271	2.00	7.5±2.6	17 ± 6	31	22

Table 3.10

$^3P_J \to \gamma\ J/\psi$ transitions

J	k (MeV)	$k^3(\times 10^7)$	$B(^3P_J \to \gamma J/\psi)$ %	theoretical Γ_J (keV) Jackson[4]	Eichten[14]	Henriques[72]	Lane[4]
2	466	10	14 ± 8	300	400	367	320
1	416	7.2	34 ± 11	230	300	258	200
0	318	3.2	3 ± 3	100	140	120	90

Compared to (3.33) (2J + 1) has been replaced by 3 and hence no balancing of the k^3 dependence occurs. The experimental results for the branching ratios are given in table 3.10. Since the total widths of the P-states are not known Γ_J cannot be determined. On the other hand, from (3.34) only Γ_J can be calculated. As a consequence a direct comparison between experimental and theoretical results is not possible. Jackson[73] has tried to estimate the total widths from sum rules and QCD but the results are not accurate enough to enable a detailed comparison.

Quantitatively one sees by inspecting table 3.10 that $B(^3P_1 \to \gamma J/\psi)$ is larger than the other two branching ratios and also its absolute value of (34 ± 11) % is remarkably big. In contrast the theoretical value Γ_J for this transition lies between the other two. This indicates that the hadronic decays of $^3P_1$ (3.51) are suppressed compared to the other 2^3P-states. This can be understood in terms of QCD as will be explained in the follwing section.

3.44 Hadronic decays of P-states

In terms of the simple charmonium picture the hadronic widths of the P-states are given approximately by the annihilation of $c\bar{c}$ into two gluons[35] for J = 0,2 and into 3 gluons (or 1 gluon and a light $q\bar{q}$ pair[74]) for J = 1.

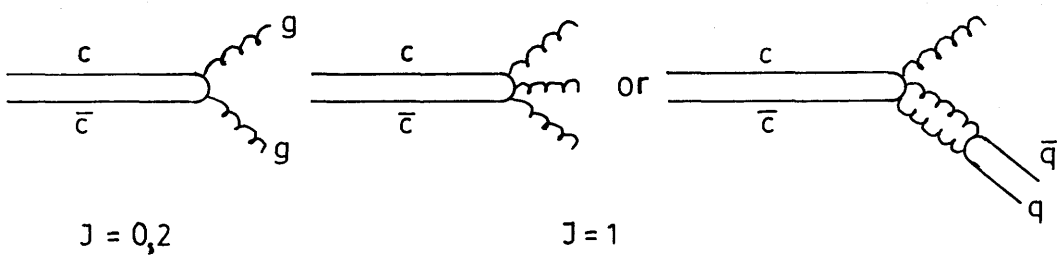

The 2 gluon annihilation can be calculated in a straightforward way using the analogy to the 2 photon annihilation of positronium which gives:

$$\Gamma(P_J \to \gamma\gamma) = N_J \frac{\alpha^2}{M^4} |R'(0)|^2 \qquad (3.35)$$

where M is the c-quark mass, R' is the derivative of the radial part of the wave function and the numerical constants are $N_0 = 256/3$ and $N_2 = 1024/45$. The 2 gluon annihilation is obtained by the substitution $\alpha^2 Q^4 \to \alpha_s^2 (2/9)$ where Q is the c-charge and one arrives at

$$\Gamma(P_J \to g\ g) = N_J^S \frac{\alpha_S^2}{M^4} \mid R'(0) \mid^2 \qquad (3.36)$$

with $N_0^S = 96$ and $N_2^S = 128/5$.
The term $|R'(0)|^2$ has to be calculated from an assumed potential and according to whether a pure Coulomb, pure linear or a mixture of both is used, one finds[4,35] $|R'(0)|^2 = 0.04$ to $0.09\ GeV^5$. From (3.36) one deduces then the estimates

$$\begin{aligned} \Gamma(P_2(3.55)) \to \text{hadron}) &\simeq 0.5\ \text{MeV} \\ \Gamma(P_0(3.41)) \to \text{hadron}) &\simeq 2.0\ \text{MeV}\ . \end{aligned} \qquad (3.37)$$

Using the experimental $P_J \to \gamma J/\psi$ branching ratios one gets estimates for the radiation widths of 70 and 60 keV, respectively. A comparison with the theoretical $\Gamma_J(P_J \to \gamma\ J/\psi)$ listed in table. 3.10 shows discrepancies of factors 4 and 2. This can be considered as a reasonable although certainly not good success of QCD.

The decay probabilities $P_J \to \gamma\gamma$ as calculated from (3.35) are completely negligible to the hadronic widths (3.37) and therefore also to the transitions $P_J \to \gamma J/\psi$. Indeed the two photon decays have not been observed[57] with $B(\psi' \to P_J\gamma \to \gamma\gamma\ \gamma) \lesssim 4 \cdot 10^{-4}$.

For the J = 1 P-states the QCD prediction is much less certain. It has been argued[74] that the annihilation into $g + q\bar{q}$ dominates the $^3P_1$ $(J=1^{++})$ decay whereas the ggg final state is most important for the $^1P_1$ $(J=1^{+-})$ state which has not been observed so far. Both of these transition rates involve logarithmic divergences at zero binding energy and

$$\Gamma(P_1 \to \text{hadrons}) = N_1 \frac{\alpha_S^3}{M^4} \mid R'(0) \mid^2 \ln\left(\frac{4\ M_c^2}{4\ M_c^2 - M^2}\right) \qquad (3.38)$$

with $N_1 = 128/3\pi$ for 1^{++} and $320/9\pi$ for 1^{+-}.
With the logarithm estimated as $2 \ln(1/\alpha_s)$ one finds for both J=1 states $\Gamma(P_1 \to \text{hadrons}) \simeq 0.15$ MeV. The width is about 1/3 of $\Gamma(P_2 \to \text{hadron})$ and the reduction is mainly due to the extra power in α_s. This delivers also the qualitative explanation for the large electromagnetic branching ratio of $P_1(3.55)$ which arises from the suppressed 3 gluon annihilation of this P-state.

The general QCD formula (neglecting logarithmic divergencies) for the annihilation of a state with orbital angular momentum ℓ into n gluons may be quoted here[59)]

$$\Gamma \simeq \frac{\alpha_s^n}{M_c^2} \left(\frac{1}{M_c}\right)^{2\ell} |R_\ell^{(\ell)}(0)|^2 \qquad (3.39)$$

where $R^{(\ell)}$ is the ℓ-th derivative of the wave function.

With respect to individual hadronic decay channels of the P-states very little theoretical work has been done. The decay $^3P \to J/\psi + \pi\pi$ is unimportant and has not been observed in contrast to $\psi' \to J/\psi + \pi\pi$ which dominates. The reason[5)] is that the decays $^3P_J \to J/\psi + \pi\pi$ have little phase space and are hindered by the centrifugal barrier.

3.5 Summary of charmonium spectroscopy

An enormous effort at SPEAR and DORIS has produced over the last few years convincing evidence for the charmonium model and for QCD.

The level scheme of the $c\bar{c}$ system as deduced from experiments is shown in fig. 3.15 including levels above the binding limit. All the various types of levels have been found. The orbital momentum $\ell = 0$ state with parallel spins $J = 1^{--}$, the triplett ^{3}P-states and the lowest ^{3}D-state. The - by now well established - $\chi(2.83)$ particle is very likely the lowest singlett ^{1}S-state although its quantum numbers have not been determined experimentally. If the state at 3.45 GeV exists and if it is the first excited ^{1}S-state remains to be clarified. The singlett $^1P_1$-state is still missing but this is plausible since it cannot be reached by radiative transitions from 1^{--} states.

The spin dependent splittings of the levels seem to pose no principal difficulties but yield on the other hand valuable information on the spin dependent forces. The rather large splitting between the triplett and singlett S-states may be associated either to anomalous gluon moments or the existence of instantons. The splitting of the P-states indicates that the long range confining potential contains Lorentz-scalar parts.

The hadronic and radiative transitions of the 1^{--} states can be explained qualitatively in the frame of QCD by the annihilation into hard gluons. Interesting information on the mechanism of OZI hinderance and the mixing of $q\bar{q}$

states can be extracted.

The electromagnetic E1 transitions involving the ^3P state are well understood and contribute to the determination of their spins. The theoretical work to explain the various hadronic decay channels is still rather scarce.

The M1 transitions involving the ^1S states present major difficulties. The real puzzle seems to be the fact that no hadronic decays of the $X(2.83)$ and the $\chi(3.45)$ have ever been seen.

Because of the exciting questions to be answered at higher energies the clarification of many details of the charmonium system has been suspended. One may hope that experimentalists and theorists will come back to these problems since many interesting information on the interaction between 2 quarks might be obtained.

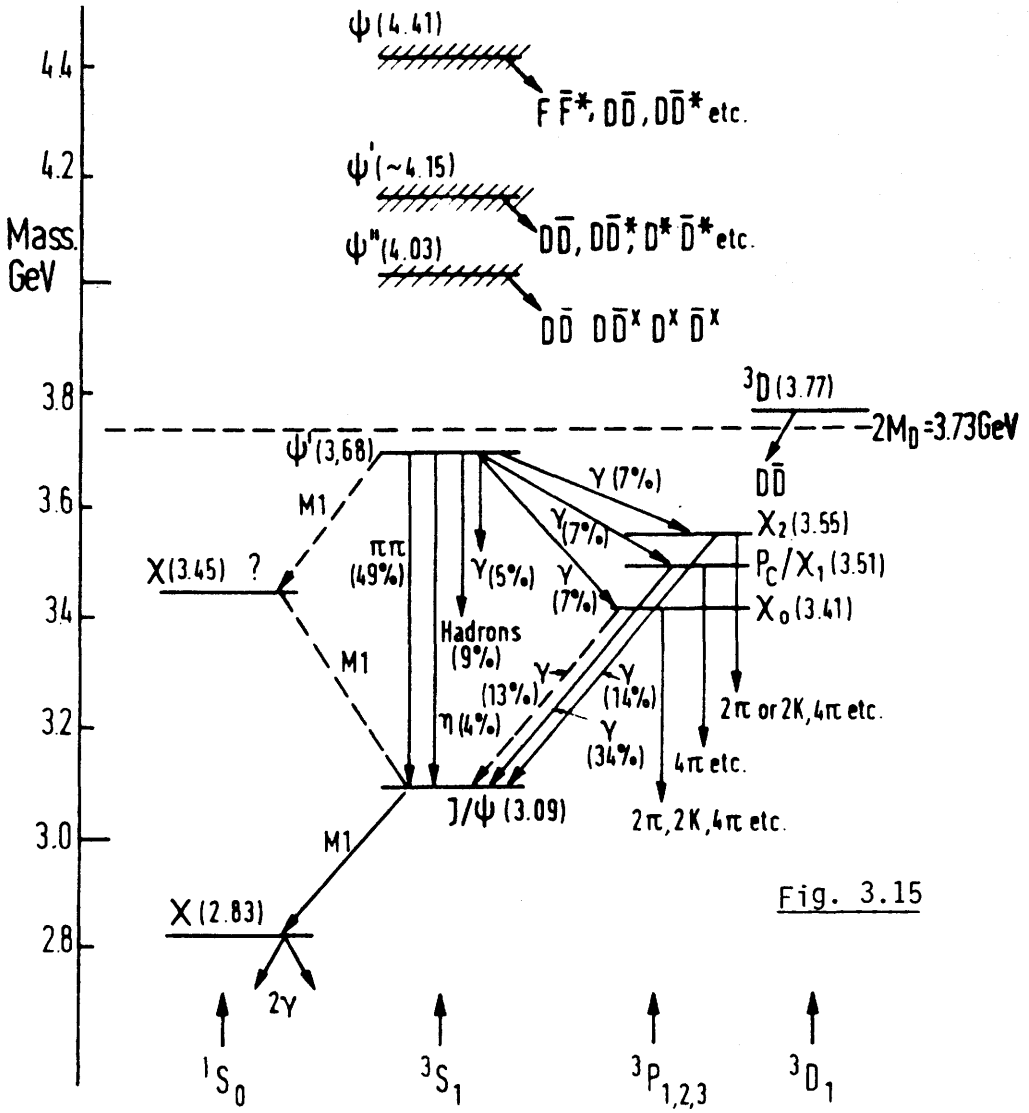

Fig. 3.15

4. Total Cross Section and Inclusive Yields

A measurement of the total cross section $e^+e^- \to$ hadrons can give important information on quarks and the strong interaction. As discussed in chap. 1.13 this process can go via an intermediate resonance state with $J = 1^{--}$ provided the total e^+e^- energy E coincides with the rest mass of the resonance.

4.1 Asymptotic limits of σ_{tot}

Away from resonances the total hadronic cross section can be estimated in the quark model on the basis of an asymptotically free theory with gluonic corrections and one finds[76)]

$$\sigma(e^+e^- \to \text{hadrons}) = \sigma_{\mu\mu}\, 3 \sum_i Q_i^2 \quad (1 + \alpha_s(E)/\pi) \qquad (4.1)$$

where Q_i are the quark charges, α_s is the gluon-quark coupling constant whose energy dependence is given by (1.1), and

$$\sigma_{\mu\mu} = (4\pi/3)\ (\alpha/E)^2 = 86.8 \text{ nb} / (E/\text{GeV})^2 \qquad (4.2)$$

is the $e^+e^- \to \mu^+\mu^-$ total cross section. The sum has to be extended over those quarks whose $q\bar{q}$ pairs can be produced at a given energy E. The factor 3 comes from the 3 colour degrees of freedom (see chap. 1.21).

Since $\alpha_s(E)$ decreases with increasing energy E the ratio $R = \sigma(e^+e^- \to \text{hadrons})/\sigma_{\mu\mu}$ tends to an asymptotic value from above. In the energy region 3 to 8 GeV α_s is of the order 0.2 (see 3.21) and hence in (4.1) the last term arising from gluonic corrections should be of the order of 10 % or less. For the 3 light quarks the asymptotic value is $R_{u,d,s} = 3(2/9+4/9) = 2$ and above the charm threshold one expects an increase by $\Delta R_c = 3(4/9) = 1.333$ which would give $R = 10/3$.

A heavy lepton with a sufficiently large mass can decay into hadrons and hence can contribute to $\sigma(e^+e^- \to \text{hadrons})$. If the lepton is pointlike its production cross section will be equal to $\sigma_{\mu\mu}\ (3\beta - \beta^3)/2$ where the term multiplying $\sigma_{\mu\mu}$ gives the threshold behaviour for a spin 1/2 particle ($\beta = v/c$ of

the lepton). The contribution to R will be $\Delta R_{lepton} = B \times (3\beta - \beta^3) / 2$ where B is the branching ratio of the lepton into hadrons. Since, however, in most experiments measuring σ_{tot} hadrons, electrons and muons are not identified decay electrons and muons are taken for hadrons and consequently B = 1 and $\Delta R_{lepton} \approx 1$ well above threshold.

4.2 Experimental results for $\sigma(e^+e^- \rightarrow \text{hadrons})$

The ratio $R = \sigma (e^+e^- \rightarrow \text{hadrons}) / \sigma(e^+e^- \rightarrow \mu^+\mu^-)$ in the range E = 2.4 to 7.7 GeV is shown in fig. 4.1, as measured at SPEAR[77]. The data at lower energies as obtained from Orsay, Frascati and Novosibirsk are still somewhat scattering. In fig. 4.1 one notices a step around 4 GeV which is attributed

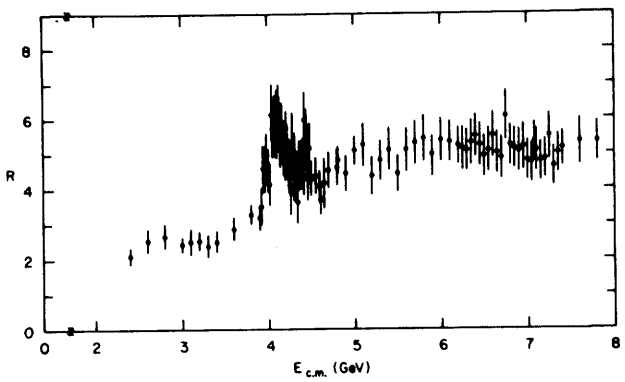

Fig. 4.1

to the opening up of the charm threshold. The resonance peaks appearing around 4 GeV will be discussed in chap. 4.2.

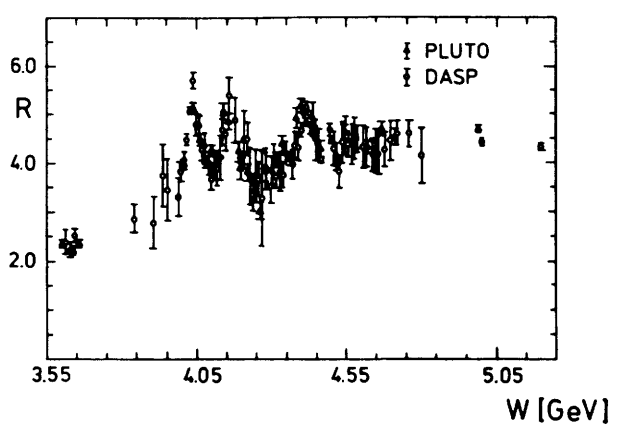

Fig. 4.2

In fig. 4.2 recent data from DORIS obtained by the PLUTO[78,79] and DASP[80] experiment are shown for the energy region 3.6 to 5.1 GeV. The data of these two groups agree very nicely and as far as the peaks are concerned their position coincides with those of the SPEAR data. However, as can be seen from fig. 4.3, where the SLAC-LBL and PLUTO data are compared, there is a discrepancy of 10 to 15 % at energies below 4.5 GeV. This difference might be due to systematic effects,

e.g. acceptance corrections. These should be smaller for PLUTO because of its larger acceptance (86 % as compared to 65 % for SLAC-LBL) and a more general trigger. Recent data from DELCO[86] seem to agree as far as the absolute values are concerened with the DORIS data but the systematic errors are still about 20 %.
It seems important to clarify the discrepancy between PLUTO and DASP on one side and MARK 1 on the other, since a 10 % difference corresponds to half a unit of R which is quite relevant for the interpretation.

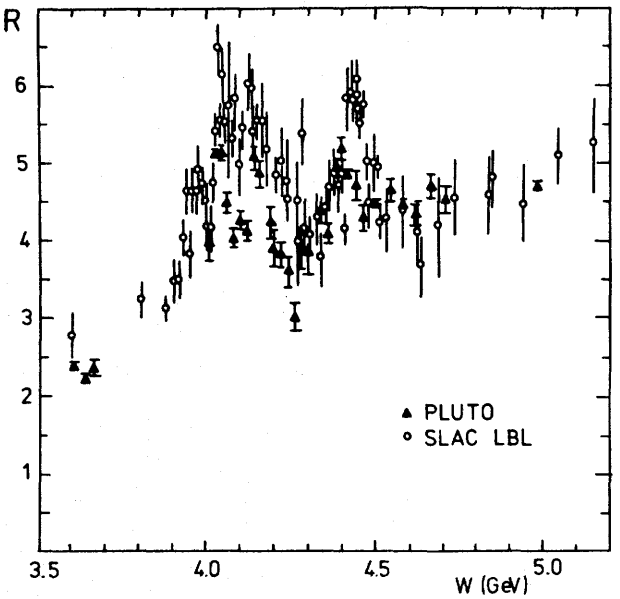

Fig. 4.3

The looser trigger enabled PLUTO to break down the total cross section into charged multiplicities, as shown in fig. 4.4. It is remarkable that

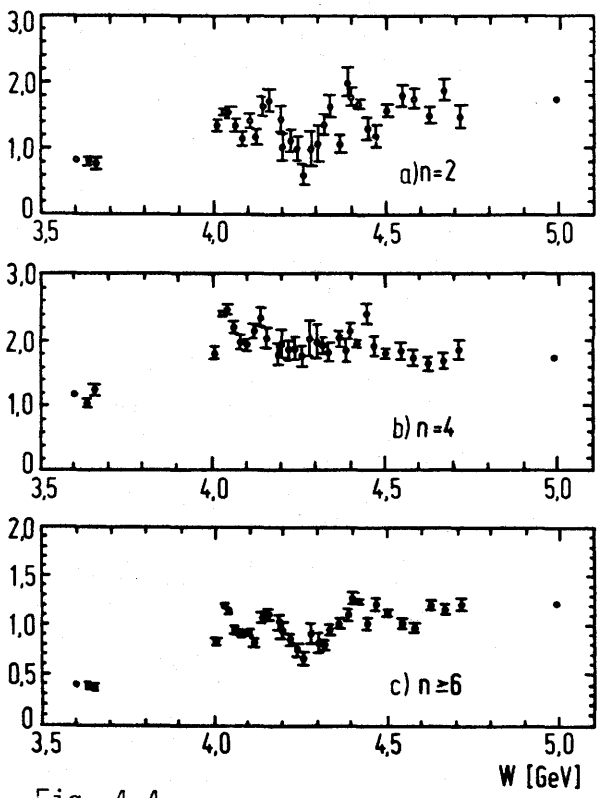

Fig. 4.4

these partial cross sections and in particular the 2prong cross sections show the same structures as σ_{tot}. The dip at 4.3 GeV is deepest in 2-prongs, and indeed at this energy R can almost alone be attributed to light quarks and the heavy lepton.

In fig. 4.5 the various contributions to $\sigma(e^+e^- \rightarrow \text{hadrons})$ are shown schematically. For the 3 light quarks the asymptotic limit R = 2 is assumed. It is remarkable that the new PLUTO results near E = 3.6 GeV are only about 10 % higher than this limit. The reason for this small difference can be due to gluon corrections as discussed above or tails of lower resonances. The contribution of the τ-lepton has been calculated for a mass[81] of 1.8 GeV. The rise above the charm threshold can only be guessed but it was assumed that the asymptotic limit of 10/3 has been reached around 5 GeV. The experimental value of R = 4.7 is higher than the expectation of about 4.2, which could be due to tails of the resonances shown or because of the opening up of new thresholds.

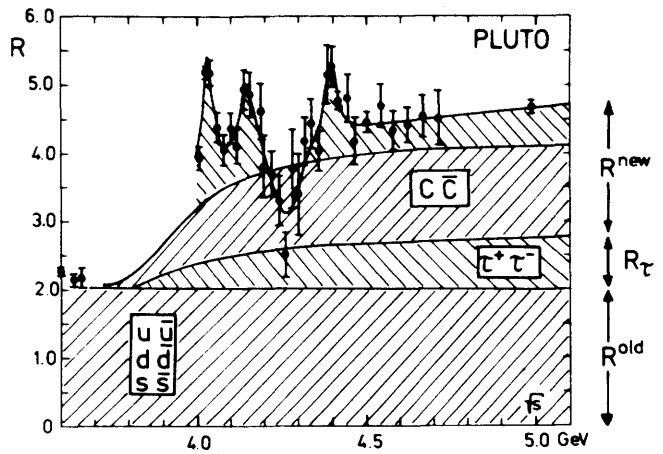

Fig. 4.5

In conclusion it can be stated that the data are in quite good agreement with the 4 quark model and the existence of the heavy lepton and they confirm explicitly the colour factor 3 in equ. (4.1).

In passing it might be mentioned that the average number of charged hadrons is given[29] by $\langle n_{ch} \rangle \approx 2.1 \pm 0.7 \ln (E/\text{GeV})^2$ with a value of about 4 in the region E = 3.6 to 5 GeV. It is remarkable that such a logarithmic rise is found also in hadron-hadron collisions.

4.3 Unbound resonances

Above the threshold for two D-mesons $E_{thr} = 2M_D = 3.726$ GeV charmonium resonances can decay into $D\bar{D}$. Above this threshold one expects therefore processes of the type $e^+e^- \rightarrow \psi^* \rightarrow D\bar{D}$ according to the quark diagram

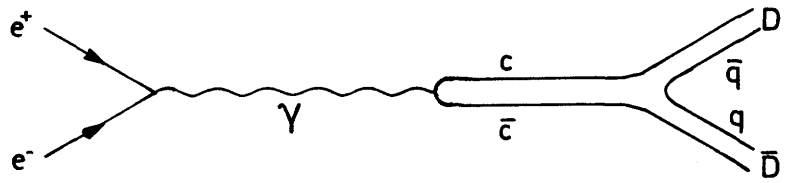

The total width of these unbound resonances should correspond to ordinary hadronic widths in contrast to J/ψ and ψ' which are below the threshold and hence can decay only by OZI hindered hard gluon intermediate states (see chap. 3.24). If the $c\bar{c}$ system has $J^{PC} = 1^{--}$ these resonances should be observed in $\sigma(e^+e^- \rightarrow \text{hadrons})$. However, a peak in this cross section does not necessarily belong to a resonance. It could also be produced by the opening of a new threshold and associated form factors which make the cross section drop fast at the high energy side of the peak. Which case is realized has to be found out by detailed studies. The situation of having discrete levels in the continuum is familiar from nuclear and atomic physics and can occur if the potential is not Coulomb-like

4.31 The $^3D(3.77)$-state

A resonance very close to the charm threshold was found at (3.77 ± 6) MeV by the SLAC-LBL collaboration[84]. Its widths was found to be $\Gamma = (28 \pm 5)$ MeV. This can be considered as a beautiful confirmation of the arguments based on charm and QCD since the ψ' which lies only 88 MeV lower but has a much smaller width. This demonstrates the difference between an allowed and a OZI hindered decay.

The mass, the total and leptonic widths have been predicted by the Cornell theory group[14,85] for the lowest $^3D_1$-state with the help of the potential model (see chap. 1.23) with astonishing accuracy. Therefore one might ask why this resonance has not been detected before. The reason becomes obvious from fig. 4.6a) which shows the uncorrected data. One notices that the resonance falls on the large tail of the ψ' and an appreciable amount of statistics had to be accumulated.

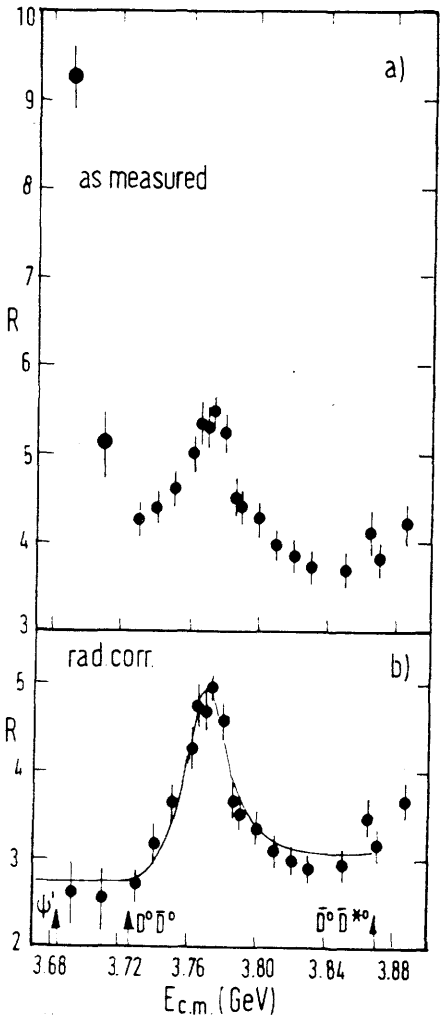

Fig. 4.6

In fig. 4.6b the results after applying radiative corrections are shown. One notices that the resonance shape is asymmetric. If one fits the data by a Breit-Wigner form one has to assume that the width $\Gamma(E)$ depends on the energy. This in turn is expected because of the proximity of the $D\bar{D}$ threshold. With these assumptions good fits to the data (see fig. 4.6b) can be obtained. The resonance parameters are given in table 4.1.

From the data to be discussed later one calculates a $D\bar{D}^*$ threshold at 3.87 GeV which is well above the resonance. As a consequence the 3.77 GeV particle should decay almost exclusively into $D\bar{D}$. The branching ratios determined from the individual D decays are listed in table 4.1. This property makes the 3.77 resonance a clean source for D particles which provides the possibility for a detailed study of these particles (see chap. 5.2).

With respect to the nature of the 3.77 level there seems to be no doubt that it should be identified with the predicted $^3D_1$ state. However, in a nonrelativistic treatment a D-state does not couple to e^+e^-. It can obtain a leptonic width by mixing with an S-state and since the ψ' is so close one expects primarily a 1^3D_1-2^3S_1 mixing. If one writes[75] for the leptonic width

$$\Gamma_{ee}(3.77) \simeq a\,\Gamma_{ee}\,(2^3S_1) + b\,\Gamma_{ee}\,(^3D_1) \qquad (4.3)$$

where a and b are mixing parameters and $\Gamma_{ee}\,(^3D_1)$ is the leptonic width of a pure $^3D_1$ state. With relativistic corrections $\Gamma_{ee}(^3D_1) \simeq 0.1$ keV was found[75]

and inserting the experimental Γ_{ee} for the 3.77 and 3.68 GeV states one obtains $a/(a+b) \simeq 0.13$. This implies an appreciable mixing. If the mixing is expressed in terms of a mixing angle one finds[84] $\Theta = (23 \pm 3)^{o}$.

Table 4.1 Parameters for unbound resonances

State	Mass MeV/c^2	Γ keV	Γ keV	Branching ratios	Experiment
$^3D_1$	3772 ± 3	28 ± 5	0.37 ± 0.09	$D^0\bar{D}^0$ 44 ± 22 % D^+D^- 44 ± 33 %	SLAC-LBL[82]
	3770 ± 6	24 ± 5	0.18 ± 0.06		DELCO[86]
	4035 ± 2	55 ± 5	0.7 ± 0.1		PLUTO[83]
	4040 ± 10	52 ± 10	0.75 ± 0.15		DASP[123]
	4146 ± 4	47 ± 11	0.4 ± 0.1		PLUTO[83]
	4156 ± 20	78 ± 20	0.77 ± 0.23		DASP[123]
	4414 ± 5	33 ± 10	0.44 ± 0.14		SLAC-LBL[82]
	4400 ± 3	33 ± 9	0.3 ± 0.1		PLUTO[83]
	4417 ± 10	66 ± 15	0.49 ± 0.13		DASP[123]

4.32 Higher resonances ($3.8\ \text{GeV} \lesssim E < 5\ \text{GeV}$)

The total e^+e^- hadron cross section shows further peaks at 4.03, 4.15 and 4.40 GeV. If they are associated with resonances one can determine the parameters given in table 4.1. These resonances could be $^3S_1$ levels or ^3D states with some S-state mixing. Unfortunately there is no direct experimental evidence to support such assignments. Also the predictions from the potential models are not very reliable because of decay channels and other corrections (see chap. 1.2). Structures can also be produced by opening thresholds, interference effects between resonances and form factors in $e^+e^- \to D\bar{D}$, $D\bar{D}^*$, $D^*\bar{D}^*$ etc. Consequently the identification of structures becomes less reliable the higher the energy.

The pronounced peak at 4.03 GeV is due to the conjunction of the 3^3S_1 state and the opening of the $D^*\bar{D}^*$ threshold at 4.012 GeV. That this peak is nevertheless a resonance can be seen in the Argand diagram for $D\bar{D}$ scattering[14,87].

The peak at 4.15 GeV could be attributed in the standard model to the 2^3D_1 state but it also lies just above the $F\bar{F}$ threshold at 4.o6 GeV. To clarify the character of this peak it would be interesting to look for F production which is difficult, however. Nevertheless some evidence for F production has been found[123] (see also 4.43). The Argand diagram supports the interpretation as a resonance[14].

The resonance at 4.4o GeV finally could be associated[85] to the 4^3S_1 state. This is supported by the splitting 4.4o - 4.o3 GeV $\simeq$ 400 MeV which agrees with the expectation for $4^3S_1 - 3^3S_1$ but does not fit so well with a D-state. A similar argument applies to the leptonic width. The ratio Γ_{ee} (4.4) / Γ_{ee} (J/ψ) $\simeq$ 0.1 seems to be compatible with an S-state but too large for a D-state (see chap. 3.21)[85].

Some broad structure seems to become apparent around 3.95 GeV (see fig. 4.7). This bump may have to do with the opening of the $D\bar{D}^*$ threshold at 3.872 GeV and with a zero in the 3S decay amplitude[87]. Similarly the broad structure around 4.35 GeV may be associated to the $F\bar{F}^*$ threshold at 4.17 GeV. To chek this it would be very interesting to look for F and F^* production in this energy region.

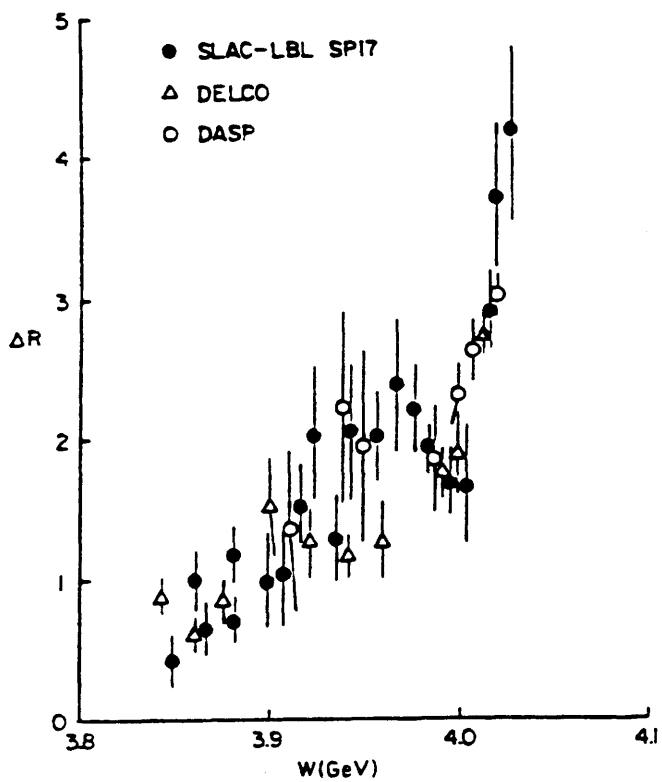

Fig. 4.7

ΔR in the region 3.9 to 4 GeV. Because of the discrepancy in the total height of R between SPEAR and DORIS a "non charm" contribution of 2.5 units has been subtracted for the SPEAR points and 1.5 units for the DASP points.

The situation in the 3.9 to 5 GeV energy region is by no means settled. The threshold and the speculative assignments are shown in table 4.2. However, the standard potential model (see chap. 2.1) may be wrong, in particular the Υ-splitting (see chap. 6) seems to indicate that the confining potential is not linear at higher energies. As a consequence the S-spacing could be much smaller and all the structures above 4 GeV could be S-wave resonances. More experimental and theoretical work is needed.

Table 4.2 Thresholds and speculative assignments to peaks in the 3.8 to 5 GeV region

Threshold		Peak		
Type	E (GeV)	E (GeV)	Interpretation	observed decays
$D\bar{D}$	3.726			
		3.772	$1^3D_1 + 2$ (2^3S_1 mixing)	$D\bar{D}$
$D\bar{D}^*$	3.872			
		~ 3.95	threshold + form factor	
$D^*\bar{D}^*$	4.012			
		4.03	3^3S_1 + threshold	$D\bar{D}$, $D\bar{D}^*$, $D^*\bar{D}^*$
$F\bar{F}$	4.06			
		4.15	2^3D_1 or threshold	$F\bar{F}$
$F\bar{F}^*$	4.17			
		~ 4.35	**threshold?**	
$F^*\bar{F}^*$	4.28			
		4.40	4^3S_1 ?	$F\bar{F}^*$

4.33 The exclusive decays of the 4.03 GeV-resonance

The 4.03 GeV resonance is above the thresholds for $D\bar{D}$, $D\bar{D}^*$ and $D^*\bar{D}^*$ decay but below the thresholds for decays into F-particles. At SPEAR a large sample of data has been accumulated and the branching ratios for the 3 decay channels (see chap. 5) have been measured[88,89]. The results are shown in table 4.3. The surprising result is that after correcting for the very different phase spaces the D^* production is very much favoured. In a naive quark model the ratios of the production probabilities should simply be given by statistical spin factors which indeed favour the $D^*\bar{D}^*$ channel but much less than experimentally found.

Table 4.3 Exclusive production of D^0 from decays of the 4.03 GeV resonance

D^0 from	$D^0\bar{D}^0$	$D^0\bar{D}^{*0}+D^{*0}\bar{D}^0$	$D^{*0}\bar{D}^{*0}$	charged D	Ref.
Fractions Experiment	0.05 ± 0.03	0.38 ± 0.08	0.40 ± 0.10	0.16 ± 0.11	88) 89)
Exp. after Phase space corrections	0.2 ± 0.1	4.0 ± 0.8	128 ± 40		70)
Statistical spin factors	1	4	7		85) 23)
node in decay amplitude	0.04	4	30		85) 87)
decoupling scheme	0.9	4	175		90)

(normalized to second column)

The Cornell theory group has tried to explain the experimental ratios in terms of a coupled channel model which produces a P-wave decay amplitude for $3^3S \to (c\bar{u}) + (\bar{c}u)$ which is oscillating and has a node. As a consequence the cross section $\sigma(e^+e^- \to D\bar{D})$ has a zero near 4 GeV and the $D\bar{D}$ production is strongly suppressed with respect to $D^*\bar{D}^*$. The ratios inferred from this model are given (after phase space corrections) in the fourth line of table 4.3. The

tendency agrees with the experimental values, but there are still differences of factors 4 to 5. While it seems possible to tune the model to get a better agreement on the ratios it seems difficult[88] to get reasonable ratios and at the same time explain the maximum of R.

An alternative explanation[91] has been offered for the large $D^{*}\bar{D}^{*}$ production by assuming that the 4.03 GeV particle is a $D^{*}\bar{D}^{*}$ 'molecule'. If this were true, one expects by a rearranging of the 4 quarks the decay into J/ψ which was estimated to occur on the 10 % level. PLUTO[92] has looked for the inclusive production of J/ψ in the energy region from 4.0 to 5.0 GeV. A cross section of 31 ± 21 pb has been found which corresponds to 0.13 % of the total hadronic cross section. Consequently no enhancement due to 'molecules' has been seen and the observed J/ψ production can be understood[93] in terms of normal OZI forbidden transitions.

Still another model[90] to explain the enhanced $D^{*}\bar{D}^{*}$ production just above threshold is based on a decoupling scheme. Its basic assumption which can be defended on quite general grounds says that of a vector particle decaying into 2 particles with spins J_1 and J_2 only the ground state and the first $J_1 + J_2$ excitations (or daughters) can couple to these 2 particles. Hence the ground state of a $J^P = 1^-$ particle can decay into two $J = 0$ particles but not the higher recurrences. This seems to hold for the ρ, ω and ϕ Regge trajectories separately (e.g. forbidding $\rho'(1520) \rightarrow 2\pi$). If applied to charmonium states, one expects the 1^3S (= J/ψ), 2^3S (= ψ'), 3^3S (= 4.03 GeV) states to couple to $D^{*}\bar{D}^{*}$ (each having spin 1 and hence $J_1 + J_2 = 2$) whereas the 3^3S state should not couple to $D\bar{D}$ which explains the suppression. A detailed analysis with form factors yields the ratios given in table 4.3 which reproduce the tendency of the experimental values, but again some discrepancies remain.

This decoupling scheme could help to sort out the structures of the total cross section. It predicts that the 4^3S state (perhaps at 4.40 GeV) should not decay into $D^{*}\bar{D}^{*}$ pairs or any lower spin configuration like $D\bar{D}$, $D\bar{D}^{*}$ etc. The 2^3D and 3^3D should couple to $D^{*}\bar{D}^{*}$ whereas the 1^3D can couple to $D\bar{D}$ (and higher spin configuration which are forbidden by energy conservation, however). The 2^3D may also decay into $D\bar{D}^{*} + \bar{D}D^{*}$ which might help to identify the 4.15 GeV peak.

4.4 Inclusive particle yields

Inclusive particle production can give interesting information in various ways. Inclusive particle spectra are related to parton models and indeed the momentum distribution of hadrons produced in e^+e^- annihilation[29] found considerable theoretical interest. However, it is beyond the scope of this review to cover this subject. Here we are rather interested to learn something about the production of new particles, which can produce steps in the total yield of one kind of particle. As will be shown in chap. 5 the D mesons decay preferentially to K-mesons and also electrons. Therefore at the threshold for D production one expects a sudden increase in the inclusive K and e production. Similarly the F mesons tend to decay to η and therefore a measurement of the η yield seems interesting. Charmed baryons will lead to final states with nucleon-antinucleon pairs, which have been looked for.

4.41 Inclusive K-production

A step in K-production at an energy where the $e^+e^- \to D\bar{D}$ channel opens up provides very good evidence for the existence of charmed particles. Strangely enough such an increase in the inclusive cross section could not be seen for quite some time. Only at the beginning of 1977 PLUTO[95] was able to see a step in the K^o_s cross section at an energy of 4 GeV. This was immediately confirmed by DASP[96] for charged K-mesons (fig. 4.8). Assuming that the increase found in the K cross section has the same origin as the step in σ_{tot} one finds that 60 to 80 % of the final states produced in the new phenomenon contain kaons. The number of K^o_s per event is 0.39 ± 0.06 and since the number of all kaons is four times larger one has 1.56 ± 0.24 kaons per event, which comes close to 2. This figure is expected if pairs of charm particles are produced and each decays into a kaon. Additional proof that the kaons are associated to charm production comes from the K-spectra.

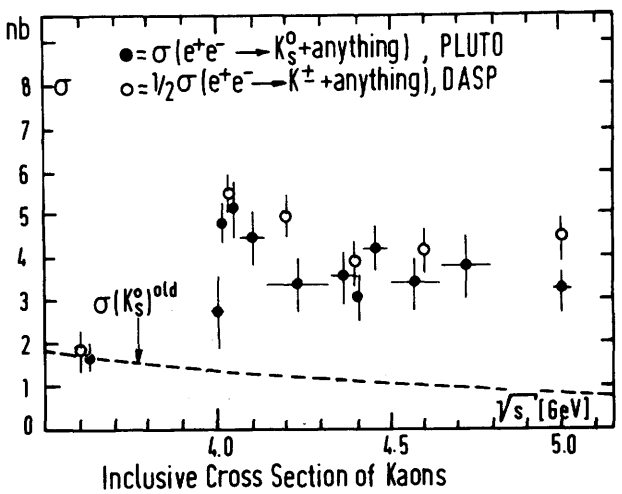

Fig. 4.8

In fig. 4.9 two spectra for charged kaons are shown as an example[96]. One spectrum was taken below, the other just above the charm threshold. The spectra agree above a K-momentum of about 1 GeV/c whereas at lower momenta a clear difference can be seen. This is exactly what one expects from D's decaying almost at rest. Each D carries roughly the beam energy and about half of this energy or less is available for the kaon, i.e. $E_K \lesssim E_{beam}/2$.

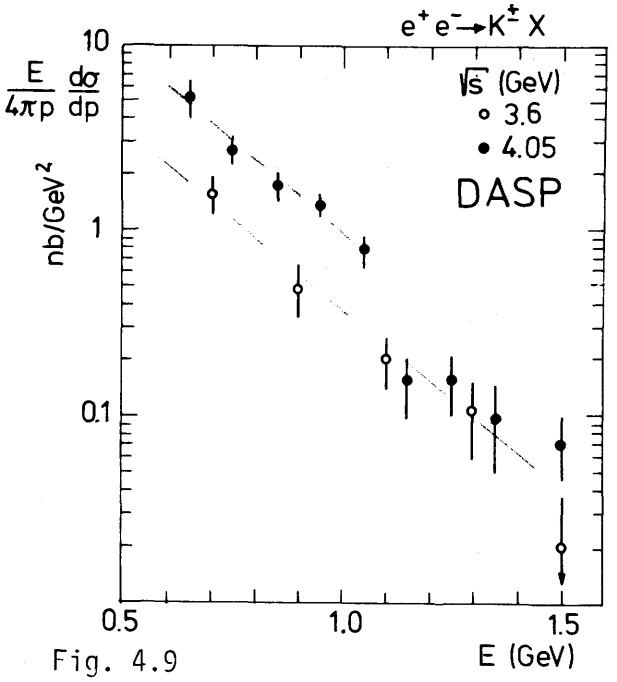

Fig. 4.9

Kaon yields obtained[97,98] by MARK 1 also show the pronounced rise at 4 GeV but the yields are larger than those found at DORIS (fig. 4.1o). However, the MARK 1 data were corrected by about 20 % for losses at low K momenta and losses in the analysis. No such corrections have been applied to the PLUTO data. The remaining discrepancy has about the same size as the difference of the total cross sections, except at an energy of 4.415 GeV. Here the MARK 1 point lies significantly higher than the PLUTO result. This could be due to the fact that the MARK 1 data were taken exactly at the peak of the resonance whereas the PLUTO data are averaged over ± 15 MeV.

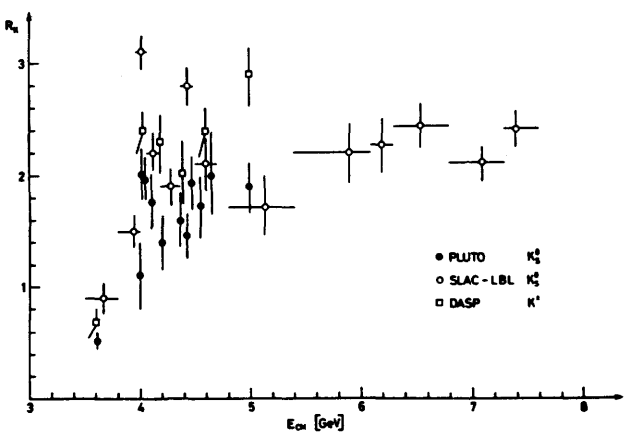

Fig. 4.10

4.42 Inclusive electron yields

Charmed particles can decay by weak interaction to final states containing only hadrons or also leptons (semileptonic decays) (see chap. 5). As a consequence one expects a step in the cross section for electron production. Indeed since ordinary hadrons have very small branching ratios for the decay into electrons, the cross section for electron production should jump from practically zero to a large value at charm threshold. The electrons originating from charm decays are accompanied by several hadrons since e.g. $e^+e^- \to D\bar{D} \to (D \to K\ e\ \nu) + (\bar{D} \to \text{hadron})$. The decay of a heavy lepton on the other hand leads preferentially to 2 prong final states, e.g. $e^+e^- \to \tau\bar{\tau} \to (\tau \to e\ \nu\nu) + (\bar{\tau} \to \mu\nu\nu)$. Therefore the electron yield is measured for events containing 2 or more additional prongs besides the identified electron.

Three groups have measured inclusive electron spectra. DASP[80)126)] and DELCO[86)] use Cerenkov counters for electron identification, whereas MARK 1 [98)] has recently be complemented by a lead glass wall. The results of the three groups are presented in fig. 4.11.

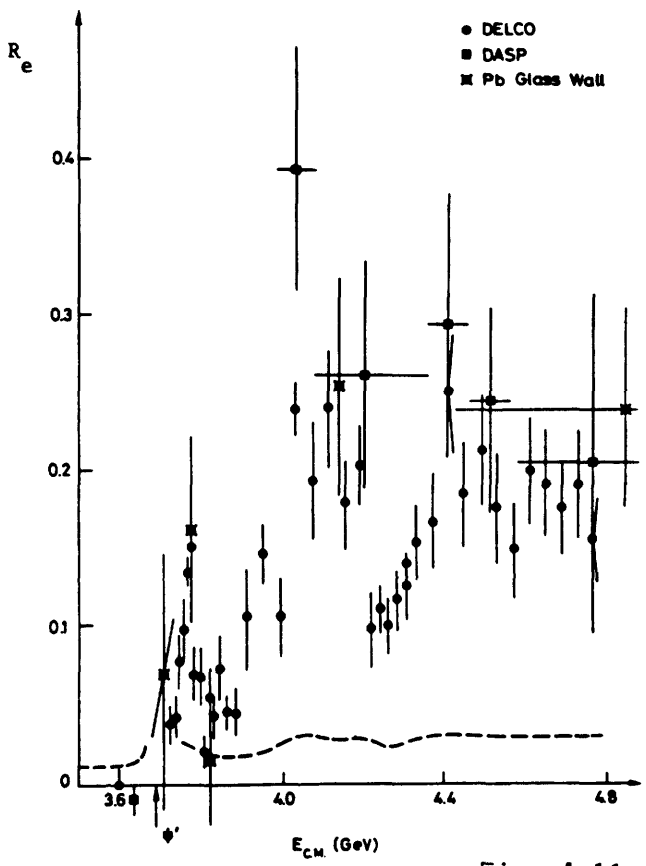

Fig. 4.11

Indeed, one notices the rise of $R_e = \sigma(e^+e^- \to e + \text{anything}) \,/\, \sigma(e^+e^- \to \mu^+\mu^-)$ from zero below charm threshold to values of the order of 0.2 above 4.0 GeV. A peak can also be seen at the 3772 GeV resonance. There is a marked difference between the DASP and DELCO data around 4.2 GeV. The dip seen by DELCO at 4.25 GeV is not present in the DASP data but this may be due to the averaging of the DASP data over 300 MeV. The dip may even be consistent with no charm production since the separation of the lepton decays was not perfect and hence the value of R_e at the dip could be entirely associated to τ decays. It should be noted that also the total cross section has a dip at that energy (see 4.2).

One can now attempt to calculate the branching ratio B_e of the charmed mesons into electrons:

$$B_e = \frac{\Gamma\,(D \to e + \text{anything})}{\Gamma\,(D \to \text{anything})} = \frac{R'_e}{2\,R_{charm}} \qquad (4.4)$$

R'_e is derived from R_e as shown in fig. 4.11 by correcting for losses of electrons at low momenta and of events with 2 charged tracks and by subtracting the contributions from τ decay (10 to 20 %). Furthermore $R_{charm} = R - R_\tau - R_{old}$, where R_{old} is the R-value below charm threshold.

The results are shown in fig. 4.12. The SPEAR data tend to be lower than the DASP-results which is mainly due to the difference in R used to calculate B_e.
Fig. 4.12 demonstrates that B_e does not change much with energy. This is remarkable since at higher energies F mesons and charmed baryons can contribute. The constancy of B_e can either mean that F and baryon production is negligible or that the branching ratios of these particles are similar to those of the D meson.

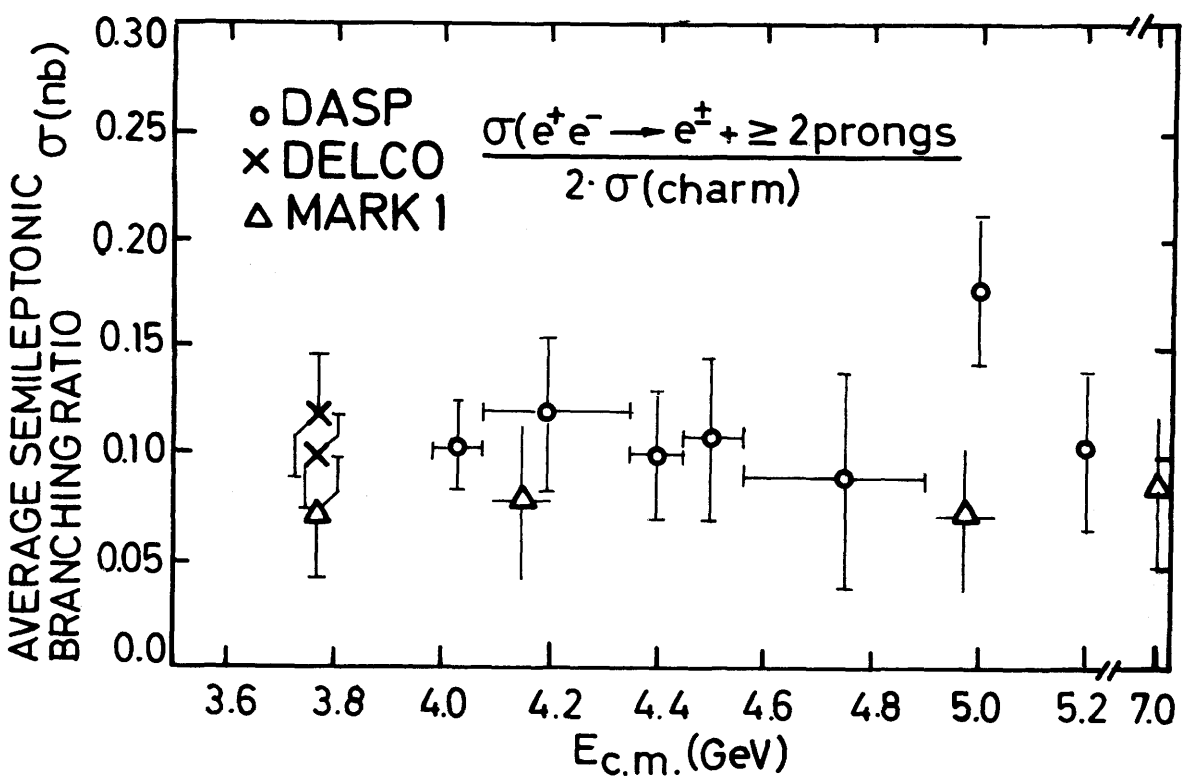

Fig. 4.12

4.43 Inclusive η production

Kaons in the final state indicate the decays of D mesons, the appearance of η is a sign of F decays (see chap. 5). The inclusive yield of η offers therefore an interesting possibility to find energies where F production is appreciable.

Unfortunately the signature to identify a η decaying into 2γ is not very strong and therefore it seemed for sometime very unlikely to find them at all. A solution to this problem was found by the DASP[80)99)123)] collaboration. Instead of looking for the reaction $e^+e^- \to F\bar{F}$ they tried to observe $e^+e^- \to F\bar{F}^*$. The F^* decays $F^* \to \gamma F$ and with an estimated photon energy of about 100 MeV (see chap. 2.22) this low energy photon yields an additional signature. With $F \to \eta\pi \to \gamma\gamma\pi$ one arrives at final states containing 3 photons, 2 originating from the η and one having low energy. The invariant mass distributions for two photons are shown[123)] for different energies in fig. 4.13a and b. For the energy interval 4.36 to 4.48 GeV a clear η signal can be seen besides a π^0 peak. For the other energy intervals no η signal appears. If the background is subtracted one obtains the inclusive η yield as function of the e^+e^- energy, as presented in fig. 4.14. The cross section is consistent with zero except at 4.4 GeV, where almost all of the η mesons are accompanied by a low energy photon. A rough estimate gives a value $\sigma_\eta \cdot \langle n_\eta \rangle \sim$ few nb, where σ_η is the production cross section and $\langle n_\eta \rangle$ the average multiplicity. These data indicate that η production is strong at the 4.4 GeV resonance but small everywhere else. This might indicate a similar behaviour as for D production where $D\bar{D}^*$ production is dominant somewhat above threshold (see chap. 4.33). Exactly because of this analogy the F search was started around $E_{cm} \approx 4.4$ GeV.

Recently the analysis of events containing η could be improved[123)] and as a result the requirement of having a low energy photon in the final state could be dropped. Hence a search for η originating from $e^+e^- \to F\bar{F}$ became possible. A clear η signal was found in the energy interval 4.10 to 4.22 GeV (fig. 4.15) which is just above the threshold at 4.06 GeV. No η's were observed in the energy interval 4.00 to 4.06 GeV as is expected. This F production just above threshold can be compared to D production at 3.77 GeV and should be an ideal source to study F decays. Indeed electrons indicating semileptonic decays have been observed (fig. 4.15).

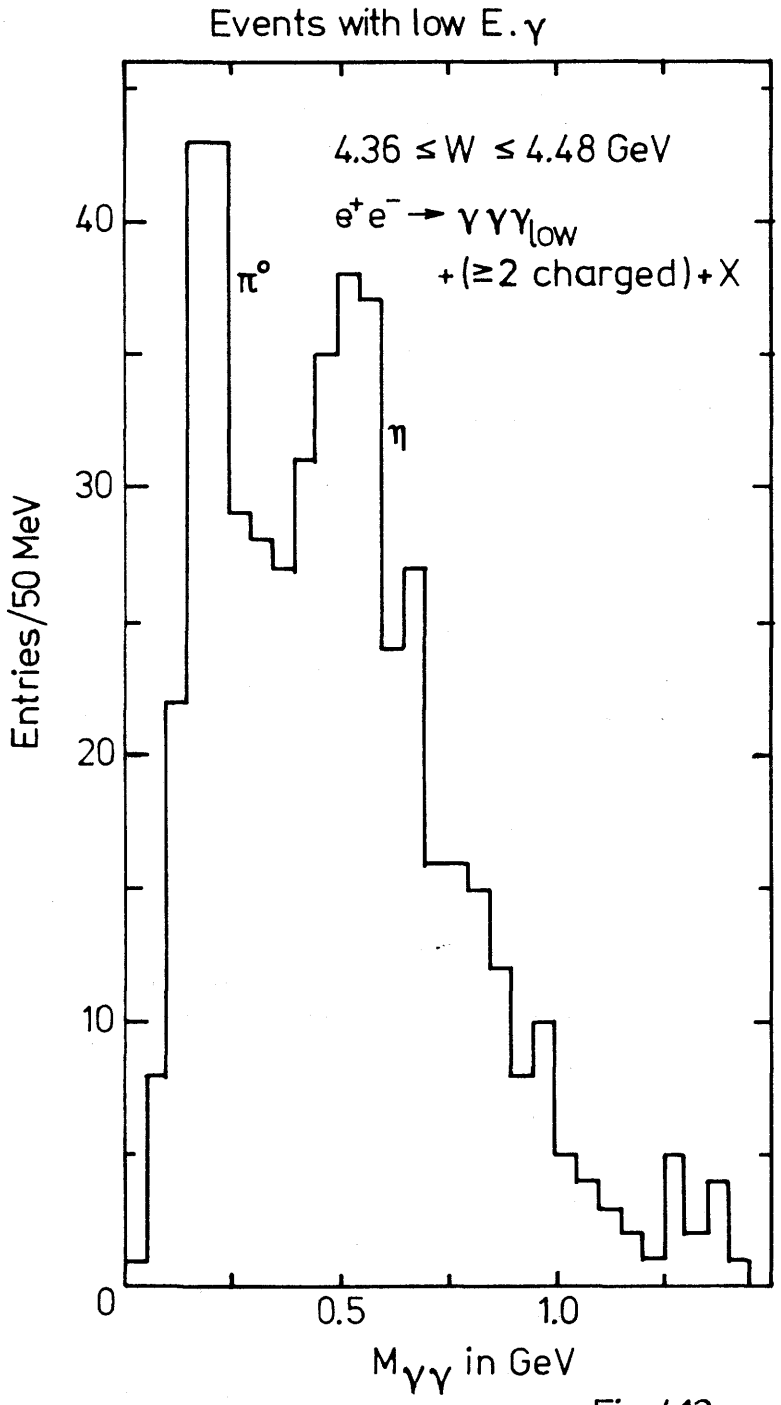
Events with low E.γ
4.36 ≤ W ≤ 4.48 GeV
e⁺e⁻ → γγγ_low
+ (≥2 charged) + X
π°
η
Entries/50 MeV
0
10
20
30
40
0.5
1.0
M_γγ in GeV

Fig. 4.13 a

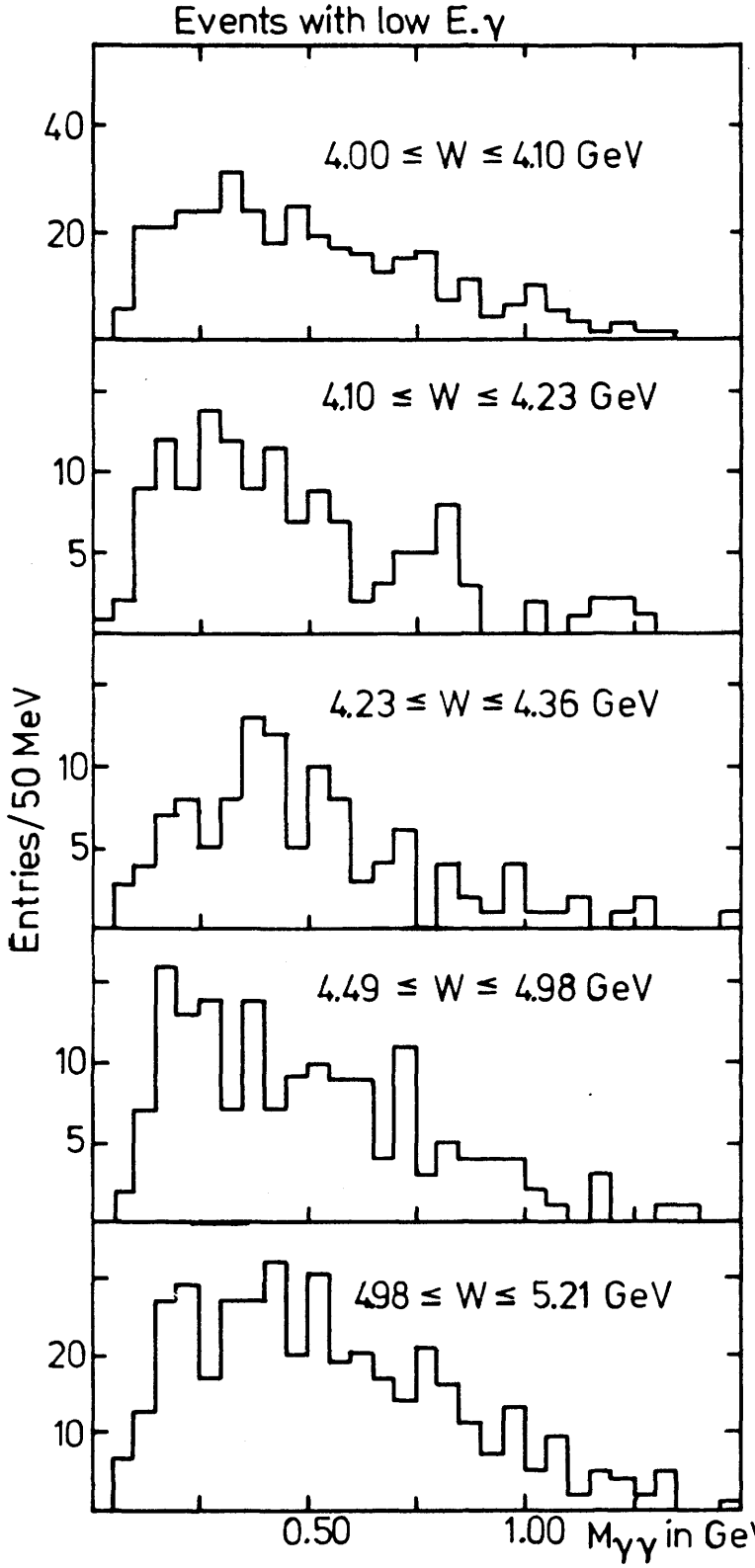
Events with low E.γ
4.00 ≤ W ≤ 4.10 GeV
4.10 ≤ W ≤ 4.23 GeV
4.23 ≤ W ≤ 4.36 GeV
4.49 ≤ W ≤ 4.98 GeV
4.98 ≤ W ≤ 5.21 GeV
Entries/50 MeV
0.50
1.00
Mγγ in GeV

Fig. 4.13 b

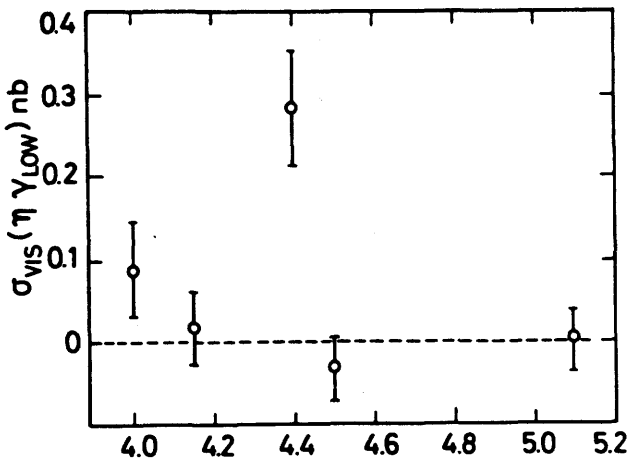

Fig. 4.14

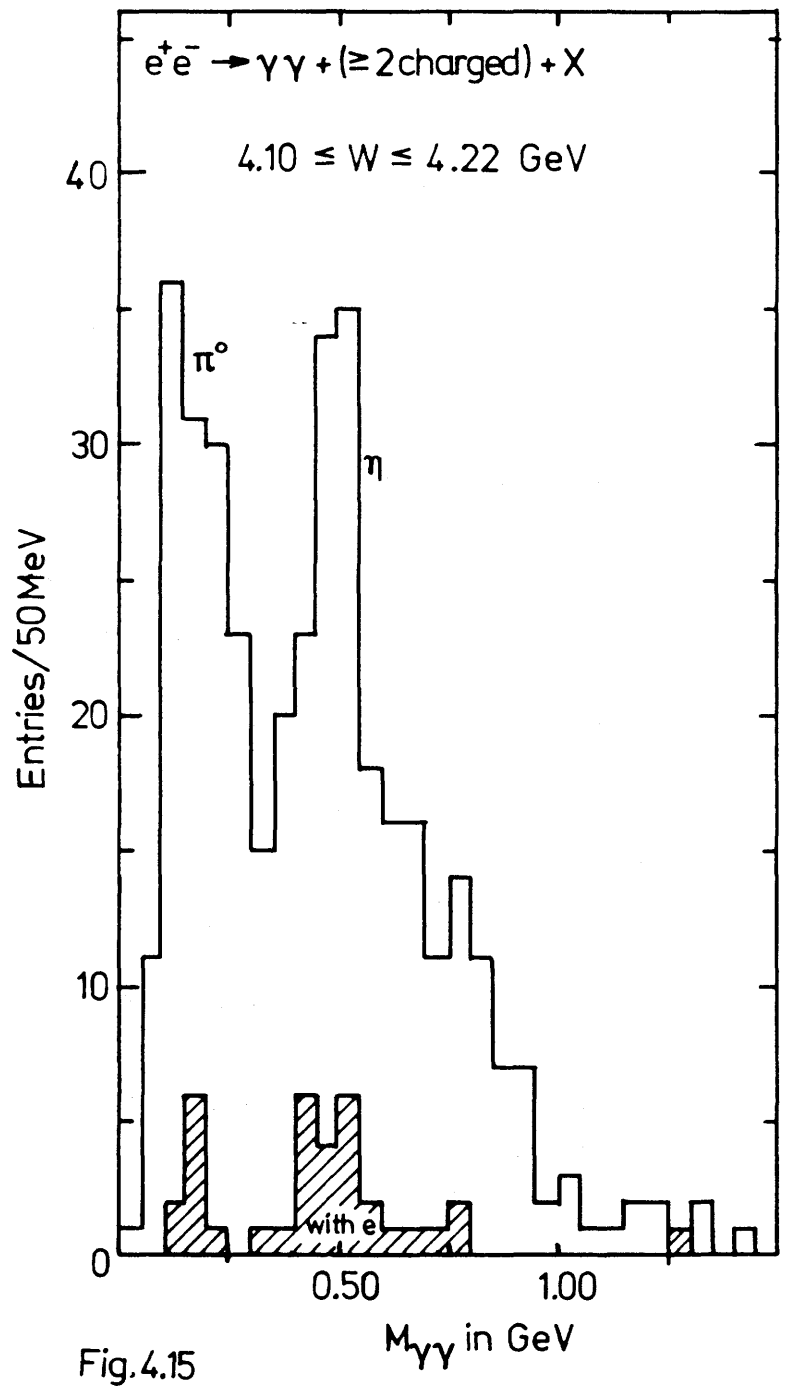

Fig. 4.15

4.44 Inclusive ρ_0, antinucleon and strange particle production

Inclusive η_0 production has been reported by PLUTO[79]. The ρ_0 spectrum follows the same exponential shape as found for charged pions but the absolute cross section is about a factor of 2 higher. The yield as function of the e^+e^- energy is shown in fig. 4.16. The large error bars indicate systematic

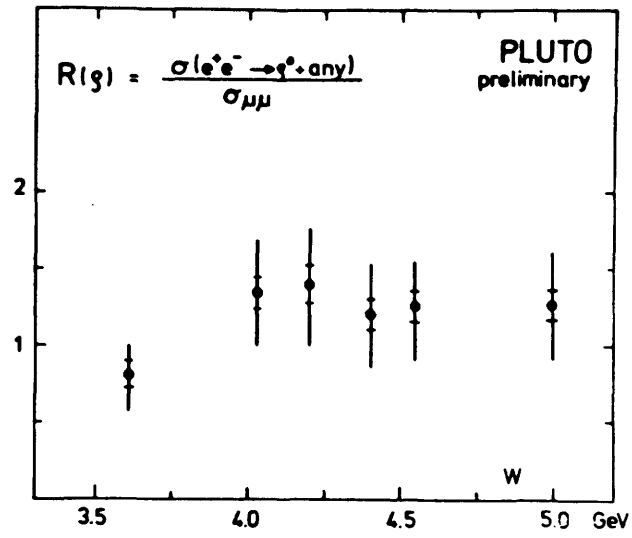

4.16

errors which are independent of energy. The data, therefore, exhibit a step just below 4 GeV, the threshold of charm, but also of heavy lepton production. The average value of $R(\rho^0) \approx 1.3$ for $W > 4$ GeV may be used to estimate which fraction of charged pions comes from vector mesons. The result is that more than 50 % of all pions originate from vector mesons. Predominance of vector mesons over pseudoscalars is expected from the quark model simply on the basis of statistical spin factors.

The observation of antinucleons and strange baryons is very interesting since it can indicate the production of charmed baryons. Some early results for $\bar{p}$ production have been obtained by DASP[100] (fig. 4.17). Very nice results from the MARK 1 detector have been published recently[101] (fig. 4.18) for $\bar{p}$ and $\Lambda + \bar{\Lambda}$ production. The antiprotons were identified by TOF measurements. The difference of $R(\bar{p} + p) = 2R(\bar{p})$ between the DASP and MARK 1 data is probably due to different cut-offs at low $\bar{p}$ momenta. The data indicate a rise by a factor of about 2 in the region between 4 and 5 GeV.

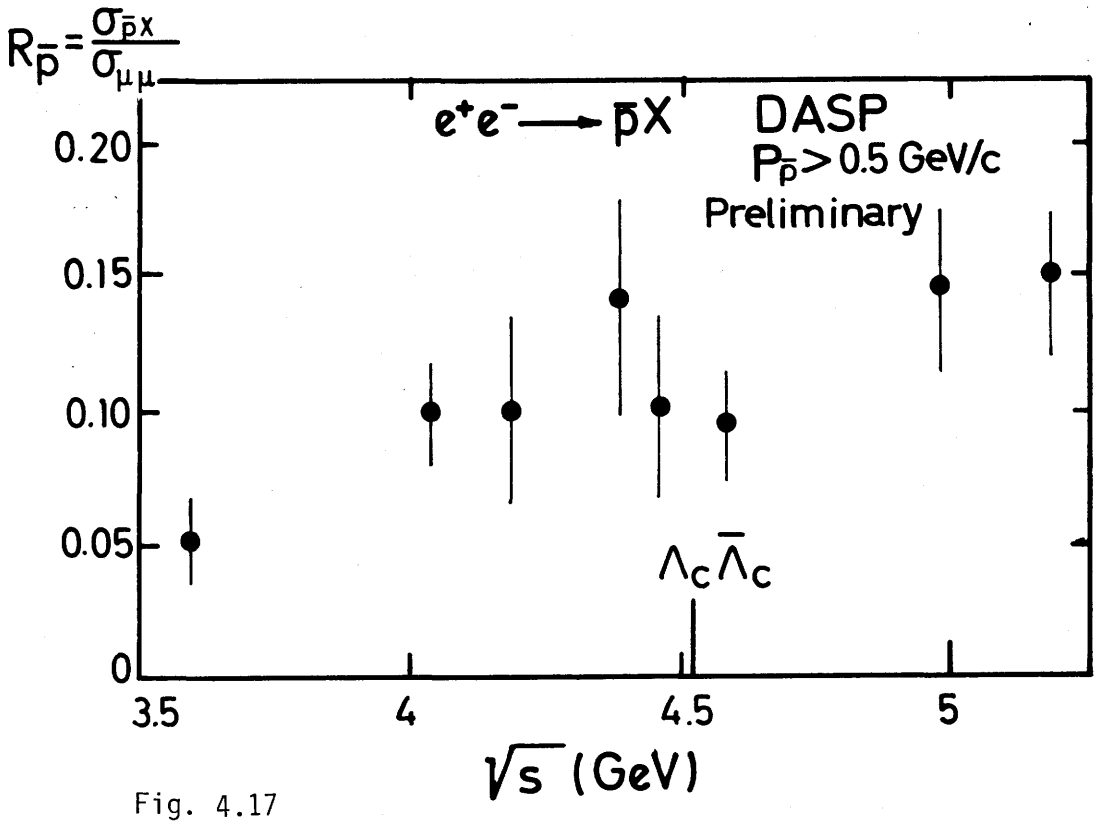

Fig. 4.17

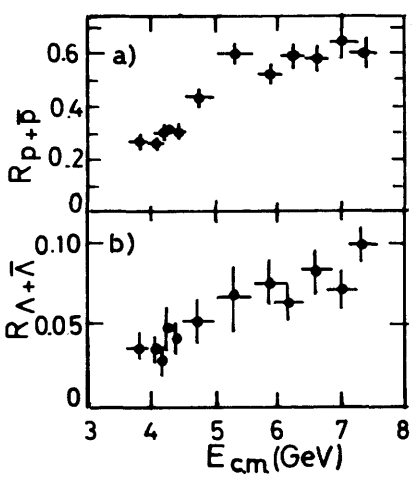

Fig. 4.18

The increase of the cross sections coincides with the expected thresholds for singly charmed baryons (strangeness 0 or 1) around 4.4 GeV. If the increase is indeed due to charmed baryon production, the ratio of charmed baryons to uncharmed baryon production is about the same as the corresponding ratios for mesons.

$R(\Lambda+\bar{\Lambda})$ is about 10 to 15 % of $R(p + \bar{p}) = 2R(\bar{p})$. The smallness of this figure indicates that the weak decays of charmed baryons prefer modes with nucleon plus strange meson and pions in the final state instead of Λ's.

The production of anti-sigmas has been measured by the UCLA-SLAC collboration[89]. The $\bar{\Sigma}$ were identified by combining the $\bar{n}$ with a $\pi^{\pm}$ in a mass plot. The $\bar{n}$ were detected through their annihilation properties, and their momentum was measured by TOF. At an e^+e^- energy of 7 GeV 27 events were observed, but practically none at 4 GeV. This gives an increase of $\Delta R(\Sigma^{\pm}) = 0.11 \pm 0.05$.

The most direct evidence for the production of charmed baryons in e^+e^- annihilation would be the observation of a peak in the mass distribution of the expected decay particles. This has not been achieved so far and a comparison with the two charmed baryon candidates found in photo[102] and neutrino[103] production is not yet possible. Here is a rich yet uncovered field for e^+e^- experimentation, although it seems that baryon production cross sections are in general relatively small.

5. Charmed Mesons and their Weak Decays

As we saw in preceeding chapters, the charm hypothesis[106,107] can explain most of the experimental findings connected with the $c\bar{c}$-system. The final proof for charm comes from the detection of mesons consisting of a charm quark and a light antiquark and their anti particles. Of course, one expects that according to the two relative spin orientations each $c\bar{q}$ state occurs as para (J = 0) and ortho (S = 1) particle. The following nomenclature is generally accepted:

C = +1:	$D^+ = c\bar{d}$,	$D^0 = c\bar{u}$,	$F^+ = c\bar{s}$	pseudoscalars
C = -1:	$D^- = \bar{c}d$,	$\bar{D}^0 = \bar{c}u$,	$F^- = \bar{c}s$	J = 0
	$D^{*+} = c\bar{d}$,	$D^{*0} = c\bar{u}$,	$F^{*+} = c\bar{s}$	vectors
	etc.			J = 1

The D^+ and D^0 form an isodoublett, whereas F^+ is an isosinglett (see chap. 1.21).

The masses of these particles were predicted[3,23,34] with astonishing accuracy on the basis of the naive model (chap. 2). The experimental masses are collected in Table 1b. The great triumph of the charm model is the existence of all the $c\bar{q}$ states that had been predicted, at least for the states where c and $\bar{q}$ have orbital angular momentum zero. P-states for the $c\bar{u}$ and $c\bar{d}$ system have been predicted with the following masses[23,24]:

$$D(1^1P_1) \simeq 2.5 \text{ GeV}$$
$$D(1^3P_0) \simeq 2.4 \text{ GeV}$$
$$D(1^3P_1) \simeq 2.6 \text{ GeV}$$
$$D(1^3P_2) \simeq 2.6 \text{ GeV}$$

None os these states has been identified so far.

The excited states can decay to the ground states by hadronic or electromagnetic interaction, e.g. $D^* \to D + \pi$, $D^* \to D + \gamma$ or $F^* \to F + \gamma$ (see chap. 5.4). The higher states are therefore expected to have rather large widths. The ground states (predicted to be the pseudoscalar states), however, can decay only by weak interaction and hence should be quite narrow. This is because the strong interaction conserves charm charge and therefore a $c\bar{q}$ system is stable, whereas the weak interaction can convert a c-quark to light quark.

In order to discuss the weak decays of the D and F mesons we shall very briefly recall the structure of weak interactions in its simplest form.

5.1 Minimal theory of weak interactions

The minimal formalism[1o9,11o,111] of weak interaction is based on $SU(2)^W$ doubletts. Assuming that there are 4 leptons and 4 quarks one has

Q	Leptons	Quarks	Q
0	$\begin{pmatrix}\nu_e\\ e^-\end{pmatrix}_L$ $\begin{pmatrix}\nu_\mu\\ \mu\end{pmatrix}_L$	$\begin{pmatrix}u\\ d'\end{pmatrix}_L$ $\begin{pmatrix}c\\ s'\end{pmatrix}_L$	2/3
- 1			-1/3

All these doublets contain left-handed particles. The right-handed quarks and leptons are singlets under $SU(2)^W$. (For larger groups see for example[1o8] and chap. 6.)

Each doublet gives rise to a current $\overline{q_1}\gamma_\mu \frac{1+\gamma_5}{2} q_2=(\overline{q}_1 q_2)$ or $\overline{\ell_1}\gamma_\mu \frac{1+\gamma_5}{2} \ell_2=(\overline{\ell}_1 \ell_2)$ where q and ℓ stand for a quark and lepton, respectively and 1 and 2 belong to the same doublet. In the following we shall use the abbreviation $(\overline{q}_1 q_2)$ and $(\overline{\ell}_1 \ell_2)$. A V-A coupling is assumed.

The d and s quarks are eigenstates of the strong interaction. This need not be true for the weak interaction. Hence the most general possibility is the Cabibbo structure, which allows mixing between isodoublets. As can be shown the most general case for 4 quarks is covered by the rotation[1o8]

$$\begin{aligned} d' &= d \cdot \cos\Theta + s \cdot \sin\Theta \\ s' &= -d \cdot \sin\Theta + s \cdot \cos\Theta \end{aligned} \qquad (5.1)$$

Where Θ is the Cabibbo angle.
A mixing for the leptons has no physical meaning if the neutrino masses are zero, since in this case the rotated as well as the unrotated states are eigenvalues of the mass matrix. The mixing between quarks ensures that there is only one conserved baryon number whereas the non-mixing of neutrinos results in separately conserved electron and muon lepton charges.

The effective weak Hamiltonian in lowest order is given by

$$H^{weak} = \frac{4G_F}{\sqrt{2}} (J_\ell + J_h)(J_\ell + J_h)^\dagger \tag{5.2}$$

The lepton current J_ℓ and the hadron current J_h can both be split in a charged current J^C and a neutral current J^N with

$$\begin{aligned} J_\ell^C &= (\bar{\nu}_e\, e) + (\bar{\nu}_\mu \mu) \\ J_\ell^N &= (\bar{\nu}_e\, \nu_e) + (\bar{\nu}_\mu\, \bar{\nu}_\mu) - (\bar{e}e) - (\bar{\mu}\mu) \end{aligned} \tag{5.3}$$

$$\begin{aligned} J_h^C &= (\bar{u}d') + (\bar{c}s') \\ &= \cos\Theta(\bar{u}d + \bar{c}s) + \sin\Theta\,(\bar{u}s - \bar{c}d) \end{aligned} \tag{5.4}$$

$$\begin{aligned} J_h^N &= \bar{u}u + \bar{c}c - \bar{d}'d' - s's - \sin^2\Theta_W J_{e\ell} \\ &= \bar{u}u + \bar{c}c - \bar{d}d - \bar{s}s - \sin^2\Theta_W J_{e\ell} \end{aligned} \tag{5.5}$$

In (5.5) the electromagnetic current $J_{e\ell}$ has been added and the Weinberg angle[111] Θ_W is the $SU(2)^W \times U(1)$ mixing angle. We shall not be concerned here with the unification of electromagnetic and weak interaction but for completeness the following relations may be quoted:

$$\begin{aligned} &\frac{4G_F}{\sqrt{2}} = \frac{g^2}{2M_W^2}\,, \quad M_W = \frac{37.3\ \text{GeV}}{\sin\Theta_W}\,, \\ &e/g = \sin\Theta_W, \quad M_Z = M_W/\cos\Theta_W \end{aligned} \tag{5.6}$$

where g is the SU(2) coupling constant, and M_W, M_Z are the masses of the charged and neutral intermediate boson.

More important for the following discussion is the GIM mechanism[107]. The existence of the charm quark had been postulated in order to explain the absence of strangeness changing neutral currents as in the decays $K^o \to \mu^+\mu^-$ or $K \to \pi\, \nu\, \bar{\nu}$. The hadronic neutral current (5.5) is invariant under rotations in the Cabibbo angle, as can be seen explicitly. J_h^N does not contain Θ and in particular the terms $\sin\Theta \cdot \cos\Theta\,(\bar{d}s + \bar{s}d)$ are cancelled. Hence transitions between the d and s quark are forbidden and the missing of the $|\Delta S| = 1$ K-decays is thus explained. However, the GIM mechanism automatically forbids also the neutral transitions between u and c quark. The experimental evidence for this expectation will be discussed later.

The charged hadronic current (5.4) contains two parts. One is proportional to $\cos\Theta$ involving the transitions $u \leftrightarrow d$ and $c \leftrightarrow s$. The other contains the factor $\sin\Theta$ associated to the transitions $u \leftrightarrow s$ and $c \leftrightarrow d$. From the hinderance of strange particle decays relative to non-strange decays one finds $\sin\Theta \approx 0.2$. Hence one calls the decays proportional to $\cos\Theta$ Cabibbo allowed and those involving $\sin\Theta$ Cabibbo forbidden.

The behaviour of the hadronic currents can nicely be summarized in fig. 5.1. Each corner of the square represents a quark whose charge is indicated in brackets.

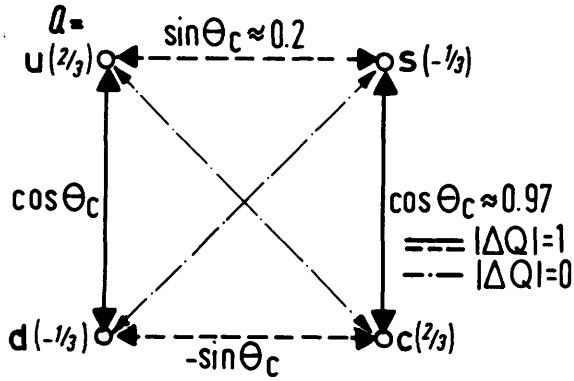

Fig. 5.1

The full arrows show the Cabibbo allowed, the broken arrows the Cabibbo forbidden decays. Both involve a change of the electric charge by one unit.

Neutral current transitions would have to be represented by diagonal arrows. The transition $d \leftrightarrow s$ has $|\Delta S| = 1$ and the transition $u \leftrightarrow c$ has $|\Delta C| = 1$. These strangness or charm changing neutral currents are cancelled by the GIM mechanism since the amplitude going from s to d via u is proportional to $\sin\Theta \cos\Theta$ whereas via c a factor $-\sin\Theta \cdot \cos\Theta$ is picked up and these two contributions cancel each other. Similarly the transition $u \leftrightarrow c$ via s and d is cancelled. The only neutral currents which exist connect each corner of the square to itself, e.g. $u \leftrightarrow u$.

It might be mentioned that the c-quark was not only invented for the GIM mechanism but also establishes symmetry between quarks and leptons. One consequence is that the sum of all fermion charges is zero (counting the quark charged three times because of colour) ensuring the absence of anomalies as required in renormalizable theories.

The most important message we get from this structure of weak interactions for the detection of charmed particles is the strong coupling between c and s, resulting in a predominance of strange particles in D and F decays. More specifically one has the diagrams

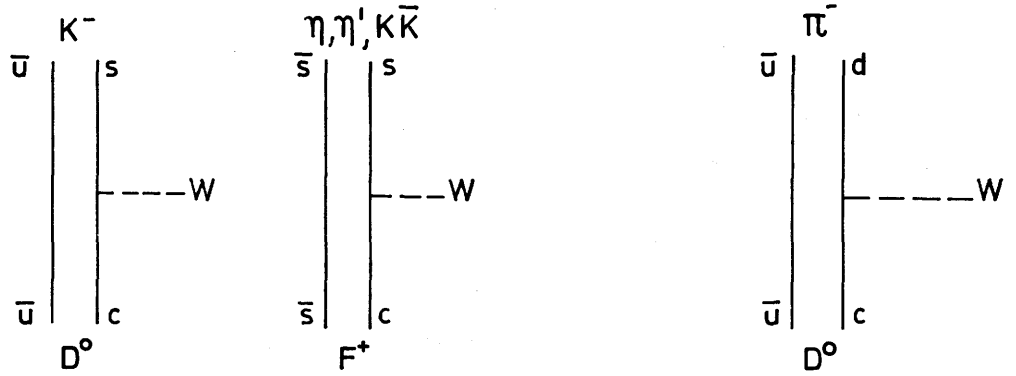

Cabibbo allowed (~ cosΘ) forbidden (~sinΘ)

where the W boson can couple on the right side to leptons (semileptonic decays) or quarks (hadronic decays). In both cases D^0 decays preferentially into K and F into η, η'. Therefore these strange particles in the final state are important signatures to observe the D and F.

5.11 Leptonic decays of D and F

From (5.4) it can be seen that the Cabibbo allowed decay transforms c↔s whereas c↔d is suppressed by tgΘ in the amplitude. Hence one expects the following decays with leptons only in the final state

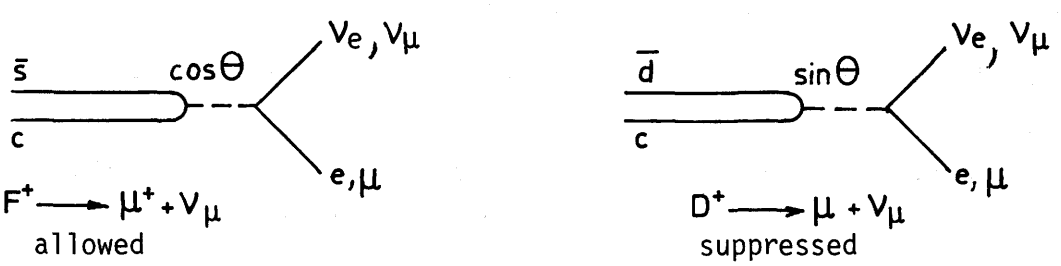

The decay $F^+ \to \mu^+ \nu_\mu$ is analogous to $\pi^- \to \mu^- \bar{\nu}_\mu$ or $K^- \to \mu^- \bar{\nu}_\mu$. Hence one expects for its decay rate[112)]

$$\Gamma(F\to\mu\nu) = \Gamma(K\to\mu\nu)\left|\frac{f_F}{f_K}\right| \operatorname{ctg}\Theta^2 \cdot \left(\frac{m_K}{m_f}\right)^3 \cdot \frac{m_F^2 - m_\mu^2}{m_K^2 - m_\mu^2} \cdot \qquad (5.7)$$

Assuming that the decay constants f_F and f_K are equal, one finds with $m_F = 2.03$ GeV

$$\Gamma(F\to\mu\nu) \simeq 4.2\times 10^9\ s^{-1}. \qquad (5.8)$$

The actual value could be larger by a factor of ~ 2 since one expects $f_F \gtrsim f_K \gtrsim f_\pi$ and indeed $f_K \simeq 1.28\ f_\pi$.

As will be shown later the decay width into hadrons is of the order $\Gamma_{tot}(F) \simeq 10^{13}\ s^{-1}$ and hence the branching ratio $B(F\to\mu\nu) \simeq 10^{-3}$ to 10^{-4} which is very small. However, the μ spectrum is characteristic for a two-body decay and might be observable.

The decay $F^+\to e^+\nu_e$ is suppressed relative to (5.7) by a factor $(m_e/m_\mu)^2$ and is negligible.

The particularly interesting decay $F^+\to\tau\nu_\tau$ is unfortunately very difficult to observe.

The leptonic decays of D particles are Cabibbo forbidden and hence are retarded by a factor $\operatorname{tg}^2\Theta \approx 0.05$ with respect to allowed decays. As a consequence their branching ratios are very small.

In summary it can be stated that leptonic decays of D and F are very weak and indeed have not been observed so far.

5.12 Semileptonic decays of D and F mesons

Such decays are of particular interest since they offer the cleanest way to study the charm current. This is because they originate from the product $J_\ell^+ J_h$ (see 5.2) which implies that the hadronic current appears only once and is multiplied by the well known leptonic current. The two possible decay modes are:

decay	amplitude	ΔS	ΔI	
$c\to s\,\ell^+\nu_e$	$\cos\Theta$	1	0	$\Delta Q = \Delta C = \Delta S$
$c\to d\,\ell^+\nu_e$	$-\sin\Theta$	0	1/2	$\Delta Q = \Delta C = \lvert 1\rvert$

If the c-quark is combined eather with $\bar{u}$ or $\bar{s}$ one has the following decays:

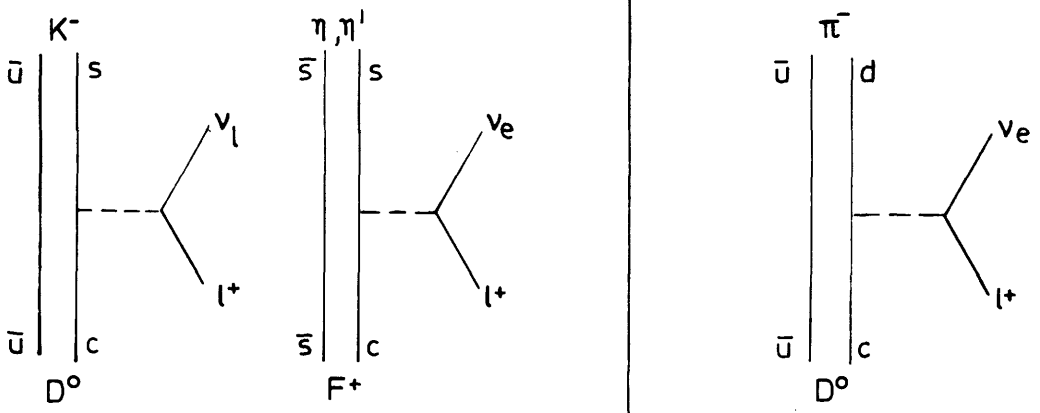

allowed forbidden

The decay rates can be estimated using symmetry arguments and making assumptions about the form factors[112,114]. One finds for example[112,114]

$$\Gamma(D^0 \to K^- e^+ \nu) \approx \left(\frac{m_D}{m_K}\right)^5 \cot^2 \Theta \cdot \Gamma(K^0 \to \pi^- e^+ \nu) \tag{5.9}$$

$$\Gamma(D^0 \to K^- \ell^+ \nu) \approx \Gamma(D^+ \to \bar{K}^0 \ell^+ \nu) \approx 1{,}4 \times 10^{11}\ s^{-1} \tag{5.10}$$

and with

$$\Gamma(D^0 \to K^{*-} \ell^+ \nu) \,/\, \Gamma(D^0 \to K^- \ell^+ \nu) \approx 0.54 \tag{5.11}$$

one obtains

$$\Gamma(D^0 \to K^{*-} \ell^+ \nu) \approx \Gamma(D^+ \to \bar{K}^{*0} \ell^+ \nu) \approx 0.7 \times 10^{11}\ s^{-1} \quad . \tag{5.12}$$

For the decays of the F meson one can derive similar expressions but they are less reliable because of η and η' mixing. Estimates are[112,114]

$$\begin{aligned} \Gamma(F^+ \to \phi\, \ell^+ \bar{\nu}_e) &\simeq 0.9 \times 10^{11}\ s^{-1} \\ \Gamma(F^+ \to \eta\, \ell^+ \bar{\nu}_e) &\simeq 1.1 \times 10^{11}\ s^{-1} \\ \Gamma(F^+ \to \eta'\, \ell^+ \bar{\nu}_e) &\simeq 0.3 \times 10^{11}\ s^{-1} \end{aligned} \tag{5.13}$$

implying

$$\Gamma(F \to \eta' \ell\, \bar{\nu}_e) \,/\, \Gamma(F \to \eta\, \ell\bar{\nu}) = 0.29 \tag{5.14}$$

The decay $F \to \omega\, \ell\, \nu$ is OZI suppressed since the ω has very little strange quark content.

For the Cabibbo forbidden decay one finds the estimate[113)]

$$\Gamma(D^0 \to \pi^- \ell\, \nu) \,/\, \Gamma(D^0 \to K^- \ell \nu) \simeq 2\, tg^2\, \Theta \simeq 0.1 \qquad (5.15)$$

and similar suppression factors for $D^+ \to \pi^0 \ell^+ \nu$ and $F^+ \to K^0 \ell^+ \nu$. The decay $F^+ \to \pi^0 \ell^+ \nu$ is Cabibbo and OZI suppressed and hence negligible.

Besides the transition rates one can calculate the momentum spectra of the leptons. These will be discussed below together with the experimental results.

Measurements of the ratios given above present an important test of the structure of the hadronic current. Significant violations could indicate new pieces in the hadronic currents.

5.13 Nonleptonic decays of D and F mesons

The understanding of nonleptonic decays is complicated by the influence of the strong interaction on the weak current product $J_h^c\, J_h^{c\dagger}$. Charmed and strange particle decays are differently affected[112)]:

1) asymptotic freedom suggests a reduced influence on charmed particle decay amplitudes
2) the quark field of strange particles contains the combination $c\bar{c} - u\bar{u}$ which couples to a gluon. In the Cabibbo-allowed decays of charmed particles, on the other hand, a corresponding coupling does not exist. For Cabibbo suppressed decays the combination $s\bar{s} - d\bar{d}$ has a small effective coupling to gluons.
3) two-body decays of charmed particles are more energetic and therefore less influenced by final state interactions.

5.131 Quark graphs for two-body nonleptonic decays

Because of the arguments given above two-body decays of charmed particle should be particularly suited to be described in terms of simple quark diagrams[112,114)]. Amplitudes are usually calculated using colour factors and exact SU(3) and ignoring gluons. This approach should allow to test the general structure of weak interactions involving c quarks. Corrections should be comparatively small to ratios of decay rates.

5.1311. Cabibbo allowed non-leptonic decays

The graphs are shown in fig. 5.2. Examples are the decays $D^0 \to K^-\pi^+$, $D^+ \to K^0\pi^+$ and $F^+ \to \eta\pi^+$. The diagrams on the right of fig. 5.2 are suppressed by a colour factor 1/9 compared to those on the left. This is because of the sum over the three colours in the outgoing meson for the diagrams on the left, whereas the colours must match in the diagrams on the right side and hence the colour enhancement is lacking. The decays of D^+ are

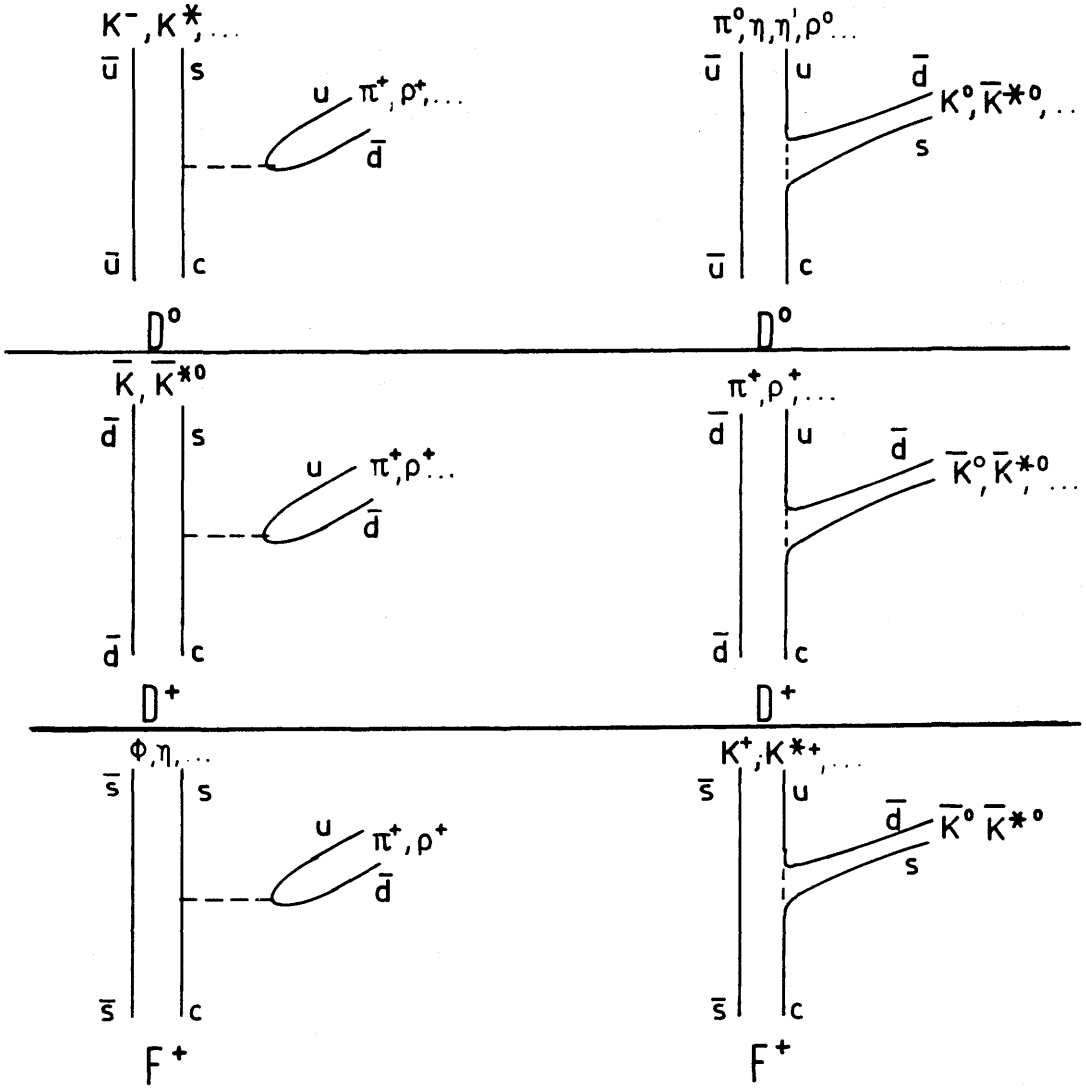

Fig. 5.2: Cabibbo allowed two-body decays of charmed particles

special since the two diagrams lead to the same final states and therefore add coherently.

One immediately finds many relations for the Cabibbo allowed decays:

$$\Gamma(D^0 \to K^-\pi^+) = 2\Gamma(F^+ \to \eta\pi^+) = (3/4)^2\,\Gamma(D^+ \to K^0\pi^+) = \\ = 18\,\Gamma(D^0 \to K^0\pi^0) = 9\,\Gamma(F^+ \to K^+K^0) \qquad (5.16)$$

One interesting consequence is the suppression of $F^+ \to K^+K^o$ which makes this decay unfavourable to look for F^+.

Decay rates for Cabibbo allowed decays have been calculated taking into account short distance gluon corrections, SU(3) breaking and form factors[112]. The results are given in table 5.1.

Table 5.1: Theoretical nonleptonic 2-body rates[112] of Cabibbo allowed decays of D and F

Decay mode	Decay width 10^{11} s^{-1}	Decay mode	Decay width 10^{11} s^{-1}
colour enhanced			
$D^o \to K^- \rho^+$	2.3	$D^o \to \bar{K}^{*o} \rho^+$	3.4
$K^{*-} \rho^+$	1.7	$\bar{K}^o \rho^+$	3.7
$K^- \pi^+$	1.7	$\bar{K}^{*o} \pi^+$	2.7
$K^{*-} \pi^+$	0.96	$\bar{K}^o \pi^+$	3.7
colour suppressed		colour enhanced	
$D^o \to \rho^o \bar{K}^{*o}$	0.14	$F^+ \to \phi\rho^+$	2.2
$\omega^o \bar{K}^{*o}$	0.14	$\eta\rho^+$	1.6
$\pi^o \bar{K}^{*o}$	0.22	$\eta'\rho^+$	0.5
$\eta \bar{K}^{*o}$	0.06	$\phi \pi^+$	1.1
$\eta' \bar{K}^{*o}$	0.0005	$\eta \pi^+$	1.1
$\rho^o \bar{K}^o$	0.09	$\eta' \pi^+$	0.6
$\omega \bar{K}^o$	0.08		
$\pi^o \bar{K}^o$	0.2	colour suppressed	
$\eta \bar{K}^o$	0.08	$F^+ \to K^{*+} \bar{K}^{*o}$	0.4
$\eta' \bar{K}^o$	0.03	$K^+ \bar{K}^{*o}$	0.5
		$K^{**} \bar{K}^o$	0.2
		$K^+ \bar{K}^o$	0.4

Besides the graphs shown in fig. 5.2 other graphs can contribute to two-body decays which are of two types

Fig. 5.3

The amplitudes for these graphs are multiplied by the factors $m_\pi^2/(m_F^2 - m_\pi^2)$ and $m_K^2/(m_D^2 - m_K^2)$, respectively, and hence they can be neglected relative to the graphs of fig. 5.2. The expectation

$$\frac{\Gamma(F^+ \to \rho^0\pi^+)}{\Gamma(F^+ \to \bar{K}^0K^+)} \ll 1 \qquad (5.17)$$

can be considered a significant test of the ideas underlying the quark graphs. If an additional $q\bar{q}$ pair is added to the final state of the left graph one obtains a prediction for the 3 body decay $F^+ \to \pi^+\pi^+\pi^-$

$$\frac{\Gamma(F^+ \to \pi^+\pi^+\pi^-)}{\Gamma(F^+ \to K^+K^-\pi^+)} \ll 1 \qquad (5.18)$$

which provides a similar test as (5.17).

5.1312 Cabibbo forbidden non leptonic decays

In non-leptonic decays the Cabibbo suppression proportional to $\sin\Theta$ can occur on either or both vertices. This is shown in fig. 5.4.

Fig. 5.4: Cabibbo forbidden non leptonic decays

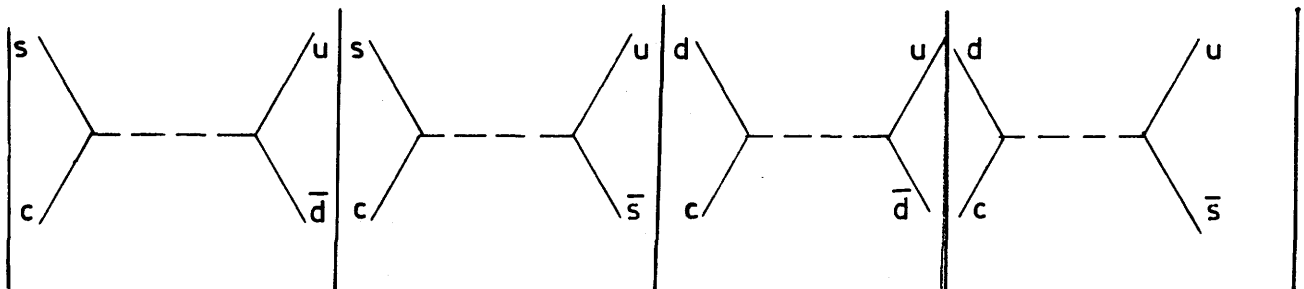

Δ S	1	0	0	-1
Δ I	1	1/2	1/2, 3/2	0,1
Amplitude ~	$\cos^2\Theta$	$\cos\Theta \cdot \sin\Theta$	$-\sin\Theta \cdot \cos\Theta$	$-\sin^2\Theta$
Example	$D^0 \to K^-\pi^+$	$D^0 \to \eta\eta'$	$D^0 \to \pi^+\pi^-$	$D^0 \to K^0\pi^0$

The corresponding single or double suppression factors are $tg^2\Theta \approx 0.05$ and $tg^4\Theta$, respecticely. From the graphs the following relations can be decuded[115]:

$$\frac{\Gamma(D^0 \to \pi^+\pi^-)}{\Gamma(D^0 \to K^-\pi^+)} = 2\,\frac{\Gamma(D^+ \to \pi^+\pi^0)}{\Gamma(D^+ \to K^0\pi^+)} = \frac{1}{2}\,\frac{\Gamma(F^+ \to K^0\pi^+)}{\Gamma(F^+ \to \eta\,\pi^+)} = 2\,\frac{\Gamma(F^+ \to K^+\pi^0)}{\Gamma(F^+ \to \bar{K}^0K^+)} \qquad (5.19)$$

All these ratios are of order $tg^2\Theta$.
For the singly suppressed decay $F^+ \to \eta K^+$ the decay rate is estimated[112] as $\Gamma(F^+ \to \eta\,K^+) = 0.05 \times 10^{11}\ s^{-1}$.

5.132 Sextet predominance

The part of the interaction that gives rise to non-leptonic decays is given by $J_h^c\,J_h^{c+}$ of (5.4). This part of the Hamiltonian transforms as a sum of the symmetric $\underset{\sim}{20}$ and $\underset{\sim}{84}$ representations of SU(4). Broken down into SU(3) representations one has

SU(4)	SU(3)	
	$\Delta C = 0$	$\lvert\Delta C\rvert = 1$
$\underset{\sim}{20}$	$\underset{\sim}{8}$ $(\Delta I = 1/2)$	$\underset{\sim}{6}$, $\overline{\underset{\sim}{6}}$
$\underset{\sim}{84}$	$\underset{\sim}{8}$,$\underset{\sim}{27}$ $(\Delta I = 3/2)$	$\underset{\sim}{15}$, $\overline{\underset{\sim}{15}}$

The decay $F^+ \to \pi^0\ell^+\nu$ is Cabibbo and OZI suppressed.

According to the well known $\Delta I = 1/2$ rule which was found experimentally, the non-leptonic decays of strange particles ($\Delta C = 0$) are enhanced. From the above table it is seen that this octet enhancement can be interpreted as 2o-plet enhancement in an exact SU(4). If this were true the octet enhancement should be associated to a sextet enhancement of the decays of charmed particles. Whether this concept is true is one of the interesting questions that can be answered from a study of non-leptonic decays of charm particles.

Of course, the predominance of the 2o-plet with respect to the 84-plet can be due either to an enhancement of the 2o-plet or a suppression of the 84-plet. An enhancement of the 2o-plet and consequently of the sextet would lead to a large non-leptonic decay rate and a small semileptonic branching ratio

for the D decays. The suppression of 84 and hence of 15 forbids the decay $D^+ \to K^0\pi^+$. As will be discussed below the semi-leptonic branching ratio for D decay is 11 ± 3 % which is not small and also the $D^+ \to K^0\pi^+$ decays have been observed. In conclusion it seems that there is no sextet predominance and a different explanation for the octet enhancement has to be found.

5.13a Multiparticle and inclusive decays and total decay rates

Decays of D and F mesons in many hadrons which are Cabibbo allowed are proportional to $\cos^4\Theta$ and have $\Delta C = \Delta S = \pm 1$. They can be written symbolically

$$\begin{aligned} D^0 &\to (\bar{K} + n\ \pi)^0 \\ D^+ &\to (\bar{K} + n\ \pi)^+ \\ F^+ &\to (\eta + n\ \pi)^+,\ (\eta' + n\pi)^+,\ (\bar{K}\ K + n\pi)^+ \end{aligned} \qquad (5.2o)$$

An example is the decay

$$D^+ \to K^-\ \pi^+\ \pi^+$$

quarks: $c\bar{d}$ $s\bar{u}$, $d\bar{u}$, $d\bar{u}$

with C = 1, S = 0 C = 0, S = -1, Q = +1

Such a final state having Q = +1, S = -1 is called "exotic" because it cannot be formed from an s quark and one $\bar{u}$ or $\bar{d}$ in the framework of SU(3) but rather needs 3 quarks. These exotic states with a strange particle are a signature of charmed particle decays. The decay to a non exotic state (total quark content $\bar{s}u$) like

$$\begin{array}{ccccc} D^+ & \to & K^+ & \pi^+ & \pi^- \\ & & \bar{s}u, & d\bar{u}, & u\bar{d} \end{array}$$

is unfavoured for charm particles, but allowed for normal particles like $K^{*+} \to K^+\pi^+\pi^-$.

The inclusive leptonic yield and the total hadronic width can be estimated[114,116] by comparing the graphs

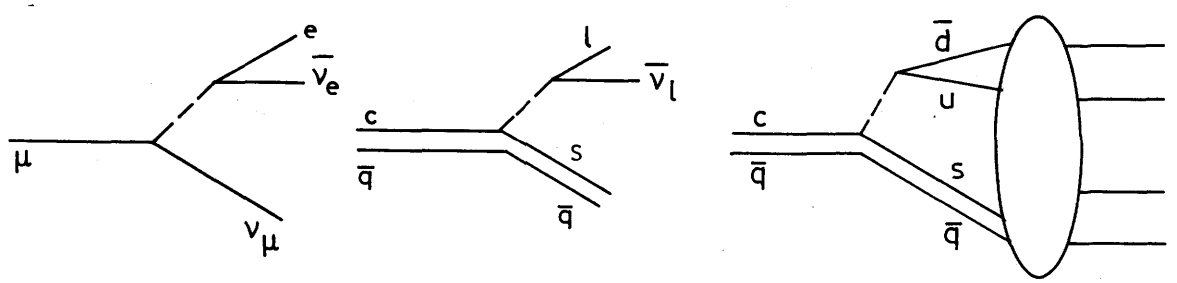

From the first two graphs one concludes

$$\Gamma(\text{charm} \to \ell\nu + \text{hadrons}) = \left(\frac{m_c}{m_\mu}\right)^5 \times \cos^2\Theta \times \Gamma(\mu \to e\nu\nu) = 0.7\times10^{12}\ s^{-1} \tag{5.21}$$

where m_c and m_μ are the c quark and μ mass, respectively and $\Gamma(\mu \to e\nu\nu) = 0.45 \times 10^6\ s^{-1}$.

Assuming that the final state interaction of the quarks indicated by the bubble in the diagram on the right goes with unit probability one finds

$$\Gamma(\text{charm} \to \text{hadrons}) = 3\left(\frac{m_c}{m_\mu}\right)^5 \times \cos^2\Theta \times \Gamma(\mu \to e\nu\nu) = 2.1 \times 10^{12}\ s^{-1} \tag{5.22}$$

where the factor 3 comes from the fact that $u\bar{d}$ occurs in three colours. If, however, a sextet enhancement as discussed in 5.132 exists $\Gamma(\text{charm} \to \text{hadrons})$ would increase by a factor of 20. If (5.21) and (5.22) are applied to D decay one expects a leptonic branching ratio

$$\frac{\Gamma(D \to \ell\,\nu K)}{\Gamma(D \to \text{hadron})} \approx \begin{cases} 30\ \% \text{ without sextet enhancement} \\ 1.5\ \% \text{ with sextet enhancement} \end{cases} \tag{5.23}$$

This provides an excellent possibility to test experimentally the existence of such an enhancement.

5.14 $D_o - \bar{D}_o$ mixing

If the life time of a D^o is sufficiently long it could mix with $\bar{D}^o$ by first order $|\Delta C| = 2$ neutral currents in a similar way as K^o and $\bar{K}^o$ mix by $|\Delta S| = 2$ currents[117]. If this were true nearly half of the decays of D^o would

decay as if it were a $\bar{D}^0$, e.g. to $K^+\pi^-$ instead of $K^-\pi^+$. An other way to look for D^0 - $\bar{D}^0$ mixing is in associated production of $D\bar{D}$, $D\bar{D}^*$ etc., where the kaon originating from the two charmed particles have opposite charge for no mixing (S conservation) and equal charge for mixing.

Mixing must compete with Cabibbo forbidden decays with $\Delta C = -\Delta S$ at a fractional level of order $\sin^4\Theta \sim 10^{-3}$ (see chap. 5.1312). A way to discriminate[115] between the two possibilities is through production and decay of $\psi(3722)$

$$e^+e^- \to \psi(3772) \to D^0 + \bar{D}^0 \longrightarrow \begin{cases} K^\pm K^\pm + \ldots \\ e^\pm e^\pm + \ldots \end{cases} \qquad (5.24)$$

The final state with two equally charged K arises through both mechanisms, whereas $e^\pm e^\pm$ solely through mixing provided the semileptonic $\Delta Q = \Delta C$ rule is valid.

Since $D_S^{0'}$ decay promptly in $\sim 10^{-13}$ s there is little time for mixing and hence the theoretical predictions for mixing are very small (much less than a percent, for literature see[113]).

5.2 Experimental results on D decays

The decisive confirmation for the charm idea introduced to explain the J/ψ particle and the other charmonium states is the existence of the charmed mesons D^0, D^+ and F^+ (see 1.21). Hence it is not surprising that a big effort was started very soon at SPEAR and at DORIS to find these particles. Initially this search was unsuccessful[118] and also the expected rise in the inclusive K-yield at charm threshold was not seen (see 4.41). The experimental work at SPEAR and DORIS was complementary since MARK 1 concentrated on the investigation of hadronic decays, whereas PLUTO and DASP were looking for semileptonic decays. Both kinds of searches became successful in spring 1976 after K-identification became possible at MARK 1 by time-of-flight measurements and electron identification was introduced at DASP by Cerenkov counters. PLUTO could establish for the first time e-K^0 correlations.

The observation of hadronic final states has the advantage that invariant and recoil masses can be measured. Hence beautiful and very precise mass values could be published from the SPEAR groups. This is not possible for the semileptonic decays since the neutrino remains undetected. However,

interesting information on the weak interaction could be extracted from the observation of these decays by the DORIS groups.

5.21 Hadronic decays of D mesons

The experimental results will not be described in their historical order but rather in a more systematic manner. We shall start with D meson production at the 3772 MeV resonance. This energy is below the threshold for D^* production and hence the decay of the 3772 MeV resonance provides a pure sample of D mesons.

5.211 D mesons from the 3.77 GeV resonance

The decay $\psi(3.77\ \text{GeV}) \to D\bar{D}$ is very close to threshold which allows a very precise determination of the D masses. The mass is calculated from $m = (E^2-p^2)^{1/2}$ where the energy E of the D must equal E_b, the energy of the incident beams. E_b is known very precisely and has a spread of about 1 MeV only. Being close to threshold $p^2 \simeq 0.08\ (\text{GeV/c})^2$ is small and thus any error in p is demagnified in its effect on the mass. As a result a mass resolution of about 3 MeV/c^2 can be obtained which is factor 5 to 10 better than normal mass resolutions (see chap. 1.13).

The data were collected[104] with MARK 1. Charged kaons are identified by time-of-flight measurements and neutral kaons by measuring the dipion mass and checking the consistency of the vertex position with the kaon decay time.

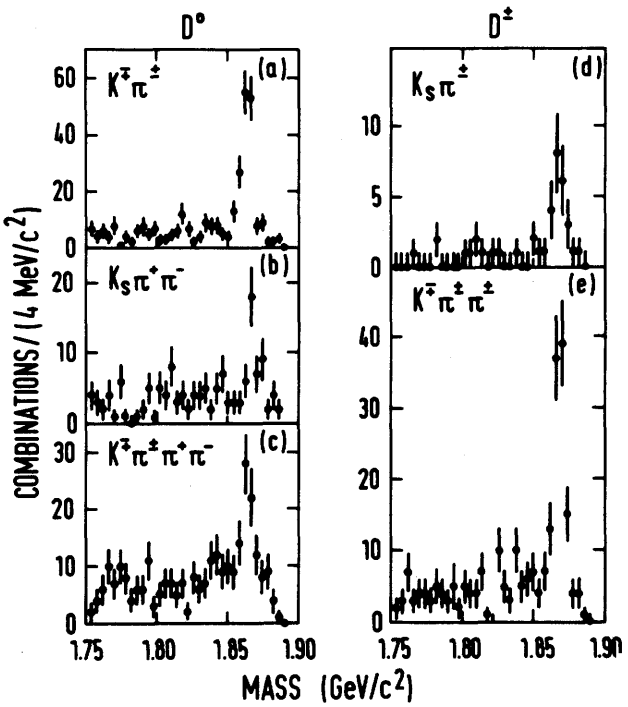

Fig. 5.5

The invariant mass spectra for different Kπ combinations are shown in fig. 5.5. Three clear mass peaks are seen in neutral final states and two decay modes for charged final states. With an additional lead glass counter also the decay into $K^{\mp} \pi^{\pm} \pi^0$ with direct observation of the π^0 could be seen[119].

The results on the masses are

$M(D^0) = 1863.3 \pm 0.9$ MeV/c^2

$M(D^+) = 1868.3 \pm 0.9$ MeV/c^2 and

$M(D^+) = M(D^0) = 5.0 \pm 0.8$ MeV/c^2

The mass difference is known more precisely since several systematic errors cancel.

The angular distribution of D's relative to the incident beams must be of the form $P(\theta) \sim (1+\alpha\cos^2\theta)$, $|\alpha| \leq 1$ for any D spin and $\alpha = -1$ for spin 0. Fig. 5.6 shows the angular distribution for D^+ and D^0 decays. The values of α are $\alpha = -1.04 \pm 0.10$ and -1.00 ± 0.09, respectively, consistent with the spin 0 assignment for the D mesons.

In order to verify that a $\bar{D}^0$ is produced together with a D^0 the recoil mass against the $K^{\pm}\pi^{\mp}$ system restricted to the D^0 mass has been determined. The result is shown in fig. 5.6a). A clear peak at the mass of the D^0 is seen. Thus associated production is verified which proves the conservation of the new quantum number charm.

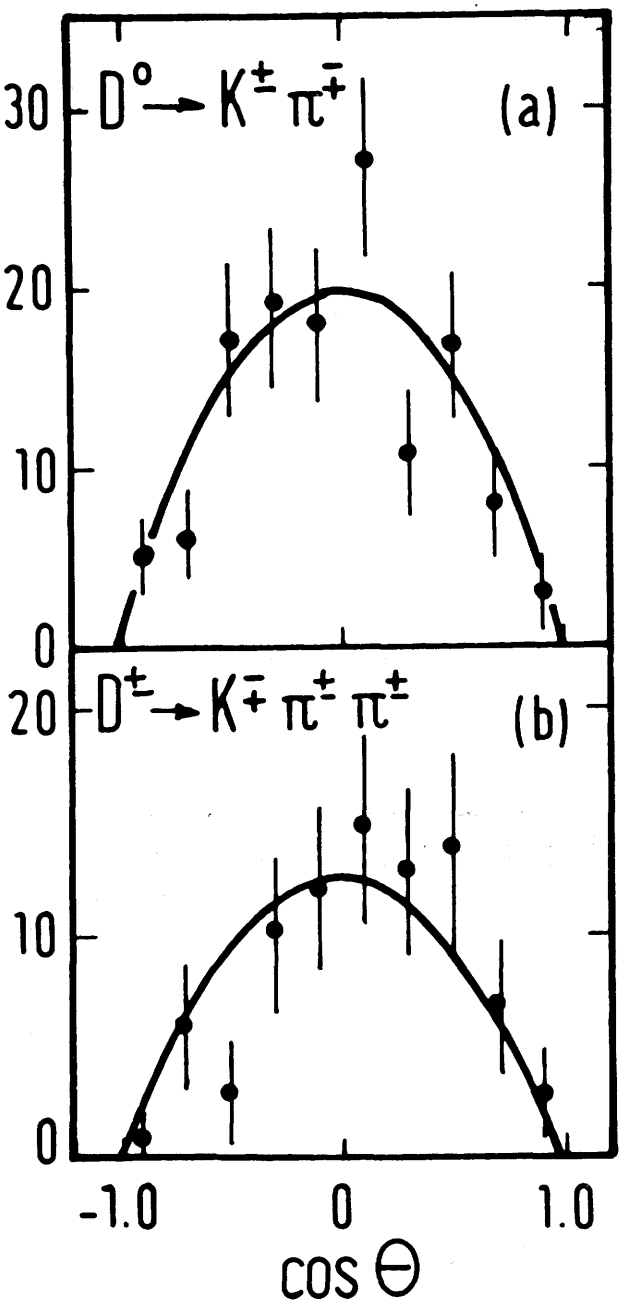

Fig. 5.6

An important point is that for D mesons originating from the 3.77 GeV branching ratios B can be determined, whereas at higher energies only $\sigma \cdot B$ can be given.
This requires, however, two assumptions: the $\psi(3.77)$ must have a definite isospin (0 or 1) and its only substantial decay mode is $D\bar{D}$. The results obtained under these assumptions are shown in table 5.2.

Table 5.2: D branching fractions

Mode		Branching fraction in %	Reference
$D^0 \rightarrow$	$K^-\pi^+$	2.2 ± 0.6	104
	$\bar{K}^0\pi^+\pi^-$	3.5 ± 1.1	
	$K^-\pi^+\pi^-\pi^+$	2.7 ± 0.9	
	$K^-\pi^+\pi^0$	12 ± 6	119
	$K^0\pi^0$	< 6	
$D^+ \rightarrow$	$\bar{K}^0\pi^+$	1.5 ± 0.6	104
	$K^-\pi^+\pi^+$	3.5 ± 0.9	

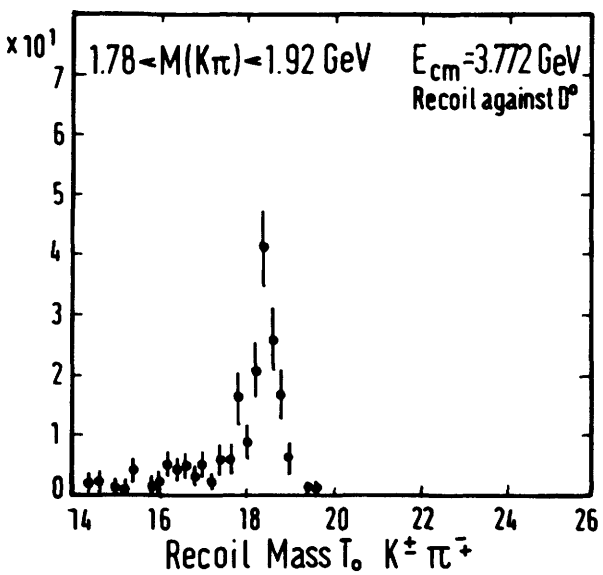

Fig. 5.6a

The channels listed in table 5.2 account only for the lesser part of the toal width. The unidentified decays are not found because of neutral particles, small branching fractions and small detection efficiencies.

Of particular interest is the decay $D^+ \rightarrow \bar{K}^0\pi^+$ which should be suppressed if sextet enhancement holds (see 5.132). The experiment[98] yields $\Gamma(D^+\rightarrow\bar{K}^0\pi^+) / \Gamma(D^0\rightarrow K^-\pi^+) = 0.70\pm0.23$ and there seems to be little suppression. Within errors the two channels $D^0 \rightarrow K^-\pi^+$ and $D^+ \rightarrow \bar{K}^0\pi^+$ are consistent with the relation (5.16).

The other branching ratio have been compared[98] to the statistical model[61]. The experimental values come out too small except for the $K^-\pi^+\pi^0$ where B is too high.

Finally it should be mentioned that the average charge multiplicities could be determined[98] as

$$\text{for} \quad D^0 \quad \langle n_{ch} \rangle = 2.3 \pm 0.2$$
$$D^+ \quad \langle n_{ch} \rangle = 2.3 \pm 0.3$$

which is in fair agreement with the statistical model.

5.212 D production at energies above 4 GeV

A large amount of data concerning hadronic decays of D and D^* were taken at SPEAR at 4.03 and 4.4 GeV where the total cross section shows peaks. From these data the results for the D mesons are corroborated, and the D^* mesons could be established.

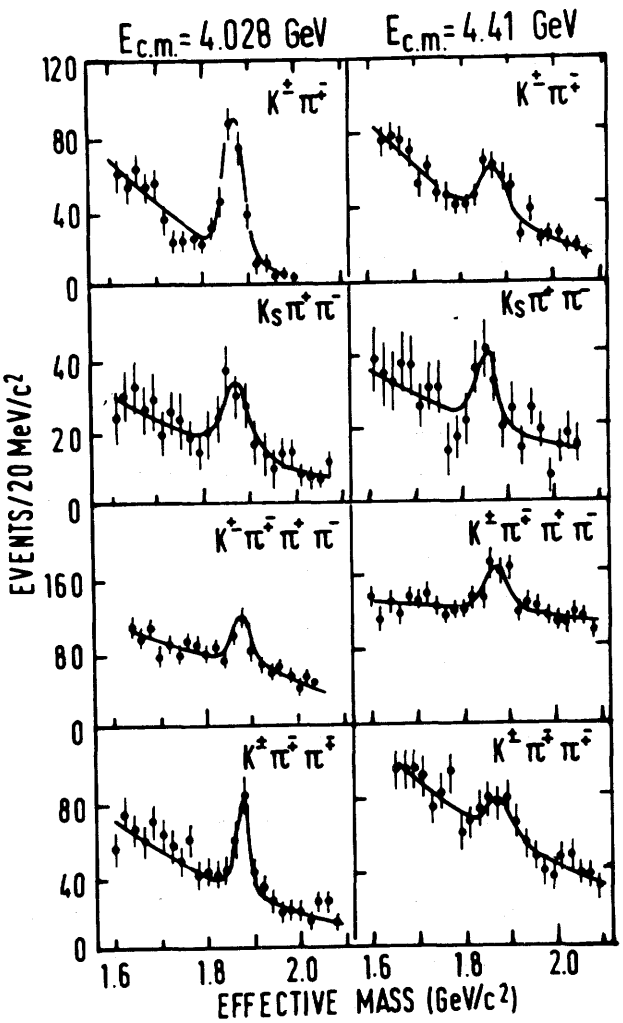

Fig. 5.7

The MARK 1 detector was used for this experiment, and again the identification of kaons by time-of-flight measurements is essential. The decay modes of the D^0 and D^* to various final states[101] is shown in fig. 5.7. The results for $\sigma \cdot B$ are summarized in table 5.3. As one sees there is not much energy dependence and the results at 3.77 GeV are confirmed. In particular the "exotic" state $K^-\pi^+\pi^+$ is seen again, whereas the Cabibbo forbidden decays are absent (fig. 5.8).
Higher multiplicities like $K3\pi$, $K^0_S\pi\pi$ are favoured over lower multiplicities like $K\pi$. The $K3\pi$ state is dominated by $K\rho\pi$ while the contribution from $K^*\pi\pi$ is small. If the maxima at 4.03 and 4.4 GeV in the total cross section are attributed entirely to charmed meson production, then the identified

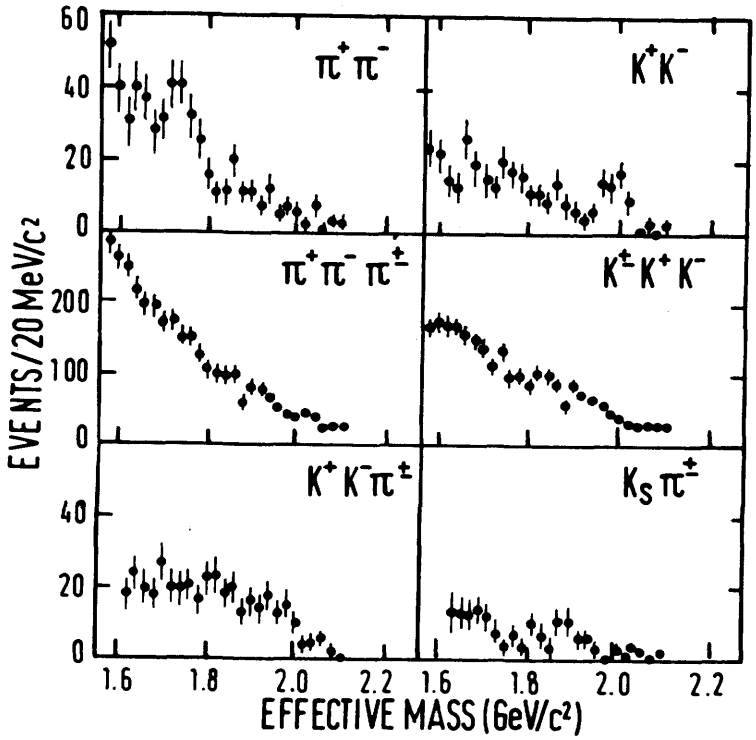

Fig. 5.8 Search for D^0, D^+ Cabibbo forbidden decay modes at 4.028 GeV

Table 5.3: $\sigma \cdot B$ in nb for various D decay modes at three values of $E_{c.m.}$

Mode		$E_{c.m.}$ (GeV)		
		3.774	4.028	4.414
D^0	$K^\mp\pi^\pm$	0.27 ± 0.05	0.57 ± 0.11	0.30 ± 0.09
	$K^0\pi^+\pi^-$ + c.c.	0.44 ± 0.11	1.09 ± 0.30	0.91 ± 0.34
	$K^\mp\pi^\pm\pi^+\pi^-$	0.34 ± 0.09	0.83 ± 0.27	0.91 ± 0.39
	$\pi^+\pi^-$	--	< 0.04	--
	K^+K^-	--	< 0.04	--
Total D^0 observed modes		1.05 ± 0.15	2.49 ± 0.42	2.12 ± 0.53
D^+	$K^0\pi^+$ + c.c.	0.15 ± 0.05	< 0.18	--
	$K^\mp\pi^\pm\pi^\pm$	0.34 ± 0.05	0.40 ± 0.10	0.33 ± 0.12
	$\pi^\pm\ \pi^+\pi^-$	--	0.03	--

hadronic decays add up to only about 10 % of all decays. The reasons for this small percentage are undetected neutrals and low detection efficiencies. As will be shown below at these energies the D mesons are predominantly produced via or associated with D^* states.

From the D decays it could also be inferred that parity is violated as should be expected for a weak decay. The $D^0 \to K^\pm\pi^\pm$ decay mode is a natural spin-parity state ($J^P = 0^+, 1^-, \ldots$) whereas $D^\pm \to K\ \pi^\pm\pi^\pm$ is compatatible with unnatural spin parity assignment, since 3 pseudoscalars cannot be in a $J^P = 0^+$ state. The cases $J^P = 1^-$ and 2^+ can be ruled out by studying the population of the Dalitz plot[12o].

5.213 D^* production and decays

If charm is a conserved quantum number, D and D^* mesons can only be produced in association. The most likely channels are for D^0 mesons

$$\begin{array}{l} e^+e^- \to D^0\,\bar{D}^0 \\ \qquad\quad D^0\,\bar{D}^{*0} + \bar{D}^0\,D^{*0} \\ \qquad\quad D^{*0}\,\bar{D}^{*0} \end{array} \qquad (5.25)$$

and similarly for D^+.

A possible way to find D^* is to determine the recoil mass $M^2_{recoil} = (E_{cm} - \sqrt{p^2 + M^2})^2 - p^2$ against a D^0 with momentum p and mass M. This has been done by the SLAC-LBL group using Mark 1[7o,89]. The recoil mass distribution against a D^0 is shown in fig. 5.9. Narrow peaks are seen at $M_{recoil} \simeq 1860$, 2005 and 2145 MeV/c^2 and a broader peak at 2440 MeV/c^2. The first two peaks can be interpreted by the first two channels of (5.25). The third peak could be due to the third channel but $e^+e^- \to D^0\,D^{**0}$ could compete. However, this interpretation is ruled out, as can be seen from two upper parts of fig. 5.9. The curves are calculated on the basis of $e^+e^- \to D^{*0}\,D^{*0}$ and one sees a shift and broadening of the peak at 2145 MeV/c^2 at $E_{cm} = 4.02$ GeV to about 2200 MeV/c^2 at 4.41 GeV, exactly as expected for this reaction.

The broad peak at 2440 MeV/c^2 could be due to multibody processes such as $D^*D^*\pi$ or to production of charm states with higher mass.

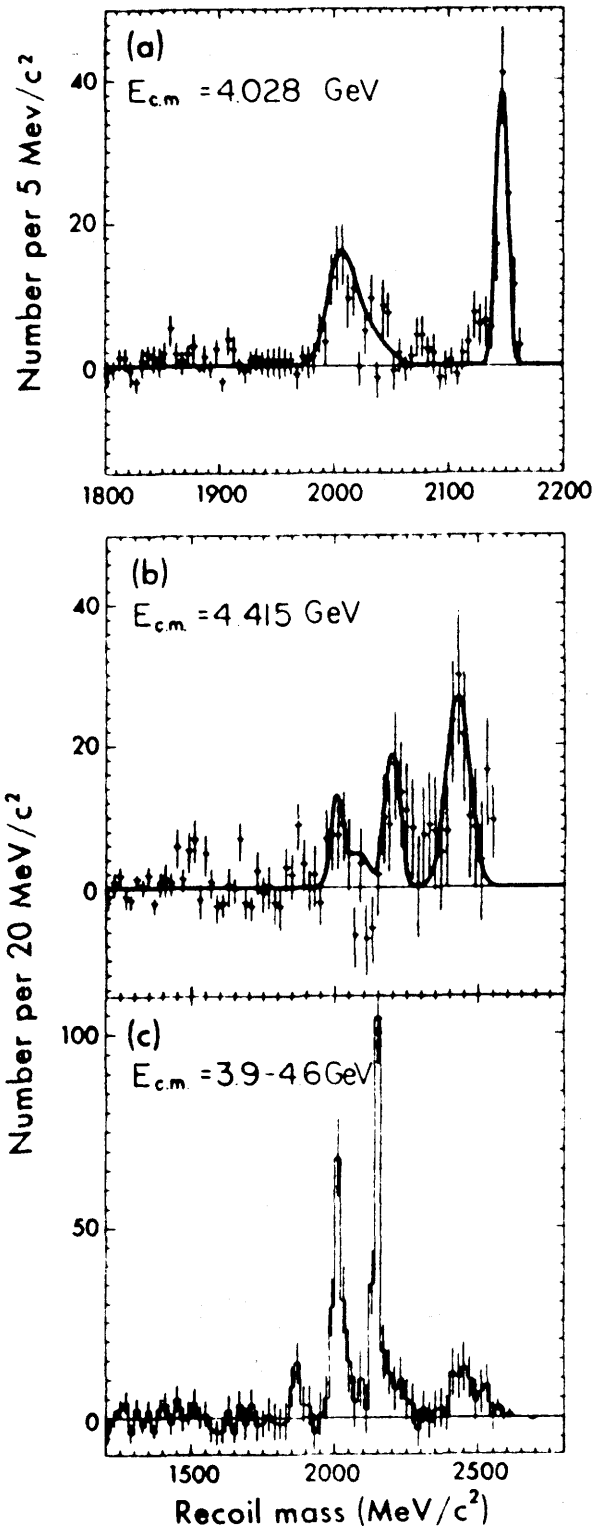

Fig. 5.9 Recoil spectra against D^0

The corresponding recoil mass distribution against a D^+ in the exotic channel $K\pi^{\pm}\pi^{\pm}$ has a much more severe background. Nevertheless a peak at 2010 MeV/c^2 was observed (fig. 5.1o) which can be interpreted as $e^+e^- \to D^+D^{*-}$ and charge conjugate. Indications for the other peaks might also be present.

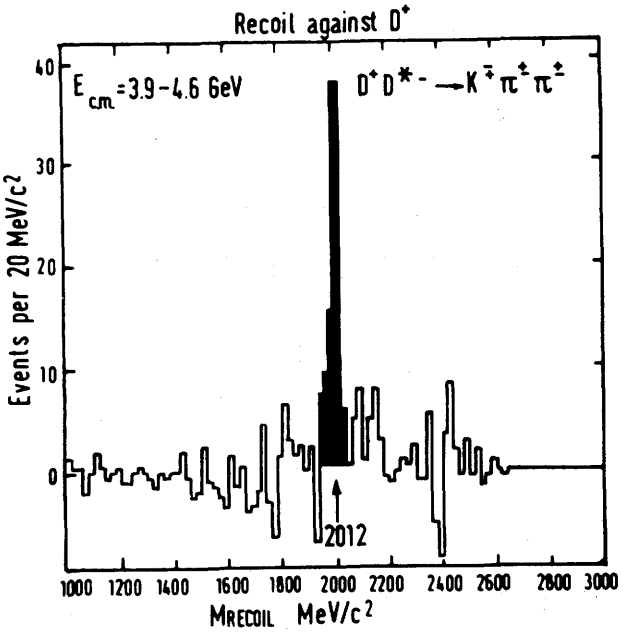

Fig. 5.10

The D^{*0} and D^{*+} being established as peaks in the recoil mass distribution against D^0 and D^+ we shall now turn to the decays of these particles. Obviously the decays $D^{*0} \to D^0\gamma$ and $D^{*+} \to D^+\gamma$ should be possible since they just involve a spin flip of the c quark (transition between HFS states). If the mass difference is large enough, the strong interaction decays $D^{*0} \to D^0\pi^0$, $D^+\pi^-$ and $D^{*+} \to D^+\pi^0$, $D^0\pi^+$ should also occur.

These decays are difficult to detect at e^+e^- energies below 5 GeV since in this case the pions originating from the D^* have low momenta and with experimental momentum cut-offs at about 100 MeV/c the detection efficiencies are low. For this reason measurements in the range $E_{m_\pm}$ = 5.0 to 7.8 GeV were performed[121]. The invariant mass distribution of $K\pi^\pm$ shows a clear D^0 peak. If the K combinations in D^0 peak are combined with the $\pi^\pm$ one expects a D^* peak in the invariant mass plot. The quantity that is precisely measured is the mass difference $M(D^0\pi) - M(D^0)$. The distribution of this difference is shown[89] in fig. 5.11. From these data the mass difference $D^{*+} - D^0$ is found to be 145.3 ± 0.5 MeV/c^2 or equivalently the Q value for the decay $D^{*+} \to D^0\pi^+$ is only 5.7 ± 0.5 MeV. Because of this small phase space the electromagnetic decays $D^* \to D\gamma$ can compete with the strong decays. The mass spectrum of fig. 5.11 gives also an upper limit on the width of the D^{*+} with $\Gamma(D^{*+}) < 2$ MeV.

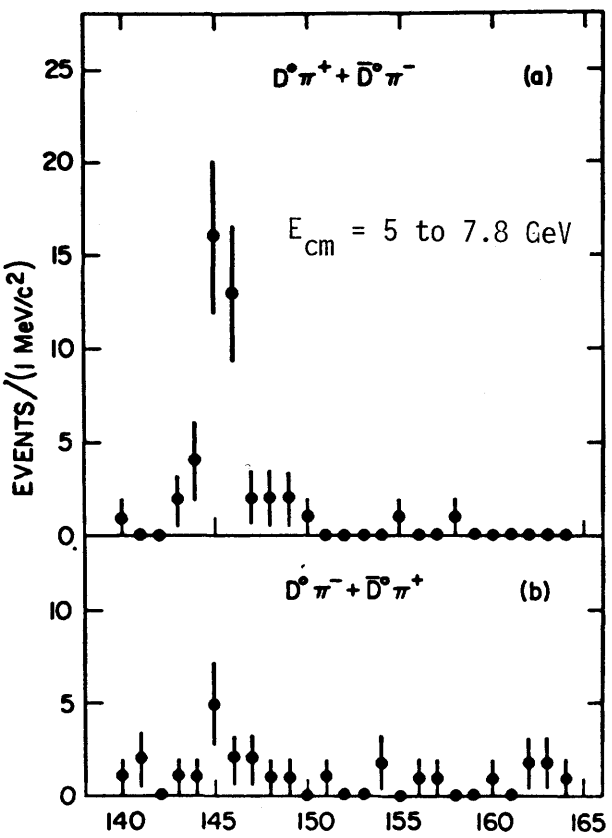

Fig. 5.11

For a precise mass determination it is of advantage to go to a e^+e^- energy just above threshold since in this case the momentum errors have less influence on the mass values (see 5.211). In fig. 5.12 the momentum spectrum of D^0 mesons decaying into 2 and 3 particles taken at 4.03 GeV is shown. In fig. 5.12a) the various processes contributing to the D^0 spectrum are shown. The peak at about 200 MeV/c is due to D^*D^*. Three channels contribute: $D^{*0} \to D^0\pi^0$, $D^{*0} \to D^0\gamma$ and $D^{*+} \to D^0\pi^+$. The distribution for the π decays should be Gaussian (curve A, B), whereas for γ decays the distribution is $dN/dp \sim p$ which results in a triangular shape (curve C). The $D^{*0} \to D^0\pi^0$ decay is clearly seen and also the evidence for $D^{*0} \to D^0\gamma$ is there. For the $D^{*+} \to D^0\pi^+$ only a faint indication might be recoginized. A precise value of the D^* mass can be inferred from the measured momentum.

The peak at 500 MeV/c and its shoulder is due to DD^* and charge conjugation: The central value determines $M(D) + M(D^*)$ while the shape of the shoulder and peak determine the ralative contributions of the different channels.

Finally the peak at about 750 MeV/c is due to direct D^0D^0 production. A similar, but simpler, situation holds for the D^+ spectrum (fig. 5.12 c).

A fit[70,89,98,104] to all these data gives the results shown in table 5.3 (isospin constraints have been used in the fit). In addition values for the production processes have been obtained from these data. Since they have been discussed already in chapter 4.41, they will not be considered here further.

Finally it should be mentioned that a detailed study[122] of angular distributions has shown that the spins of D^* are compatible with 1 as expected.

The approximate equality of the decay probabilities of $D^{*0} \to \gamma D^0$ and $D^{*+} \to \pi^+ D^0$ is in qualitative agreement with the theoretical expectation[85]. The main reason is, of course, the suppression of the strong decay by its small phase space.

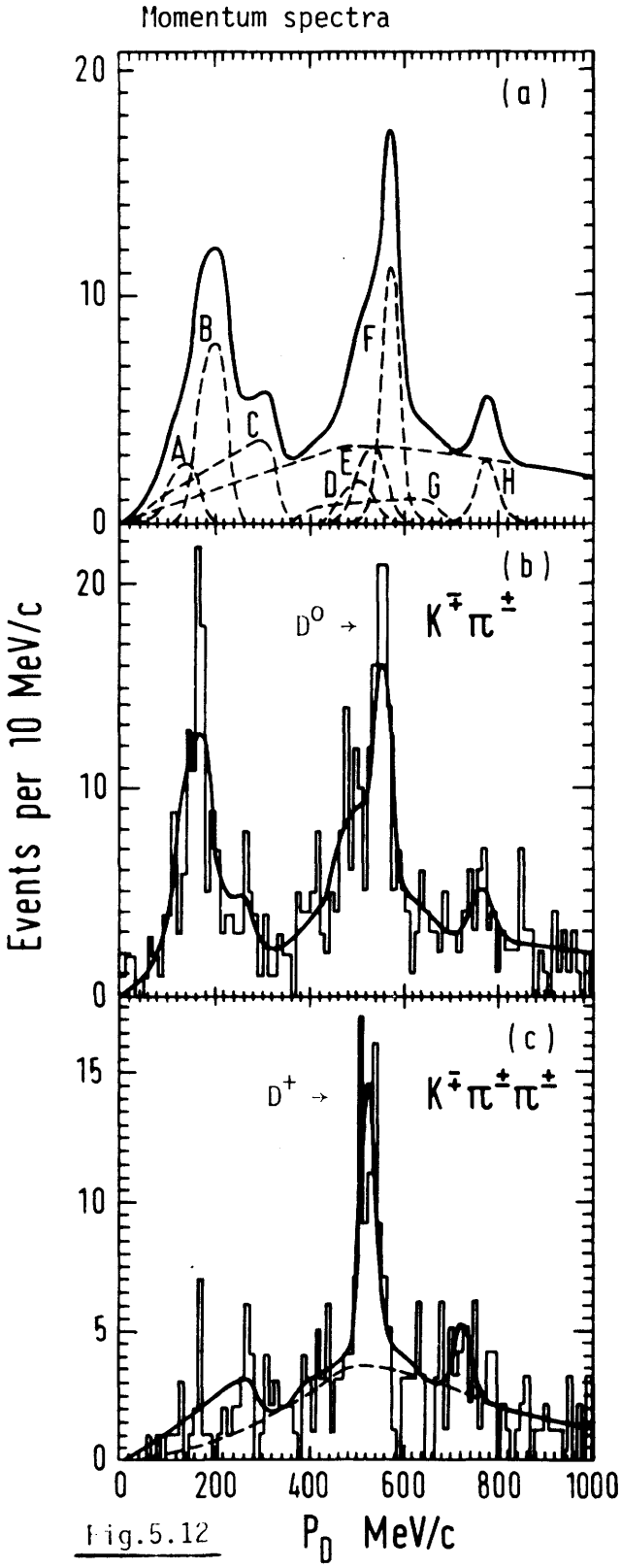

Fig.5.12

A: $D^{*+}D^{*-}$ $\to \pi^0 D^0$

B: $D^{*0}\bar{D}^{*0}$ $\to \pi^0 D^0$ (Gaussian)

C: $D^{*0}\bar{D}^{*0}$ $\to \gamma D^0$ $(\frac{dN}{dp} \sim p)$

E,D: D^*D $\to \pi D$

F: $D^{*0}D^0$

H: $D^0\bar{D}^0$

Table 5.4: Masses and decays of D^*

Particle	Mass $(MeV/c)^2$
D^{*o}	2006. ± 1.6
D^{*o}	2008.6 ± 1.0
D^o	1863 ± 3
D^+	1874 ± 5

Decay	Branching ratio
$D^{*o} \rightarrow \gamma D^o$	0.75 ± 0.05
$D^{*+} \rightarrow \pi^+ D^o$	0.60 ± 0.15

Mass differences (MeV)		Q-values (MeV)	
$D^+ - D^o$	5.0 ± 0.8	$D^{*o} \rightarrow D^o\ o$	7.7 ± 1.7
$D^{*+} - D^{*o}$	2.6 ± 1.8	$D^{*o} \rightarrow D^+ -$	- 1.9 ± 1.7
$(D^+ - D^o) - (D^{*+} - D^{o+})$	2.4 ± 2.4	$D^{*+} \rightarrow D^o +$	5.7 ± 0.5
		$D^{*+} \rightarrow D^+ o$	5.3 ± 0.9

The masses of D^o and D^+ agree well with those determined at 3.77 GeV (see chap. 5.211).

In fig. 5.11b the non exotic $K\pi\pi$ combinations are shown. From the data at the position of the D^*-mass the limit[89]

$$\frac{D^o \rightarrow K^+\pi^-}{D^o \rightarrow K\pi} < 16\ \%\ \ (90\ \%\ CL) \qquad (5.26)$$

can be derived which puts a limit on $D^o - \bar{D}^o$ mixing (see chap. 5.14). From the number of events where the K in the $\bar{D}^o$ recoil has the same sign as in D^o a different limit on $D^o - \bar{D}^o$ mixing can be obtained[89]:

$$\frac{D^o \rightarrow K^+\pi^-}{D^o \rightarrow K\pi} < 18\ \%\ \ (90\ \%\ CL) \qquad (5.27)$$

If we introduce the parameter

$$\varepsilon = \frac{N(K_{opposite}) - N(K_{same})}{N(K_{opposite}) + N(K_{same})} \tag{5.28}$$

where N(K) gives the number of events with kaons of oppsitve and same sign respectively, one obtains experimentally $\varepsilon \gtrsim 0.8$.
For complete $D^0 - \bar{D}^0$ mixing $\varepsilon = 0$ and for no mixing $\varepsilon = 1$. The experiments are thus compatible with the non-existence of a neutral flavour changing current.

The data also yield the limits for the Cabibbo forbidden decays

$$\frac{\Gamma(D^0 \to \pi^+\pi^-)}{\Gamma(D^0 \to K^-\pi^+)} < 0.07 \tag{5.29}$$

$$\frac{\Gamma(D^0 \to K^+K^-)}{\Gamma(D^0 \to K\pi)} < 0.07$$

and hence $tg^2\Theta < 0.07$.

5.22 Semileptonic decays of D and F mesons

The observation of semileptonic decays of charmed mesons is very interesting since the hadronic current appears only once and therefore a rather clean test of the weak charm current is possible (see chap. 5.12).

Semileptonic decays of charmed mesons with an electron in the final state were observed for the first time by the DASP collaboration[124] in spring 1976 at the time when the hadronic decays were found at SPEAR. Very soon PLUTO[125] could show that the electrons are associated to K^0 mesons as one would expect for the decay $D \to e\nu\bar{K}$ (see fig. 5.14 and 5.15).

Semileptonic decays into electrons require a clean identification of the electron. In the DASP experiment this was achieved by Cerenkov counters, in the PLUTO experiment by the showering property of electrons. Following a whim nature has chosen the mass of the D meson (1.86 GeV/c^2) cery close to the mass of the heavy lepton[81] (1.80 GeV/c^2). Hence the corresponding lepton

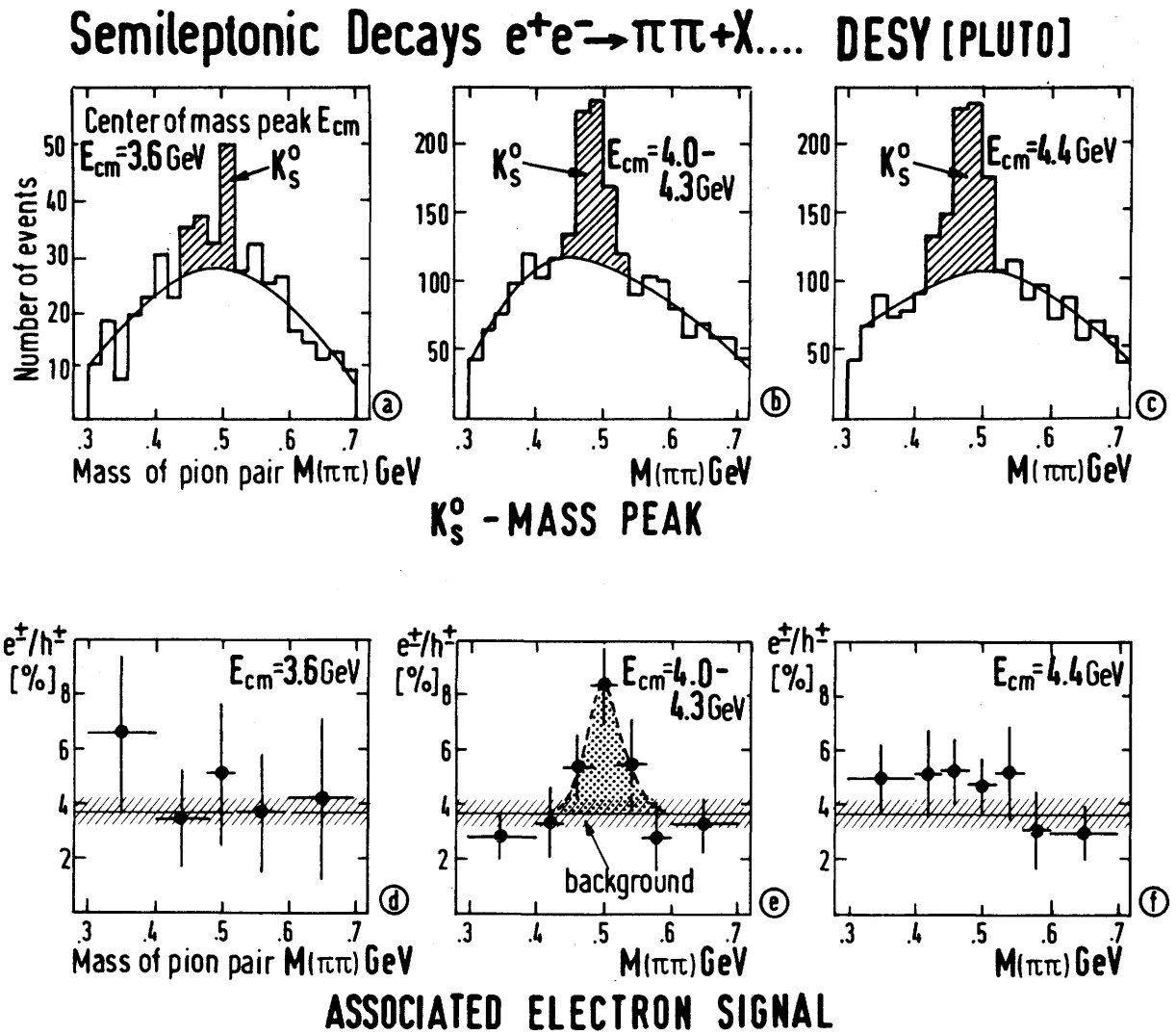

Fig. 5.14

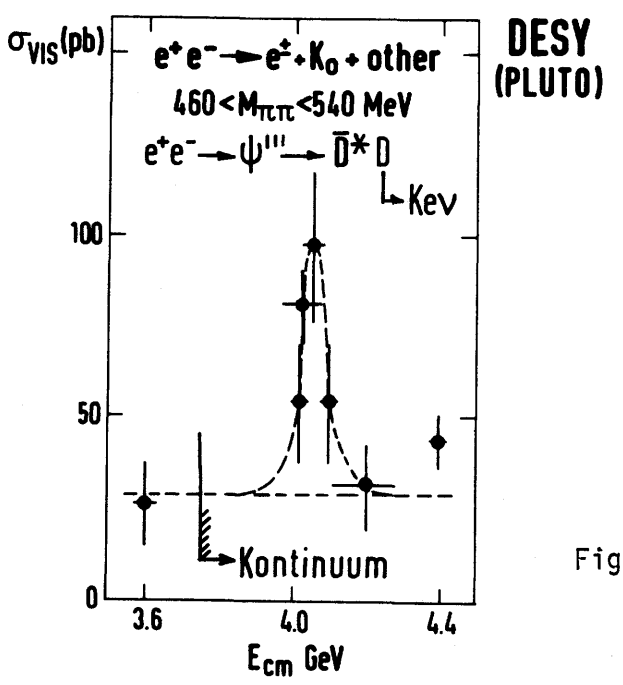

Fig. 5.15

spectra cover similar energy regions and one has to find ways to separate the two phenomena. This can be done on the basis of two criteria:

1.) The charmed mesons tend to produce final states with more than 2 charged tracks, whereas the heavy lepton has predominantly two tracks in the final state.

2.) The D mesons decay mainly into K mesons whereas the heavy lepton has a very low branching ratio for kaons.

In this way one can distinguish two types of events: high multiplicity, large kaon content versus low multiplicity, few kaons. These two kinds of events have been invetigated[127] quite carefully and it could be shown that the meson and lepton decays can be separated quite well. The average number of charged kaons was found to be 0.90 ± 0.18 per multiprong event and 0.07 ± 0.06 per to prong event. This also shows that for charmed particles (i.e. high multiplicity) the weak current couples strongly to strangeness in accordance with the GIM mechanism.

The inclusive electron spectrum measured by DASP[126] for the range E_{cm}=3.99 to 5.2 GeV is shown in fig. 5.16 before having been corrected. One notices that the contamination from the heavy lepton is quite small. In fig. 5.17 the electron spectrum taken close to $E_{cm}\simeq 4$ GeV is shown after subtracting the background. Two theoretical curves[128] are drawn for the decays $D\to K\, e\, \nu$ and $D\to K^{*}\, e\, \nu$. The accuracy is not good enough to distinguish between the two channels. The best fit is obtained for a mixture of both. Since the contribution of the two decay modes to the D decays depends sensitively on the V, A structure of the weak current, it seems very important to improve the measurements such that a separation of the two channels becomes possible. This might be achieved

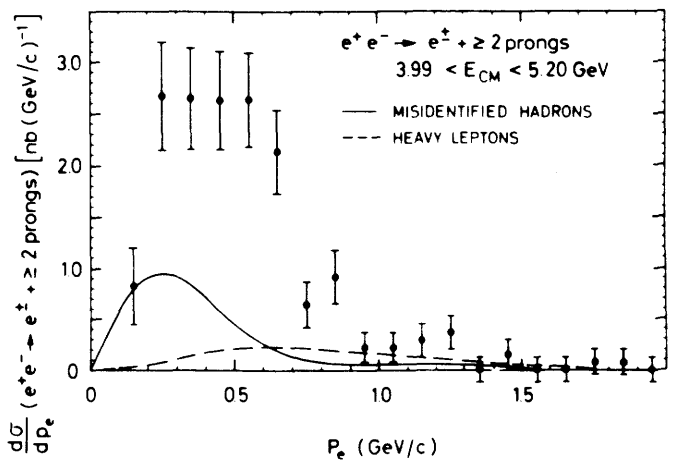

Fig. 5.16

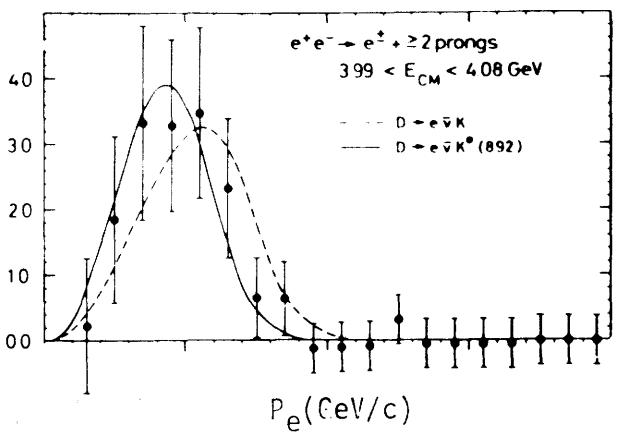

Fig. 5.17

by the DELCO detector at SPEAR which covers a much larger solid angle with C-counters than DASP (60% compared to 7% of 4π). So far the statistical accuracy that could be obtained does not allow such a separation yet[129]. Some results with lower statistical accuracy have recently also be obtained by MARK 1 [13o]. All these data are in good agreement.

DASP data[126] taken at higher E_{cm} show no drastic change of the spectrum which is not trivial since they were taken above the thresholds for F and charmed baryon production.

From the spectrum displayed in fig. 5.17 one can infer a limit on the leptonic decay $D \to e\nu$ which would produce a peak near $p_e \approx 1$ GeV/c. One finds $\sigma(D \to e\ \nu_e) / \sigma(D \to eX) < 0.09$ (90 % C.L.) in agreement with the theoretical expectation (see chap. 5.11). The Cabibbo-suppressed decay $D \to \pi\ e\ \nu$ (see chap. 5.12) produces a spectrum similar to those from $D \to K\ e\nu$ and $D \to K^*\ e\ \nu$ but it is shifted to higher momenta. From the fits to the measured spectrum it can be excluded that the decay $D \to \pi\ e\ \nu$ is the sole leptonic decay mode.

Integrating over the spectra and comparing to the total cross section one can derive the leptonic branching ratios. These have already been discussed in chap. 4.42.

Recently an indication of the semileptonic decay of the F meson has been found by DASP[123]. The η's found at $E_{cm} \approx 4.16$ GeV are associated to electrons (fig. 4.15, hatched events). A value for the branching ratio cannot yet be given, since the evaluation of the efficiencies is still under progress.

Electron spectra for the decays $F \to \eta\ e\nu$, $\eta'\ e\nu$, $\phi\ e\ \nu$ have been calculated[131].

No semileptonic decays of charmed mesons with muons in the final states have been seen. This is because the detection and identification of muons with momenta below 1 GeV/c is very difficult.

5.23 Discovery of F mesons

As has been explained in chap. 5.13 the lowest states of the F mesons tend to decay to final states containing $s\bar{s}$ which results in η and η'. Since ıce it is more difficult to detect η's than K's the discovery of the F mesons has to be considered much more difficult than those of the D mesons which are characterized by kaons in the final state. A first indication of F production was obtained from the inclusive yield of η which shows an abandance at $E_{cm} = 4.4$ GeV (see chap. 4.43). Since η is a frequent byproduct of η' decay, a search for η includes a search for η'.

The DASP group[1o5] succeeeded in detecting F mesons by their decay $F \to \eta\pi$, however, this could be achieved only by using a "trick". The signature of this decay channel is not specific enough to separate the F decays from the large background. The theoretical prediction was that the first excited state F^* (the ortho $c\bar{s}$ state having parallel spins) should be close to the spin-zero ground state F (see chap. 2.22) and the favoured decay should be $F^* \to F\,\gamma$ with a photon energy of about 100 MeV. This low energy photon delivers an additonal selection criterium. What has been observed are events of the type

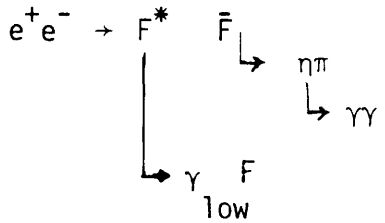

(5.26)

A good event is characterized by 3 photons, one of which has a low energy, the other two forming a mass in the η region. In addition an identified charged pion with momentum above 0.6 GeV/c had to be seen. These events could, however, also originate from the reaction

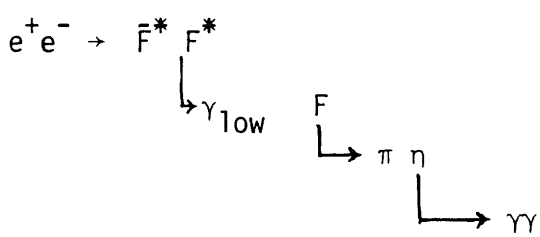

(5.27)

$$e^+e^- \longrightarrow F\bar{F}^* \longrightarrow F\gamma F$$
$$\qquad\qquad\qquad\qquad\qquad\quad \llcorner\!\!\rightarrow \eta\pi$$

$4.36 \leq W \leq 4.48$ GeV

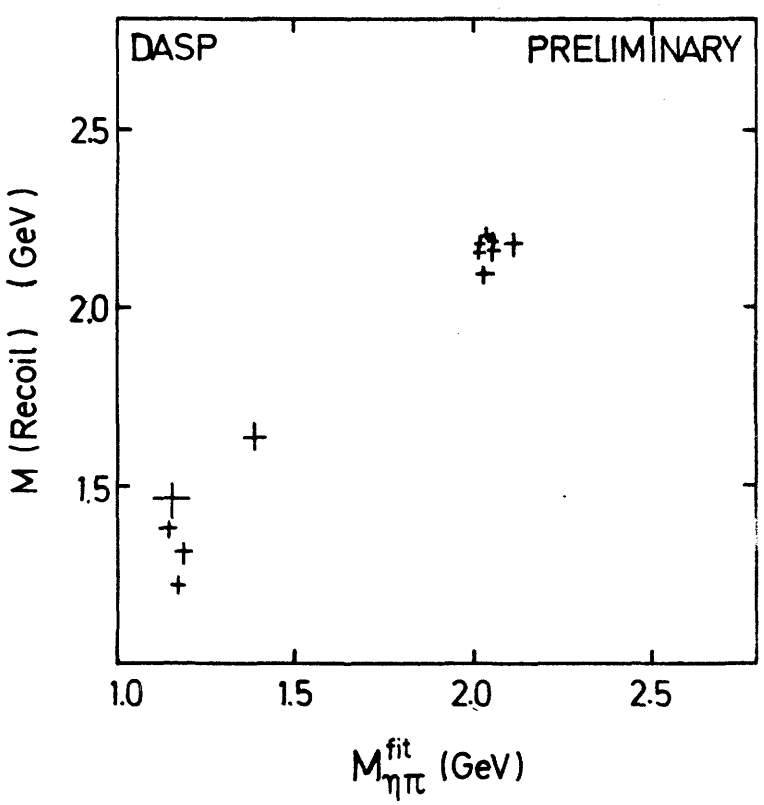

Fig. 5.18

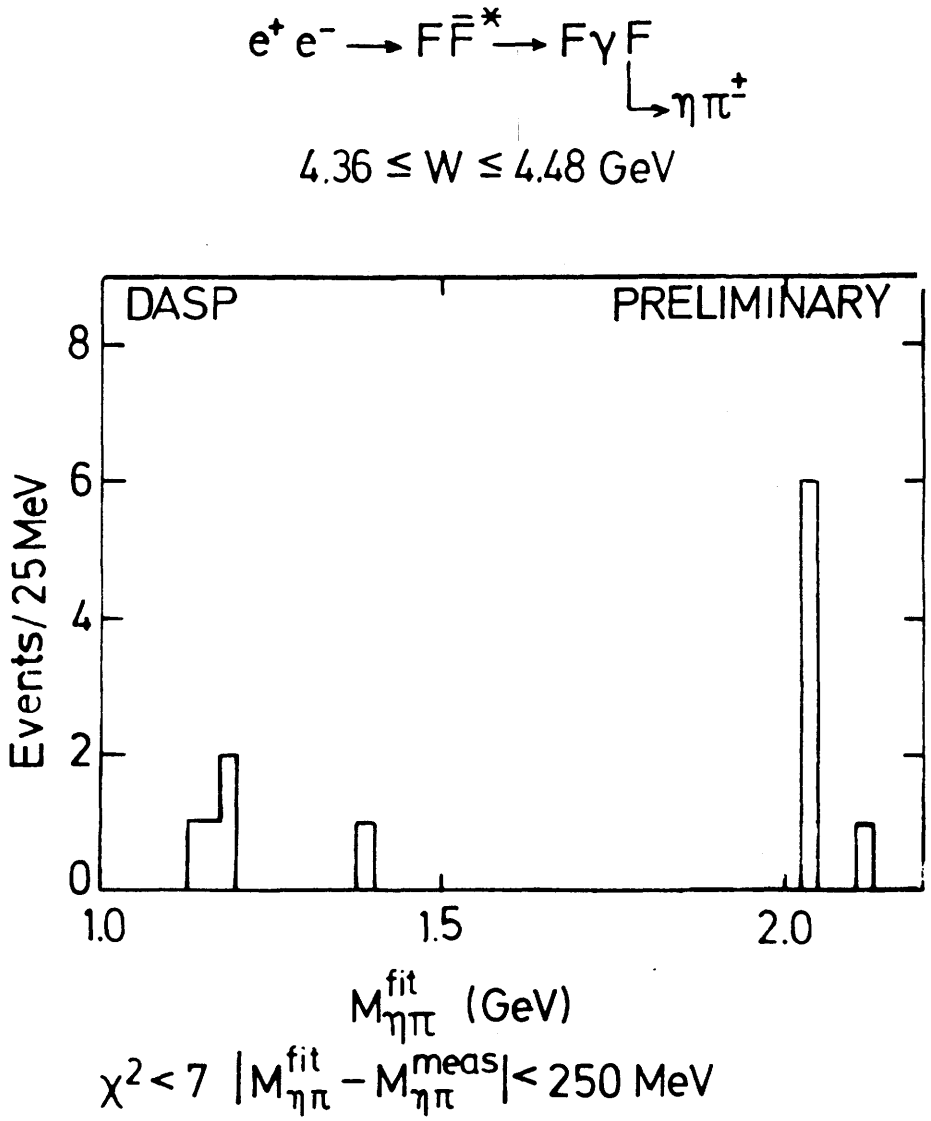
$e^+ e^- \rightarrow F\bar{F}^* \rightarrow F\gamma F$
$\hookrightarrow \eta\pi^\pm$
$4.36 \leq W \leq 4.48$ GeV
DASP
PRELIMINARY
Events/25 MeV
0
2
4
6
8
1.0
1.5
2.0
$M^{fit}_{\eta\pi}$ (GeV)
$\chi^2 < 7 \quad |M^{fit}_{\eta\pi} - M^{meas}_{\eta\pi}| < 250$ MeV

Fig. 5.19

The observed events were fit for both processes. The most recent results are shown[123] in fig. 5.18, where the invariant $\pi\eta$ mass is plotted against the recoil mass. A clear clustering of events can be seen corresponding to (5.26) or (5.27). In fig. 5.19 the projected $\eta\pi$ mass distribution is shown. The peak in the mass bin 2.025 to 2.050 GeV is attributed to the F.The events at lower masses could originate from A_2 decays.

The conclusion on the masses is

$$\begin{aligned} m(F) &= 2.03 \pm 0.06 \quad GeV/c^2 \\ m(F^*) &= 2.14 \pm 0.06 \quad GeV/c^2 \end{aligned} \tag{5.28}$$

where the uncertainty originates essentially from the ambiguity (5.26) or (5.27). The mass difference F^* - F can be determined directly from the energy of γ_{low} and the result is:

$$m(F^*) - m(F) = 120 \pm 40 \text{ MeV} \tag{5.29}$$

The interpretation of the HFS-splitting has already be discussed in chap. 2.2. It agrees astonighsingly well with the theoretical expectation.

These data were taken at E_{cm} = 4.4 GeV where the inclusive η production shows a prominent peak (see fig. 4.13). However, it would be very interesting to observe $F\bar{F}$ production just above its threshold at 4.06 GeV (see table 4.2) where $F\bar{F}^*$ is not yet possible, in complete analogy with $D\bar{D}$ production at 3.77 GeV. The right place for such a search seems to be the peak at 4.1 GeV and indeed a clear η peak has recently been found[123] in the $\gamma\gamma$ invariant mass distribution (fig. 4.15). In this case no low energy photon was required, of course. The shaded events in fig. 4.15 show events with an additional electron. One notices that the η peak is correlated with electrons indicating that a weak decay was involved. No η peak was seen for e^+e^- energies 4.0 to 4.06 GeV, i.e. below $F\bar{F}$ threshold.

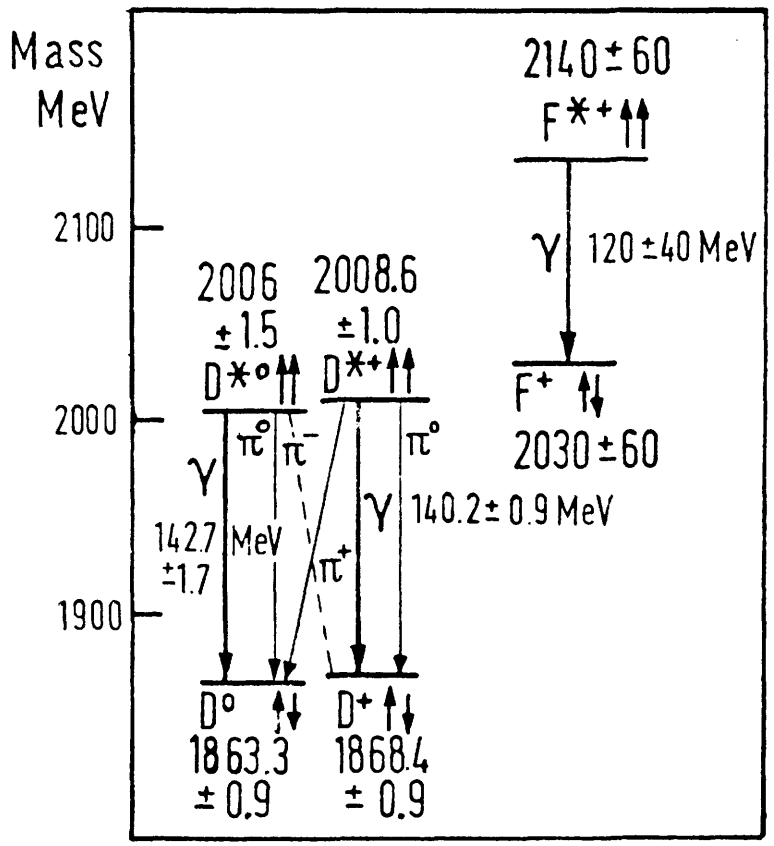
Mass
MeV
2100
2000
1900
2140 ± 60
F*+
γ
120 ± 40 MeV
F+
2030 ± 60
2006
± 1.5
D*°
2008.6
± 1.0
D*+
π°
π⁻
γ
142.7
± 1.7
MeV
π+
π°
γ
140.2 ± 0.9 MeV
D°
1863.3
± 0.9
D+
1868.4
± 0.9

Fig. 5.20

5.24 Summary on charm particles

Perhaps the most striking success of the charm model is the discovery of the charmed mesons predicted by the model.The most important results are:

1.) Both the isospin doublet D^0, D^+ and the isospin singlett with strangeness F^+ have been seen. As expected the lowest states are the ones with J = 0 (quarks spins opposite). The corresponding states with J = 1 have also be found and the HFS splitting agrees with the expectation of the potential model (see chap. 2.22). These ortho states decay to the ground states by strong or electromagnetic transitions. The transition rates present no problems to their theoretical interpretation.

The mass spectrum of the charm mesons and the observed transitions are summarized in fig. 5.20.

Higher excited states, e.g. P-states have not been seen yet.

2.) The weak decays of the ground states of charm mesons are compatible with the expectations of the minimal model of weak interaction (see chap. 5.1). The rule $\Delta C = \Delta S = \pm 1$ which is implied by the minimal theory is dramatically confirmed by the dominance of kaons in the final states. Also the Cabibbo structure of the charm current is evident by the suppression of $\Delta C = \pm 1$, $\Delta S = 0$ decays. Parity violation has been demonstrated.

3.) The chirality structure of the charm current could not been verified yet. The accuracy of the semileptonic decay spectra is not sufficient to distinguish between V-A and V+A. A distinction between $D \to e\ \nu\ K$ and $D \to e\ \nu\ K^*$ would help, since the first decay goes by pure V, whereas the second contains V and A components.
Polarization measurements would be the most direct way to clarify the chirality structure. Λ_0 polarization from charmed baryon decays could offer a possible way.

4.) No sextuplet enhancement is found in charm meson decays. As a consequence, the $\Delta I = 1/2$ enhancement found in ordinary strange particle decays cannot be explained by 20-plet enhancement.

5.) No $D^0 - \bar{D}^0$ mixing is found. The present accuracy excludes the existence

of neutral currents with $\Delta C = 0$ of order G_F.

6.) Although there is evidence for charm baryons in neutrino reactions, they could not be identified so far in e^+e^-. Indirect evidence is provided by steps in the $\bar{p}$ and Λ inclusive cross section.

So far all the observations on charm mesons are compatible with the minimal theory. This model, however, cannot be exact if embedded in a world with 6 leptons and more than 4 quarks. Hence it would be very interesting to find deviations.

6. The Upsilon

6.1 Experimental results

In 1977 a Columbia-Fermilab-Stony Brook Collaboration[132] under the guidance of L.M. Lederman bombarded nuclear targets by 400 GeV portons and observed the reaction

$$p + \text{Nucleus} \rightarrow \mu^+ + \mu^- + \text{anything} \qquad (6.1)$$

in a two-arm spectrometer which allowed the identification of the muons and the measurement of their momenta. From these the invariant mass of the muon pair can be computed and the distribution of the invariant masses is shown in fig. 6.1.Superimposed on an exponentially decreasing background one notices enhancements at the J/ψ and ψ' masses and a broad structure between 9 and 10 GeV/c^2. If the smooth background is subtracted one obtains the data displayed in fig. 6.2. The experimental resolution in this region is 200 MeV.

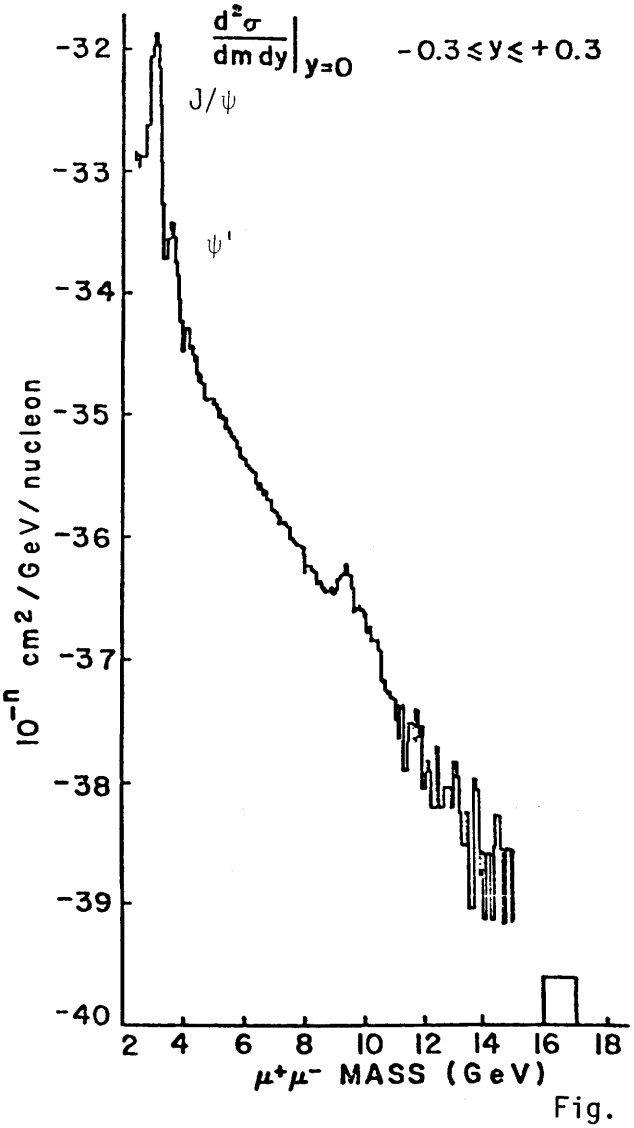

Fig. 6.1

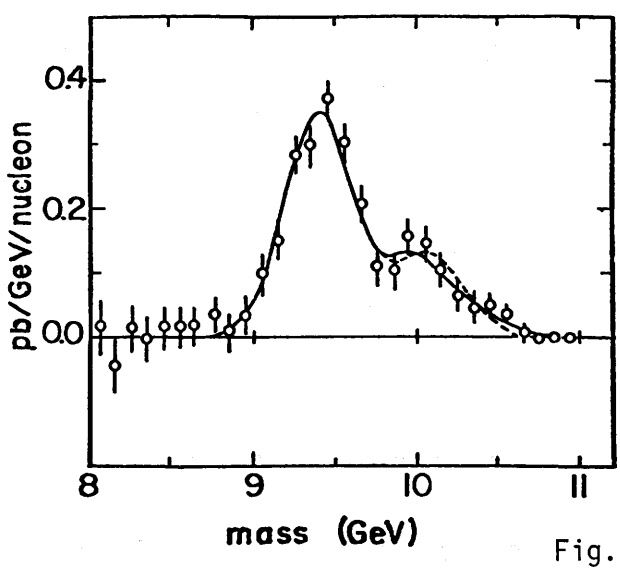

Fig. 6.2

Hence the width of the structure cannot be due to the experimental resolution but indicates some complicated structure. Indeed, just looking at the data of fig. 6.2 one would assume peaks around 9.4 and 10 GeV/c^2.

The authors have fitted the data by two different assumptions, by 2 or 3 aussian peaks, respectively. The position of the peaks and their branching ratio x production cross section are given in table 6.1.

The existence of the T'' is statistically not certain, of course. Not much can be said about the width of the peaks. In the fits it is assumed that their widths are small compared to the experimental resolution of about 200 MeV.

Table 6.1: Resonance Fit Parameters

	2 peak	3 peak	
Υ M_1	9.41 ± 0.013	9.40 ± 0.013	GeV
Υ $B\frac{d\sigma}{dy}\Big\|_{y=0}$	0.18 ± 0.01	0.18 ± 0.01	pb
Υ' M_2	10.06 ± 0.03	10.01 ± 0.04	GeV
Υ' $B\frac{d\sigma}{dy}\Big\|_{y=0}$	0.069 ± 0.006	0.065 ± 0.007	pb
Υ'' M_3	---	10.40 ± 0.12	GeV
Υ'' $B\frac{d\sigma}{dy}\Big\|_{y=0}$	---	0.011 ± 0.007	pb
χ^2 / DF	19.3 / 18	14.2 / 16	

From the figures of table 6.1 one can extract the following data which will be important for the discussion in chap. 6.2.

		2 peaks	3 peaks
$M(\Upsilon') - M(\Upsilon)$		650 ± 30 MeV	610 ± 40 MeV
$M(\Upsilon'') - M(\Upsilon)$		--	1000 ±120 MeV
Ratio of $B\frac{d\sigma}{dy}\Big\|_{y=0}$	Υ'/Υ	0.38 ± 0.04	0.37 ± 0.04
	Υ''/Υ	--	0.06 ± 0.04

Clearly it seems very important to resolve experimentally the complex structure in its components. This might be possibly only by producing the Υ in e^+e^- collisions. Although not being designed for such high energies, DORIS might be pushed to reach the T region and this will be tried in spring 1978.

6.2 Possible interpretation of the T family

After the discovery of the T there appeared a flood of theoretical papers making the assumption that the T family is just a replay of the J/ψ story. This means that there exists a family of $Q\bar{Q}$-bound states, where Q is a heavy quarks of charge ± 2/3 or ± 1/3 and the mass of Q is about half the T mass, i.e. $m_Q \simeq 4.6$ GeV.

6.21 Excitation energies

Even before the detection of T the standard model with a linear confining potential has been extended[133] to larger quark masses. The excitation energies above the lowest lying state are shown in fig. 6.3 as function of the quark mass. The essential point is that for a linear potential the excitation energy is reduced proportional to $m_Q^{-1/3}$. Since the continuum boundary on the other hand goes up one expects more bound states. For $m_Q \simeq 4.6$ GeV not only the 1S and 2S states are bound but also the 3S level.

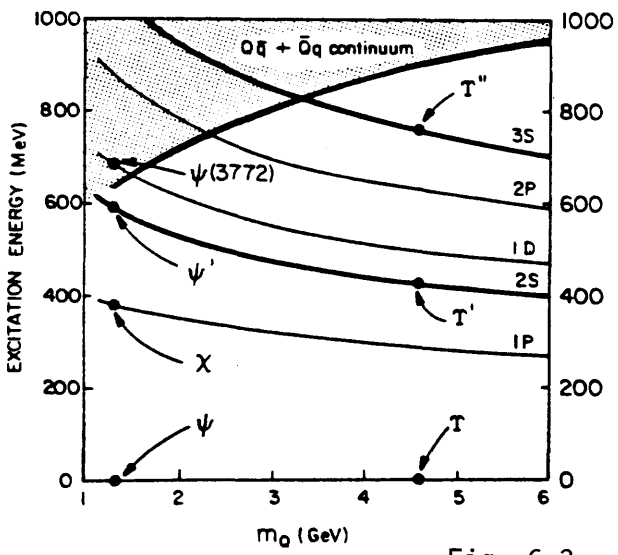

Fig. 6.3

According to this model one expects $M(\Upsilon') - M(\Upsilon) = 420$ MeV and $M(\Upsilon'') - M(\Upsilon) = 750$ MeV, values which are smaller than the experimental ones. Indeed, the experimentally found splittings imply $M(\Upsilon') - M(\Upsilon) \simeq M(\psi') - M(J/\psi)$ in contradiction to the prediction of the linear confining potential. This perhaps is not very surprising since the naive standard model failed to give the proper positions of the charmonium P states. One possible remedy was to assume that the confining potential is not a Lorentz vector but a scalar (see chap. 1.232). Indeed it was shown[134] that a scalar linear potential gives splittings independent of m_Q and of the right magnitude.

An other possibility is to look for a vector potential with m_Q-independent excitation energies. Indeed it could be shown[135] that a logarithmic potential $V(r) \sim \ln r$ does exactly that. It also gives good account on the charmonium levels and even is better than the linear potential, as far as the P levels are concerned. However, it predicts too large E1 transition rates and gives uncomfortably large relativistic corrections[87].

If the interpretation of the Υ family as a new $Q\bar{Q}$ system is right then the study of the excitation levels of this system together with that of charmonium offers us a unique possibility to learn something about the quark-quark forces. The spectrum of the $Q\bar{Q}$ system could even be much richer than the charmonium decay scheme[133] but we shall not discuss it here further, since the scaling of the excitation energies is not clear yet.

6.22 Production and decays

The interesting question is whether Υ is made of charge 2/3 (top) or 1/3 (bottom) quarks. A number of authors have tried to answer this question by comparing the measured production cross section to different models[136]. Clearly $B \cdot d\sigma/dy$ is 4 times larger for a 2/3 charge than for 1/3. Most of the theoretical estimates are in favour of 1/3 (for a comparison see Ref. 132), but the uncertainties are so large that no definite conclusion can be drawn.

A surprising fact is the large ratio of $B \cdot d\sigma/dy$ for T' compared to T. In analogy to ψ' one would expect[87] a large branching ratio for the transition $T' \to T + 2\pi$. For the ψ'/ψ couple the ratio is $R = (1.7 \pm 0.5)$ % whereas for T' / T one has $R \simeq 0.4$. This could be taken as evidence against the assumption that all states belong to the same family. However, from a somewhat naive application of ACD one can find[87] plausible arguments that the $T' \to \gamma + 2\pi$ transition is suppressed by OZI mechanism by a factor of about 10. More experimental information is needed to clarify this issue.

Of particular interest will be the hadronic decays of the Υ family. The masses of these particles are large enough that hadron jets originating from gluons should be well developed. This might provide an excellent test of the ideas of QCD. Because of conservation laws a $^3S_1$ state can decay into 3 photons (e.g. ortho positronium) or 3 gluons (J/ψ family, see chap. 3.2) but not 2 photons or gluons. A ^3P state on the other hand decays into 2 photons or 2 gluons. Hence it is expected that Υ (9.4) decays into 3 gluons which should appear[137] as 3 coplanar hadron jets.

The excited states of Υ are expected to decay to P states by electromagnetic transitions and one expects[138] decays like

$$\Upsilon'(10.0) \to \gamma + {}^3P_2(9.8) \to \gamma + 2\ g \to \gamma + 2 \text{ jets}$$

where one finds two jets with distinct lab energies ($\approx$ 5 GeV) accompanied by a monochromatic photon. The angular distribution allows to differentiate between jets originating from gluons and from quarks.

If the $Q\bar{Q}$ interpretation of Υ is right, particles with $Q\bar{q}$ etc. should also exist where q is one of the 4 lighter quarks. Obviously they are analogous to the D and F mesons and their ground states would be stable with respect to strong interactions. Their weak decays and possible mixing between B^0 - $\bar{B}^0$ and T^0 - $\bar{T}^0$ has been discueed ($B^0 = b\bar{q}$, $T^0 = t\bar{q}$)[136)137)138)139].

6.3 Sequential quarks and leptons

The existence of the charm quark made is possible to group the 4 quarks and 4 leptons into weak $SU(2)^W$ doublts and a minimal theory with GIM mechanism

could be formulated for the weak interaction. It is compatible with all experiments (see chap. 5.1), except for the non-observation of parity violation in atomic transitions[140] which, however, needs confirmation and the small CP violation in K decays. The beauty of this model is the symmetry between quarks and leptons which is needed to cancel the triangle anomalies which would otherwise have destroyed the renormalizability of the weak and electromagnetic gauge theory[141].

With the discovery of an other heavy lepton τ and probably another quark it is tempting to extend the Weinberg-Salam-Ward-GIM model by adding further lefthanded quark and lepton doublets:

$$\begin{pmatrix} \nu_e & \nu_\mu & \nu_\tau \\ e & \mu & \tau \end{pmatrix}_L \qquad \begin{pmatrix} u & c & t \ldots \\ d' & s' & b' \ldots \end{pmatrix}_L \tag{6.2}$$

The extension to a 6 quark- 6 lepton model was first proposed by Kobayashi and Maskawa[142]. It retains the natural suppression of $\Delta S = 1$ and $\Delta C = 1$ effects as observed and preserves the phenomenological succes as far as neutrino scattering is concerned.

A very important point is, however, that the 6 quark model gives CP violation in a natural way. This is achieved by a generalization of the Cabibbo structure of the hadronic current (see chap. 5.1). The most general way of mixing the lefthanded charge 1/3 quarks is[143]

$$\begin{aligned} d' &= c_1 \cdot d + s_1 c_3 \cdot s + s_1 s_3 \cdot b \\ s' &= -s_1 c_2 \cdot d + (-s_2 s_3 e^{i\delta} + c_1 c_2 c_3) \cdot s + (c_1 c_2 s_3 + s_2 c_3 e^{i\delta}) \cdot b \\ b' &= s_1 s_2 \cdot d - (c_1 s_2 c_3 + c_2 s_3 e^{i\delta}) \cdot s + (c_1 s_2 c_3 + c_2 c_3 e^{i\delta}) \cdot b \end{aligned} \tag{6.3}$$

whereas the 2/3 charge quarks u, c and t remain unchanged. Here the abbreviated notation $s_1 = \sin \Theta_1$, $c_1 = \cos \Theta_1$, $s_2 = \sin \Theta_2$, ... has been

used and Θ_1 is identical to the Cabibbo angle. The 4 quark model is reproduced by $\Theta_2 = \Theta_3 = \delta = 0$.

Since the original Cabibbo structure agrees well with observations c_3 has to be close to one. A more quantitative analysis (Ellis et al.[136]) of the coupling in μ decay and in $(\bar{u}d)$ and $(\bar{u}s)$ gives $s_1^2 \cdot s_3^2 < 0.003$ and with $s_1^2 \simeq 0.05$ this means $s_3^2 < 0.06$. Hence Θ_3 cannot be much larger than the Cabibbo angle Θ_1 but it may, of course, be much smaller. The restrictions on Θ_2 are much weaker and depend on the quark masses. For $m_t \simeq 5$ GeV one finds $s_2^2 < 0.2$ and for $m_t \simeq m_W \simeq 65$ GeV $s_2^2 < 0.03$.

The phase parameter δ introduces CP violation and appears only if one has at least 6 quarks. From the measured CP violation parameter $\varepsilon \approx 10^{-3}$ one deduces that δ cannot be arbitrarily small: $|\sin\delta| > 3 \times 10^{-3}$ for $m_t = 5$ GeV and $|\sin\delta| > 6 \times 10^{-4}$ for $m_t = 65$ GeV.

Because of the limits for Θ_2 and Θ_3 one might speculate if they are exactly zero. This has quite amusing consequences. The decay of the strange particles to ordinary hadrons is only possible because of the d-s mixing. Without this "feed-through" the lightest strange particles would be absolutely stable. With $\Theta_2 = \Theta_3 = 0$, b would not mix with d and s, as can be seen from (6.3) and as a consequence particles like $b\bar{q}$ would be stable if the b quark is lighter than the t quark or v.v. Such stable particles of a new kind of matter could be captured in nuclei and the consequences for the ensueing X-ray spectra and formation of hypernuclei have been recently discussed in detail[144].

If the interpretation of the Υ family as a $Q\bar{Q}$ spectrum of a new kind of quark turns out to be right then a number of questions arises, e.g.

1) is there one more quark to complete the couple (t,b)?
2) which one is the lighter, t or b?
3) is the structure of the weak current such as expected from a minimal theory?
4) are 6 quarks and 6 leptons the basic elements of matter or are there more sequential leptons and quarks?
5) are electrons and muons elementary contituents or are they made up of smaller entities having 1/3 and 2/3 charges?

It is hoped that the e^+e^- storage rings PETRA, CESR and PEP which will come into operation soon might make it possible to shed some light on these exciting and fundamental questions.

Appendix 1 (see p. 30)

Table A1: Decay modes of the ψ into mesons

Topology	Decay Mode	Observed Number of Events	Efficiency	Branching Ratio
$K_S MM$	$K_S K_L$	< 4	0.23	$< 8.9 \times 10^{-5}$
$\pi^+\pi^-$	all	1.7 ± 1.7 *	0.040	$(1.6 \pm 1.6) \times 10^{-4}$
K^+K^-	all	1.8 ± 1.4 *	0.036	$(2.0 \pm 1.6) \times 10^{-4}$
$K_S K^\pm \pi^\mp$	all	126 ± 15	0.13	$(2.6 \pm 0.7) \times 10^{-3}$
	$K^0\bar{K}^{*0} + \bar{K}^0K^{*0}$	45 ± 7.8	0.044	$(2.7 \pm 0.6) \times 10^{-3}$
	$K^+K^{*-} + K^-K^{*+}$	48 ± 7.7	0.040	$(3.2 \pm 0.6) \times 10^{-3}$
	$K^0\bar{K}^{**0} + \bar{K}^0K^{**0}$	1 ± 2.7	0.007	$< 2.0 \times 10^{-3}$
	$K^+K^{**-} + K^-K^{**+}$	-1 ± 2.7	0.006	$< 1.5 \times 10^{-3}$
$\pi^+\pi^-K^+K^-$	all	205 ± 17	0.076	$(7.2 \pm 2.3) \times 10^{-3}$
	$K^{*0}\bar{K}^{**0} + \bar{K}^{*0}K^{**0}$	$40 \geq 8.4$	0.016	$(6.7 \pm 2.6) \times 10^{-3}$
	$K^{*0}\bar{K}^{*0}$	1.5 ± 4	0.048	$< 0.5 \times 10^{-3}$
	$K^{**0}\bar{K}^{**0}$	2.5 ± 4.5	0.009	$< 2.9 \times 10^{-3}$
	$\phi\pi^+\pi^-$	23 ± 5	0.043	$(1.4 \pm 0.6) \times 10^{-3}$
	ϕf	≤ 1	0.023	$< 3.7 \times 10^{-4}$
$\pi^+\pi^-\pi^+\pi^-K^+K^-$	all	30 ± 6	0.026	$(3.1 \pm 1.3) \times 10^{-3}$
	$\phi\pi^+\pi^-\pi^+\pi^-$	≤ 3	0.013	$\leq 1.5 \times 10^{-3}$
$K^+K^-K^+K^-$	all	19 ± 5	0.075	$(0.7 \pm 0.3) \times 10^{-3}$
	ϕK^+K^-	14 ± 5	0.040	$(0.9 \pm 0.4) \times 10^{-3}$
	$\phi f'$	6 ± 3	0.020	$(0.8 \pm 0.5) \times 10^{-3}$
$\pi^+\pi^-K^+K^-\pi^0$	all	309 ± 50	0.073	$(1.2 \pm 0.3) \times 10^{-2}$
	ωK^+K^-	22 ± 12	0.068	$(0.8 \pm 0.5) \times 10^{-3}$
	$\omega f'$	-2 ± 2.4	0.034	$< 1.6 \times 10^{-4}$
	$\phi\eta$	5 ± 2.5	0.013	$(1.0 \pm 0.6) \times 10^{-3}$
$\pi^+\pi^-K^+K^-$ MM	$\phi\eta'$	≤ 2	0.011	$\leq 1.3 \times 10^{-3}$
$2(\pi^+\pi^-)\pi^0$	all	675 ± 40 *	0.17	(4.0 ± 1.0) %
	$\omega\pi^+\pi^-$	348 ± 40	0.14	$(6.8 \pm 1.9) \times 10^{-3}$
	ωf	81 ± 20	0.11	$(1.9 \pm 0.8) \times 10^{-3}$
	$\rho^0A_2^0 + \rho^\pm A_2^\mp$	36 ± 12	0.018	$(8.4 \pm 4.5) \times 10^{-3}$
$3(\pi^+\pi^-)\pi^0$	all	181 ± 26*	0.062	(2.9 ± 0.7) %
	$\omega 4\pi$	140 ± 30	0.044	$(8.5 \pm 3.4) \times 10^{-3}$
$4(\pi^+\pi^-)\pi^0$	all	13 ± 4 *	0.014	$(9.0 \pm 3.0) \times 10^{-3}$
$\pi^+\pi^-\pi^0$	$(\rho^0\pi^0 + \rho^\pm\pi^\mp)$	153 ± 13 *	0.12	(1.3 ± 0.3) %
$2(\pi^+\pi^-)$	all	76 ± 9 *	0.19	$(4.0 \pm 1.0) \times 10^{-3}$
$3(\pi^+\pi^-)$	all	32 ± 7 *	0.80	$(4.0 \pm 2.0) \times 10^{-3}$

Modes marked with an asterisk were calculated from a smaller data sample,

References

1. H. Fritzsch, M. Gell-Mann and H. Leutwyler, Phys. Lett. B47 (1973),365
   D.J. Gross, F. Wilczek, Phys. Rev. D8 (1973),3633
   S. Weinberg, Phys. Rev. Lett. 31(1973),494

2. T. Appelquist and H.D. Politzer, Phys. Rev. Lett. 34(1975),43
   T. Appelquist, A. De Rújula and H.D. Politzer, Phys. Rev. Lett.34 (1975),365
   A. De Rújula and S.L. Glashow, Phys. Rev. Lett. 34(1975),46

3. A. De Rújula, H. Georgi, and S.L. Glashow, Phys. Rev. D12(1975),147
   R. Barbieri, R. Kögerler, Z. Kunszt, and R. Gatto, Nucl. Phys. B1o5 (1976),125

3.a A. De Rújula, R.C. Giles and R.L. Jaffe, MIT-preprint CTP No. 635, June 1977

4. J.D. Jackson, Summer Institute of Particle Physics, SLAC, August, 1976 and papers quoted there

5. E. Eichten, K. Gottfried, T. Kinoshita, J. Kogut, K.D. Lane, T.-M. Yan, Phys. Rev. Lett. 34(1975),369

6. M. Krammer and H. Krasemann, Nuov. Cim. 32A(1976),394

7. H.J. Schnitzer, Phys. Rev. Lett. 35(1975),1540 and Phys. Rev. D13 (1975),74

8. J. Pumplin, W. Repko and A. Sato, Phys. Rev.Lett.35(1975),1538

8.a A. Martin, Phys. Lett 67B(1977),330
   H. Grosse, Phys. Lett.68B(1977),343
   H. Grosse, and A. Martin, Nucl. Phys. B132(1978),125

9. C.E. Carlson and F. Gross, College of Willam and Mary Preprint WM-PP-21 (March 1977)

10. A.B. Henriques, B.K. Kellett and R.G. and R.G. Moorhouse, Phys. Lett. 64B(1976),85

11. H.J. Schnitzer, Phys. Lett. 65B(1976),239

12. A. Arneodo and G.L. Kane, Preprint, Michigan Univ., UM-HE 77-5(1977)

13. T. De Grand, R.L. Jaffe, K. Johnson and J. Kiskis, Phys. Rev. D12(1975), 2060

14. E. Eichten, K. Gottfried, T. Kinoshita, K.D. Lane and T.-M. Yan, Phys. Rev. Lett.36(1976),500

15. S. Okubo, V.S. Mathur and S. Borchardt, Phys. Rev. Lett. 34(1975),236
Ngee-Pong Chang and C.A. Nelson, Phys. Rev. D35(1975),1492

16. A. Kazi, G. Kramer, D.H. Schiller, DESY 75/11 (1975) and
Acta Phys. Austriaca 45(1976),65
S. Borchardt, V.S. Mathur, S. Okubo, Phys. Rev.Lett.34(1975),38
B.J. Edwards and A.N. Kamal, Phys. Rev.D39(1977)66

17. G. Källen, Elementary Particle Physics, Addison-Wesley, 1964, pp29

18. H.J. Schnitzer, preprint, Brandeis Univ., March 1977

19. W. Celmaster, Harvard Univ., Preprint 1977, HUTP77-A024

20. H. Fritzsch, preprint CERN, July 1977

21. C.E. Carlson and F. Gross, preprint, College of William and Mary, Williamsburg, WM-PP-21, March 1977

22. A.B. Henriques, B.K. Kellet and R.G. Moorhouse, Phys. Lett. 64B(1976),85

23. A. De Rújula, H. Georgi and S.L. Glashow, Phy. Rev. Lett. 37(1976), 398
see also K. Lane and E. Eichten, Phys. Rev.Lett. 37(1976),477

24. K.D. Lane, and S. Weinberg, Phys.Rev.Lett.37(1976),717

25. J.J. Aubert et al., Phys.Rev.Lett. 33(1974),1404

26. J.-E. Augustin et al., Phys.Rev.Lett.33(1974),1406

27. G.S. Abrams et al., Phys.Rev.Lett. 34(1975),1181
W. Tannenbaum et al., Phys. Rev. Lett.36(1976),4o2

28. G.J. Feldman, Summer Inst. on Particle Physics, SLAC, August 1976, SLAC-PUB 1852
recent data see G. Goldhaber, European Conf. on Particle Physics, Budapest, July 1977, LBL-6732

29. B.H. Wiik and G. Wolf, Les Houches Summer School 1976, DESY Report 77/01 (1977)

3o. A.M. Boyarski et al., Phys. Rev. Lett. 34(1975),1357
V. Lüth, SLAC-PUB-1599 (1975)

31. W. Braunchweig et al., Phys. Lett 63B(1976),115

32. L. Criegee et al., DESY Report 75/32 (1975)
J. Burmester et al., 1976 Tblisi Conference and DESY Report 76/53 1976)

33. C. Bemporad, 1975 Stanford Conference, p.113

34. W.Braunchweig et al., Phys. Lett.57B(1975),297 and Phys. Lett. 63B(1976) and Phys. Lett.63B(1976),487

35. R. Barbieri, R. Gatto and R. Kögerler, Phys. Lett.60B(1976),183

36. S. Okubo, Phys. Lett. 5(1963),1o5
G. Zweig, CERN Rep. TH-401,412 (1964)
J. Iizuka, K. Okada and O. Shito, Prog.Theor. Phys. 35(1966),1o61

37. J. Burmester et al., DESY report 77/50 (1977)
and Phys. Lett. 72B(1977),135

38. F. Vanucci et al., Phys.Rev. D15(1977),1814

39. J.S. Whitaker et al., Tblisi Conference 1976

4o. W.Braunchweig et al., Phys. Lett.67B(1977)243

41. W. Bartel et al., DESY rep. 76/40(1976), Phys. Lett.64B(1976),483
and Phys. Lett. 66B(1976),489

42. W. Bartel et al., DESY report 77/70 (1977)

43. G. Knies, DESY report 77/74 (1977) and Proc. of the 1977 International Symposium on Lepton and Photon Interactions at High Energies, Hamburg, August 1977, p.93,
G. Alexander et al., DESY Rep. 77/72 (1977)

44. A. De Rújula, H. Georgi, and S.L. Glashow, Phys.Rev.D12(1975),154
and Phys. Rev. Lett.34(1975),46

45. H. Fritzsch and P. Minkowski, Nuov. Cim. 30A (1975),393

46. H. Fritzsch and J.D. Jackson, CERN report TH-2264 (1976)

47. W. Braunchweig et al., Phys. Lett.67B(1977)249

48. B.J. Edwards and A.N Kamal, Phys.Rev.Lett.39(1977),66

49. T.F. Walsh, DESY report 76/13 (1976) and unpublished information

50. R. Brandelik et al., DESY report 78/01 (1978)

51. M. Krammer, DESY report 78/06 (1978)

52. W. Braunchweig et al., Phys. Lett.67B(1977),243

53. W.Bartel et al., DESY report 77/70 (1977)

54. C.J. Biddick et al., Phys.Rev.Lett.38 (1977), 1324

55. J.S. Whitaker et al., Phys. Rev. Lett. 37(1976), 1596

V. Blobel, XII Rencontre de Moriond (1977)

56. W.D. Apel et al., Phys. Lett. 72B(1978),500

57. W. Braunchweig et al, Phys. Lett. 67B(1977 249

58. W. Tannenbaum et al., Phys. Rev. Lett. 35(1975),1323

59. J.D. Jackson, European Conf. on Particle Physics, Budapest, 1977

6o. G. Feinberg and J. Sucher, Phys.Rev. Lett. 35(1975),1740

61. C. Quigg and J.L. Rosner, FNAL-report 77/40 (1977)

62. F. Wilczek and A. Zee, Phys. Rev. Lett. 40(1978),83

63. H. Krasemann and M. Krammer, DESY report 77/34 (1977) and Phys. Lett. 70B(1977 457

64. D.H. Boal, Phys. Rev. Lett. 37(1976), 1333

65. M. Greco and M. Krammer, DESY report 77/3C (1977) and Phys. Lett. 69B(1977),313

66. W. Braunschweig et al., Phys. Lett. 57B(1975),4o7

B. Wiik, Tblisi Conference 1976

67. D. Badtke et al., Tblisi Conference 1976

68. W. Bartel et al., Tblisi Conference 1976

J. Olsson, Proc. of the 1977 Intern. Symposium on Lepton and Photon Interactions at High Energies, Hamburg, 1977, pp 117

69. U. Timm, DESY report 77/52 (1977) and European Conference on Particle Physics, Budapest, 1977

7o. G. Goldhaber, European Conference on Particle Physics, Budapest 1977 and LBL-6732 (1977)

71. M.S. Chanowitz and F.J. Gilman, SLAC-PUB 1746 (1976)

72. A.B. Henriques, B.H. Kellett and R.G. Moorhouse, Phys. Lett. 64B (1976),85

73. J.D. Jackson, Phys. Rev. Lett.37(1976),11o7

92. J. Burmester et al., DESY report 77/17 (1977)

93. T.F. Walsh, DESY report 76/13 (1976)

R. Kögeler, G. Schierholz and G. Kramer, Phys. Lett. 65B(1976),441

94. M. Tonutti, Proc. of the 1977 Inter. Symposium von Lepton and Photon Interactions at High Energies, Hamburg, 1977, pp135

95. J. Burmester et al., DESY report 77/14 (1977)and Phys. Lett. 67B(1977)367

96. R. Brandelik et al., Phys. Lett. 67B (1977), 363

97. V. Lüth et al., Phys. Lett. 70B (1977), 120

98. A. Barbaro-Galtieri, Proc. of the 1977 Intern. Symposium on Lepton and Photon Interactions at High Energies, Hamburg, 1977, p. 21

99. R. Brandelik et al., DESY report 77/44 (1977)

100. G. Wolf, Intern. School of Physics "Enrico Fermi", Varenna, July, 1977

1o1. M. Piccolo et al., Phys. Rev. Lett. 39(1977) 15o3

1o2. B. Knapp et al., Phys. Rev. Lett. 37(1976), 882

1o3. E.G. Gazzoli et al., Phys. Rev. Lett. 34(1975),1125

1o4. I. Peruzzi et al., Phys. Rev. Lett. 39 (1977), 13o1

1o5. R. Brandelik et al., Phys. Lett. 70B (1977), 132

1o6. J.D. Bjorken and S.L. Glashow, Phys. Lett. 11 (1964), 255

1o7. S.L. Glashow, J. Illiopoulos, and L. Maiani, Phys. Rev. D2 (1970), 1285

1o8. H. Fritzsch, Intern. School of Physics "Enrico Fermi", Varenna, July 1977, CERN-TH 2359 and Intern. Summer Institute for Theor. Physics, Bielefeld, September 1977

1o9. S.L. Glashow, Nucl. Phys. 22 (1961), 579

11o. A. Salam and J.C. Ward, Phys. Lett. 13 (1964), 168

111. S.Weinberg, Phys. Rev. Lett.19 (1967), 1264

112. D. Fakirov and B. Stech, Heidelberg THEP 77-8 (1977) and contribution to the 1977 Intern. Symposium von Lepton and Photon Interactions at High Energies, Hamburg, 1977

113. T.F. Walsh, DESY report 77/76 (1977) and Proc. of the 1977 Intern. Symposium on Lepton and Photon Interactions at High Energies, Hamburg, 1977, pp 711

114. A. Ali and T.C. Yang, Phys. Lett. 65B(1976), 275
and DESY report 77/54 (1977)

74. R. Barbieri, R. Gatto and E. Remiddi, Phys. Lett. 61B(1976),465

75. J.D. Jackson, European Conference on Partilce Physics, Budapest, 1977

76. T.W. Appelquist and H. Georgi, Phys. Rev. D8(1973),4000
A. Zee, Phys. Rev. D8(1973), 4o38

77. A.M. Boyarski et al., Phys. Rev. Lett.34(1975),764

78. U. Timm, DESY report 77/52 (1977) and European Conference on Particle Physics, Budapest, 1977

79. G. Knies, DESY report 77/74 (1977) and Proc. of the 1977 Intern. Symposium on Lepton and Photon Interactions at High Energies, Hamburg, 1977, pp 93

J. Burmester et al., Phys. Lett. 66B(1977)395

8o. S. Yamada, Proc. of the 1977 Intern. Symposium on Lepton and Photon Interactions at High Energies, Hamburg, 1977, pp.69

81. R. Brandelik et al., Phys.Lett. 73B(1978), 1o9

82. G.J. Feldman, SLAC-PUB-2000 (1977)

83. A. Bäcker, PHD-Thesis, University Siegen, DESY report F33-77/03 (1977)

84. P.A. Rapidis et al., Phys. Rev. Lett. 39(1977), 526

85. K.D. Lane and E. Eichten, Phys. Rev. Lett. 37(1976), 477

86. J. Kirkby, SLAC-PUB-2040 (1977) and Proc. of the 1977 Intern. Symposium on Lepton and Photon Interactions at High Energies, Hamburg, 1977, pp 3

87. K. Gottfried, Proc. of the 1977 Intern. Symposium on Lepton and Photon Interactions at High Energies, Hamburg, 1977, pp 667

88. G. Goldhaber et al., Phys. Lett. 69B (1977), 5o3

89. H. Sadrozinski, Proc. of the 1977 Intern. Symposium on Lepton and Photon Interactions at High Energies, Hamburg, 1977, pp.47

90. J.G. Körner, M. Kuroda, G. Schierholz, Phys. Lett. 70B(1977),1o6

9o.a J.G. Körner and M. Kuroda, Phys. Rev. D16(1977),2165

91. L.B. Okun and M.B. Voloschin, JETP 23(1976), 369
A. DeRújula, H. Georgi and S.L. Glashow, Phys. Rev. Lett. 38(1976),317

114.a J. Ellis, M.K. Gaillard, and D.V. Nanopoulos, Nucl. Phys. B100 (1975),313

115. R.L. Kingsley et al., Phys. Rev. D11(1975), 1919

116. M. K. Gaillard, B.W. Lee, J.L. Rosner, Rev. Mod. Phys. 47(1975),277

117. S.L.Glashow and S. Weinberg, Phys. Rev. D15 (1977),1958
E.A. Paschos, Phys. Rev. D15 (1977), 1966

118. A.M. Boyarski et al., Phys. Rev. Lett. 35 (1975), 196

119. D.L. Scharre et al., SLAC-PUB 2019, September 1977,
Phys. Rev. Lett 40(1978), 74

120. J.E. Wiss et al., Phys. Rev. Lett. 37(1976), 1531

121. G. Feldman et al., Phys. Rev. Lett. 38(1977), 1313

122. H.K. Nguyen et al., Phys. Rev. Lett.39 (1977), 262

123. DASP-Collaboration; DPG-Spring Meeting, Heidelberg, March 1978,
and G. Wolf, private communication

124. W. Braunchweig et al., DESY report 76/37 (1976) and Phys. Lett. 63B(1976),417

125. J. Burmester et al., DESY report 76/50 (1976), and Phys. Lett. 64B(1976),369

126. R. Brandelik et al., Phys. Lett. 70B(1977), 387

127. R. Brandelik et al., Phys. Lett. 70B(1977),125

128. A. Ali and T.C. Yang, Phys. Lett. 65B (1976), 275

129. J. Kirkby, SLAC-PUB 2040, November 1977

13o. J.M. Feller et al., Phys. Rev. Lett. 40(1977),274

131. A. Ali and T.C. Yang, DESY report 77/54 (1977)

132. S.W. Herb et al., Phys.Rev. Lett.39(1977),252
L.M. Lederman, Proc. of the 1977 Intern. Symposium on Lepton and
Photon Interactions at High Energies, Hamburg, 1977, pp 567

133. E. Eichten and K. Gottfried, Phys. Lett. 66B(1977),286

134. D. Pignon and C.A. Piketty, preprint Nov. 1977
Lab. de Phys. Theor. de l'Ecole Norm. Sup.

135. C. Quigg and J.L. Rosner, FERMILAB Pub-77/82 (1977)

136. C.E. Carlson and R. Suaya, Phys. Rev. Lett. 39(1977),9o8

R.N. Cahn and S.D. Ellis, Univ. Michigan Report 76-45 (1976)
J. Ellis et al., Nucl. Phys. B131(1977), 285
T. Hagiwara, Y. Kazama and E. Takasugi, Phys. Rev. Lett. 40(1978), 76

137. K. Koller and T.F. Walsh, DESY report 77/68 (1977)

138. M. Krammer and H. Krasemann, Phys. Lett. 73B(1978), 58

139. A. Ali, CERN report TH.2411 (1977)
A. Ali and Z.Z. Aydin, DESY report 78/11 (1978)

140. P.G.H. Sandars, Proc. of the 1977 Intern. Symposium on Lepton and Photon Interactions at High Energies, Hamburg, 1977, pp 599

141. C. Bouchiat, J. Illiopoulos and Ph. Meyer, Phys. Lett.38B(1972),519

142. M. Kobayashi and K. Maskara, Prog. Theor. Phys. 49(1973), 652

143. H.Fritzsch, CERN TH-2539 (1977)

144. R.N. Cahn, Phys. Rev. Lett.40(1978), 80